AD_____

Award Number: DAMD17-99-1-9528

TITLE: The Integrin-Regulated Kinase PYK-2: A Therapeutic
Target for Prostate Cancer

PRINCIPAL INVESTIGATOR: Magnus Edlund, Ph.D.
                         Leland W. K. Chung, Ph.D.

CONTRACTING ORGANIZATION: University of Virginia
                           Charlottesville, Virginia 22906-9003

REPORT DATE: September 2001

TYPE OF REPORT: Annual Summary

PREPARED FOR: U.S. Army Medical Research and Materiel Command
               Fort Detrick, Maryland 21702-5012

DISTRIBUTION STATEMENT: Approved for Public Release;
                        Distribution Unlimited

The views, opinions and/or findings contained in this report are
those of the author(s) and should not be construed as an official
Department of the Army position, policy or decision unless so
designated by other documentation.

20020717 026

REPORT DOCUMENTATION PAGE

Public reporting burden for this collection of information is estimated to average 1 hour per response, including the time for reviewing instructions, searching existing data sources, gathering and maintaining the data needed, and completing and reviewing this collection of information. Send comments regarding this burden estimate or any other aspect of this collection of information, including suggestions for reducing this burden to Washington Headquarters Services, Directorate for Information Operations and Reports, 1215 Jefferson Davis Highway, Suite 1204, Arlington, VA 22202-4302, and to the Office of Management and Budget, Paperwork Reduction Project (0704-0188), Washington, DC 20503

1. AGENCY USE ONLY (Leave blank)	2. REPORT DATE September 2001	3. REPORT TYPE AND DATES COVERED Annual Summary (1 Sep 00 – 31 Aug 01)

4. TITLE AND SUBTITLE
The Integrin-Regulated Kinase PYK2-: A Therapeutic Target for Prostate Cancer

5. FUNDING NUMBERS
DAMD17-99-1-9528

6. AUTHOR(S)
Magnus Edlund, Ph.D.
Leland W. K. Chung, Ph.D.

7. PERFORMING ORGANIZATION NAME(S) AND ADDRESS(ES)
University of Virginia
Charlottesville, Virginia 22906-9003

E-Mail: nme7c@virginia.edu

8. PERFORMING ORGANIZATION REPORT NUMBER

9. SPONSORING / MONITORING AGENCY NAME(S) AND ADDRESS(ES)

U.S. Army Medical Research and Materiel Command
Fort Detrick, Maryland 21702-5012

10. SPONSORING / MONITORING AGENCY REPORT NUMBER

11. SUPPLEMENTARY NOTES
Report contains color

12a. DISTRIBUTION / AVAILABILITY STATEMENT
Approved for Public Release; Distribution Unlimited

12b. DISTRIBUTION CODE

13. ABSTRACT (Maximum 200 Words)

A prostate cancer cell's growth, differentiation and survival are guided by its interactions with the surrounding extracellular matrix (ECM). A number of promising therapeutic targets for androgen-independent and metastatic prostate cancers are contained within the signaling cascades downstream of the ECM-binding Integrin molecules. My research focuses on one component of these cascades, the phospho-tyrosine kinase PYK-2, whose expression levels and activity I aim to manipulate in cell culture and within tumors in mice. This past year, after redirecting my research approach somewhat because of technical difficulties, I can now report that I have: 1) characterized PYK-2 expression in prostate tissues and cell lines; 2) linked Green Fluorescent Protein (GFP) to both PYK-2 and dominant-negative PYK-2 (PRNK), transiently transfected cells with these constructs, and studied protein localization and construct effects on cell growth, apoptosis and migratory behaviors; 3) quantified integrin subunit expression levels in cell lines of different metastatic potential and assayed the tyrosine phosphorylation states of endogenous PYK-2, following cell adhesion to different ECM substrata; 4) generated a virus expression vector with a tissue-specific promotor that will be used for in vivo animal experiments; and finally 5) begun microarray analysis of gene expression changes accompanying shifts in the levels of PYK-2 and PRNK. The work is ongoing and will continue in my new position at Emory University.

14. SUBJECT TERMS
Prostate Cancer

15. NUMBER OF PAGES
74

16. PRICE CODE

17. SECURITY CLASSIFICATION OF REPORT	18. SECURITY CLASSIFICATION OF THIS PAGE	19. SECURITY CLASSIFICATION OF ABSTRACT	20. LIMITATION OF ABSTRACT
Unclassified	Unclassified	Unclassified	Unlimited

NSN 7540-01-280-5500

Standard Form 298 (Rev. 2-89)
Prescribed by ANSI Std. Z39-18
298-102

Table of Contents

Introduction

In the prostate, cell-matrix adhesion, cell motility and invasive behaviors are regulated by an interplay of signals between the epithelia and surrounding stroma. Changes in the signals, their reception, or the intracellular interpretation of their meaning affects adhesion-based behaviors and can result in cancerous progression in the prostate. The signaling cascades downstream of Integrin extracellular-matrix-binding proteins contain a number of promising therapeutic targets for metastatic prostate cancers. My research focuses on one component of these cascades, phospho-tyrosine kinase PYK-2, whose expression levels and activity I aim to manipulate in cell culture and within tumors in mice. PYK-2 manipulation, in cells of different metastatic potentials, may allow us to push cells forward or backward in cancerous progression, affecting cell proliferation, differentiation, migration and/or apoptosis.

This past year, after building PYK-2 overexpression and dominant-negative constructs, I hoped to express them in LNCaP-derived prostate cancer cells of different metastatic protential and to control construct expression using tetracyclin inducible promoters. Because of technical problems with the inducible promoter system, I have turned now to transient overexpression assays, which are proving fruitful, and in preliminary studies now suggest that PYK-2 has a negative regulatory effect on cell migration and growth. A second accomplishment of this past year was the development of a virus vector containing a PSA (prostate specific antigen) promotor and PYK-2. This virus expression system should prove valuable for both in vitro and in vivo experiments and potentially also clinical trials. If intentional PYK-2 modulation is sufficient to control LNCaP prostate cancer model cell proliferative, migratory or apoptotic behaviors, our laboratory is uniquely equipped to develop the approach into a clinical therapy, by delivering the genes in an adenoviral vector, first to LNCaP tumors in mice, and eventually to men.

My mentor Dr. Leland Chung's laboratory has moved this year from the University of Virginia, significantly delaying my research. This fall, I will become an Assistant Professor with the Molecular Urology and Therapeutics Program (MUT) within Winship Institute at Emory (Atlanta, GA), where one of my research plans is to continue the work outlined in this grant proposal, evaluating PYK-2's value as a therapeutic target for prostate cancer.

Body

      This research project focuses on Proline-rich Tyrosine Kinase (PYK-2), a key component of the signaling cascades downstream of the integrin cell-matrix adhesion molecules. We hypothesize that manipulation of PYK-2 activity and expression in prostate cancer cells will disrupt a link between the extra cellular matrix and the nucleus, allowing the intentional control of cell behaviors such as growth, migration, and apoptosis. During the grant period, I have focused on assessing and changing PYK-2 expression levels in vivo and in the LNCaP prostate cancer progression model of cell lines, and have additionally developed a virus vector that should be useful both in vitro and as a potential therapeutic vehicle. Each area of progress during the grant period is presented below:

1) Characterization of PYK-2 expression patterns in prostate tissues and cell lines

      The non-receptor tyrosine kinase PYK-2 is expressed broadly, but is particularly enriched in prostate tissues, brain, and hematopoetic cells (Avraham et al, 1995; Sasaki et al., 1995; Lev et al., 1995; Berg et al., 1997; Yu et al., 1996). Recently, Stanzione et al. (2001) reported that PYK-2 is expressed *in vivo* in normal epithelia and in benign prostate hyperplasia, as well as in low-grade adenocarcinoma, but is lacking in higher grades of adenocarcinomas. We find PYK-2 expressed in normal prostate endothelia, muscle stroma and basal cells beneath columnar epithelia, but see elevated expression in these locations during Prostate Intra-epithelial Neoplasia (PIN) and in adenocarcinomas (Fig. 1). Among cell lines, PYK-2 is strongly expressed in both LNCaP and C4-2 lines, but is lacking in the aggressive DU145, PC3 and ARCaP prostate cancer lines and expressed only at low levels in PC3M. Together these results support a model in which increased PYK-2 expression might revert cancerous progression, although it is suprising then that the p69 cell line, an immortalized prostate epithelial line commonly used as a normal cell line, also expresses PYK-2 at low levels (Fig. 2). Note that it was necessary to check for antibody cross-reactivity between PYK-2 and FAK (focal adhesion kinase), to confirm specificity for PYK-2 in LNCaP and C4-2 cells (Fig. 3).

5

2) Construction of tetracycline-regulated expression vectors of four PYK-2 variants, including constitutively-active and dominant-negative acting variants

Technical problems have thwarted my plan to manipulate PYK-2 expression levels with a tetracycline-inducible promoter expression system. After successfully building the constructs and going though the time-consuming selection process for stable inducible clones, I repeatedly discovered multiple *uninduced* clones with increased levels of construct proteins, due to "leaky" promoters. Phenotypic differences that I originally believed to be PYK-2 construct-based may also then have only been clonal variations. I've stopped attempting to use these systems and am concentrating instead on transient transfection of a PYK2-GFP (green fluorescent protein) construct and a newly constructed virus vector. See below.

3) Protein localization, cell migration, cell growth, and apoptotic behaviors in cells over-expressing GFP-labeled PYK-2 and dominant-negative PYK-2 (PRNK)

LNCaP and C4-2 cells prostate cancer cells were transiently transfected with green fluorescent protein (GFP)-labeled PYK-2 and dominant-negative PYK-2 (PRNK) and evaluated for protein localization, changes in cell migration, cell growth, and apoptotic behaviors.

Protein Localization: PYK-2 protein localization is known to be cell line dependent; for example, PYK-2 is found concentrated in focal contacts within megakaryocytes (Li et al., 1996), but in a diffuse perinuclear pattern within rat fibroblast and smooth muscle cells (Matsuya et al., 1998, Zheng et al. 1998). PYK-2's localization was not known in the LNCaP model cell lines we are using, partly because of previous problems with cross-reactivity between antibodies against PYK-2 and the similar protein Focal Adhesion Kinase (FAK). The GFP-tagged PYK-2 construct was distributed in a diffuse cytoplasmic pattern in all the LNCaP model cell lines, and had a somewhat higher concentration in the cell-cell borders of the p69 cells. This same pattern was seen in immunofluorescence studies, as well. No elevated PYK-2 localization was visible at structures important for cell migration, such stress fibers or focal adhesions (Fig. 4).

6

Migratory Behaviors: Both PYK-2 and the closely-related Focal Adhesion Kinase (FAK) are components of the Mitogen-Activated Protein Kinase (MAPK) pathway, making them likely regulators of cell motility. Overexpression of FAK has been correlated with *increased* metastatic and invasive behaviors in a variety of cells (Sieg et al., 1999; Gu et al., 1999). In contrast, I find that overexpression of either full-length or PRNK-truncated versions of PYK-2 significantly *reduces* migration of metastatic C4-2 prostate cancer cells (Fig. 5). The change in migratory behavior is correlated with the transfection efficiency, which must be normalized in order to compare individual experiments. I will next check these exciting results using the newly constructed virus vector, in order to infect 100% of the cells. PYK-2 expression levels may also prove to be important for substrate specificity and/or growth factor response. So far these studies have been conducted on Laminin only, but past work on FAK phosphorylation reveals a Laminin-specific (not fibronectin, vitronectin or collagen) response following growth factor stimulation (Edlund et al., see attached); I plan to use the constructs to assess whether PYK-2 levels affect this specific response.

Cell Growth and Apoptosis: Fluorescence Activated Cell Sorting (FACS) confirmed that, like other metastatic cells, neither LNCaP nor C4-2 cells were dependent upon anchorage for cell growth. When cells from either line were detached from the substrate or deprived of serum, neither line displayed marked apoptosis, as assayed with TUNEL staining and FACS. To investigate PYK-2's involvement in cell proliferative and apoptotic decisions, I first followed cell growth responses to transient transfection of PYK-2 and dominant-negative PYK-2 (PRNK), using a 3-(4,5-dimethylthiazol-2-yl)-2,5-diphenyltetrazolium bromide (MTT) assay, and found that expression of either construct *decreased* cell growth relative to controls, with PYK-2 expression resulting in a slightly larger decrease than PRNK (Fig. 6A). Surprisingly, though, when PSA levels from the two transfected cell lines were compared, PYK-2 overexpression lowered PSA, whereas PRNK did not (Fig. 6B). Correlations between cell growth and PSA levels must now be explored further. Given that PYK-2 and PRNK overexpressions affect cell growth and PSA levels, I next used microarray analysis to ask how gene expression changed in

7

transfected cells. These studies were ongoing when the Chung laboratory moved, but following a delay due to the move, I can now prepare array filters again and expect more results shortly.

5) Characterization of integrin subunit expression in prostate cancer cell lines, and assessment of PYK-2 tyrosine phosphorylation, following cell adhesion to different extracellular matrices

While activation of β3-containing integrins has previously been linked to PYK-2 phosphorylation (Duong et al, 1998; Damsky and Werb, 1992; Juliano and Haskill, 1993), and while we have found that somewhat elevated expression patterns of PYK-2 and αvβ3 integrins are coincident, no comprehensive comparison had been made of integrin subunit expression patterns in prostate cell lines, nor had attachment-dependent PYK-2 phosphorylation been verified in our cell lines, or comparisons made using different substrata. We have now used Fluorescence Activated Cell Sorting (FACS) analysis to determine the integrin subunit expression levels in a number of prostate cell lines, including LNCaP and C4-2 (Fig. 7). While very little change in integrin subunit *expression* was noted between the linage related cell lines (LNCaP, C4, C4-2 and C4-2B), integrin subunit *usage* was markedly variable, with cells of different metastatic potential using different heterodimers to attach and spread on the same matrix (Edlund et al., 2001). We have also assayed the tyrosine phosphorylation state of endogenous PYK-2 in LNCaP and C4-2 cells, following cell re-attachment to different extracellular matrices. We found that PYK-2 was phosphorylated in a time-dependent manner, as detected by immunoprecipitation and Western blotting, in both LNCaP and C4-2 cells, following attachment to both laminin and collagen IV. These studies address our second proposed aim of simultaneously assessing both upstream integrin regulation of PYK-2 and downstream PYK-2 regulation of cell behaviors.

6) Construction and use of a new Virus Expression Vector

Because of the "leakiness" of the tetracycline inducible system and the resulting undesired, low level of protein expressed in uninduced cells, I have set out to create an expression system that depends upon adenovirus infection instead. This system will give us the tools to do our experiments on whole cell populations, within a short window of time, thus minimizing phenotypic and genotypic drifting of the cells. Our laboratory has experience in making effective tissue-specific promotors for the delivery of constructs to prostate cancer cells (Fig. 8), and has developed tissue specific promotors (Yeung et al, 2000) that I will use in these PYK-2 vectors.

Research Accomplishments

- Characterization of PYK-2 expression in prostate tissues and cell lines

- Linkage of green fluorescent protein (GFP) to both PYK-2 and dominant-negative PYK-2 (PRNK), transient transfection of LNCaP and C4-2 cells with these constructs, and assay of protein localization and construct effects on cell migration, growth and apoptosis .

- Quantification of integrin subunit expression levels in several prostate cell lines, along with assay of PYK-2 tyrosine phosphorylation states, following cell adhesion to different extracellular matrix substrata.

- Construction of virus expression vector with tissue specific promotor for animal experiments

- Experiments begun to study gene expression changes following shifts in PYK-2 and PRNK levels

Reportable Outcomes

Edlund, M., Bradely, M., Sikes, R.A. and L. Chung. (2001) "c-met Independent Hepatocyte Growth Factor regulation of cell adhesion in prostate cancer cell lines" (To be submitted)

Sikes, R.A., Koeneman, K.S., **Edlund,M.**, Bissonette, E.A., Nicholson, B., Bradley, M.J., Pienta, K.J. amd Chung, L.W.K. (2001) "Cellular interactions in the tropism of prostate cancer to bone" (To be submitted)

Bekir, C., Koeneman, K.S., **Edlund, M.**, Prins, P.G., Zhau, H.E., and L.W.K. Chung. (2001) "Androgen Receptor Mediates the Reduced Tumor Growth, Enhanced Androgen Responsiveness, and Selected Target Gene Transactivation in a Human Prostate Cancer Cell Line" Cancer Research 61(19) 7310-7317

Edlund, M., Miyamoto, T., Sikes, R.A., Ogle, R, Laurie G.W., Farach-Carson, M.C., Otey, C.A., Zhau, H.E., and Chung, L.W.K. (2001) "Integrin expression and utilization by LNCaP prostate cancer cells on laminin substrata" Cell Growth and Differentiation, 12(2) 99-107

Other Papers published during grant period

Edlund, M., Lotano, M. and Otey, C. (2001) "Dynamics of α-actinin in focal adhesions and stress fibers visualzed with α-Actinin-Green Fluorescent Proteins cultured cells. *Cell Motility and Cytoskeleton,* 48(3) 190-200.

Knight, B., Laukaitis, C., Akhtar, N., Hotchin, N., **Edlund, M**. and A.F. Horwitz. (2000) "Visualizing cell migration in situ" *Current Biology* 10, 576-585.

11

References

Avraham, S., London, R., Fu, Y., Ota, S., Hiregowdara, O., Li, J., Jiang, S., Pasztor, J.M., White, R.A. and Groopman, J.E. (1995) Identification and characterization of a novel related adhesion focal tyrosine kinase (RAFTK) from megakaryocytes and brain. *J. Biol. Chem.* 270: 27742-2775.

Berg, N.N. and Ostergaard, H.L. (1997) T cell receptor engagment induces tyrosine phosphorylation of FAK and PYK2 and their association with Lck. *J. of Immunol.* 159: 1753-1757.

Damsky, C.H. and Werb, Z. (1992) Signal transduction by integrin receptors for extracellular matrix: co-operative processing of extracellular information. *Curr. Opin. Cell Biol.* 4: 772-781.

Duong, L. T., Lakkakorpi, P. T., Nakamura, I., Machwate, M., Nagy, R. M. and Rodan, G. A. (1998) PYK2 in osteoclasts is an adhesion kinase, localized in the sealing zone, activated by ligation of alpha(v)beta3 integrin, and phosphorylated by src kinase. J. Clin. Investig. 102:881-892.

Edlund, M., Miyamoto, T., Sikes, R.A., Ogle, R., Laurie, G.W., Farach-Carson, M.C., Otey, C.A., Zhau, H.E. and W.K. Chung (2001) Integrin expression and utilization by LNCaP prostate cancer cells on laminin substrata. *Cell Motility and Cytoskeleton,* 48(3) 190-200.

Gu, J., Tamura, M., Pankov, R., Danen, E.H., Takino, T., Matsumoto, K. and Yamada, K.M. (1999) Shc and FAK differentially regulate cell motility and directionality modulated by PTEN. *J. Cell Biology.* 146(2):389-403.

Li, J., Avraham, H., Rogers, R. A., Raja, S. and Avraham, S. (1996) Characterization of RAFTK, a novel focal adhesion kinase, and its integrin-dependent phosphorylation and activation in megakaryocytes. *Blood.* 88:417-428.

Juliano, R.L. and Haskill, S. (1993) Signal transduction from the extracellular matrix. *J. Cell Biol.* 120: 577-585.

Lev, S., Moreno, H., Martinez, R., Canoll, P., Peles, E., Musacchio, J.M., Plowman, G.O., Rudy, B. and Schlessinger J. (1995) Protein tyrosine kinase PYK2 involved in Ca2+-induced regulation of ion channel and MAP kinase function. *Nature* 376: 737-745.

Matsuya, M., Sasaki, H., Aoto, H., Mitaka, T., Nagura, K., Ohba, T., Ishino, M., Takahashi, S., Suzuki, R. and Sasaki, T. (1998) Cell adhesion kinase beta forms a complex with a new member, Hic-5, of proteins localized at focal adhesions. *J. Biol. Chem.* 273:1003-1014.

Sasaki, H., Nagura, K., Ishino, M., Tobioka, H., Kotani, K. and Sasaki, T. (1995) Cloning and characterization of cell adhesion kinase b, a novel protein-tyrosine kinase of the focal adhesion kinase subfamily. *J. Biol. Chem.* 270: 21206-21219.

Sieg, D.J., Hauck, C.R. and Schlaepfer, D.D. (1999) Required role of focal adhesion kinase (FAK) for integrin-stimulated cell migration. *J. Cell Science.* 112:2677-2691.

Stanzione R., Picascia A., Chieffi P., Imbimbo C., Palmieri A., Mirone V., Staibano S., Franco R., De Rosa G., Schlessinger J., and Tramontano, D. (2001) Variations of proline-rich kinase Pyk2 expression correlate with prostate cancer progression. *Laboratory Invest. 81:51-59.*

Yeung, F., Li, X., Ellett, J., Trapman, J., Kao, C. and Chung. L.W.K. (200) Regions of prostate-specific antigen (PSA) promoter confer androgen-independent expression of PSA in prostate cancer cells. *J.Biol. Chem.* 275:40846-40855.

Yu, H., Li, X., Marchetto, G.S., Dy, R. Hunter, D. Calvo, B., Dawson, T.L., Wilm, M., Anderegg, R.J., Graves, L.M. and Earp, H.S. (1996) Activation of a novel calcium dependent protein-tyrosine kinase. Correlation with c-jun N-terminal kinase but not mitogen-activated protein kinase activation *J. Biol. Chem* 271: 29993-29998.

Zheng, C., Xing, Z., Bian, Z. C., Guo, C., Akbay, A., Warner, L. and Guan, J. L. (1998) Differential regulation of Pyk2 and focal adhesion kinase (FAK). The C-terminal domain of FAK confers response to cell adhesion. *J. Biol. Chem.* 273:2384-2389.

Figure 1. PYK-2 staining in tissue sections of human prostate. (A) In normal tissue, PYK-2 is expressed at low levels in vessel endothelia, basal cells. (B) PYK-2 is also expressed in hypoplasia.

Figure 2. Western blot analyses of PYK-2 and FAK expression in whole cell lysates from LNCaP, C4-2, DU145, PC3, and SV40T prostate cell lines. Note that only LNCaP and C4-2 cell lines express PYK-2.

Figure 3. PYK-2 antibody specificity. FAK and PYK-2 were immunoprecipitated from whole cell lysates, and stained with either FAK or PYK-2-specific antibodies to check for cross-reactivity.

Figure 4. Cytoplasmic localization of PYK-2-GFP in C4-2 cells. No distinct co-localization with focal adhesions or stress fibers is visible.

Figure 5. Cell migration comparisons in matrigel-coated Boyden chambers between mock-transfected and GFP-PYK-2 and GFP-PRNK transiently-transfected C4-2 cells. Invasion was assayed as an increase over time in fluorescence intensity in the lower chamber. Transfection with either PYK-2 or PRNK construct reduced C4-2 migration.

Figure 6. (A) Growth inhibition of C4-2 cells following expression of either full-length PYK-2 or truncated PYK-2 (PRNK) constructs. (B) PSA levels upon PYK-2 and PRNK expression.

Figure 7. Fluorescence Activated Cell Sorting (FACS) characterization of integrin subunit expression in prostate cell lines p69, LNCaP, C4-2, C4-2B, and ARCaP. Values are shown as the average of two independent experiments, with the value range in parentheses.

Figure 8. Virus expression vectors developed for use in further PYK-2 and PRNK transfections and assessment of PYK-2's roles in prostate cancer progression.
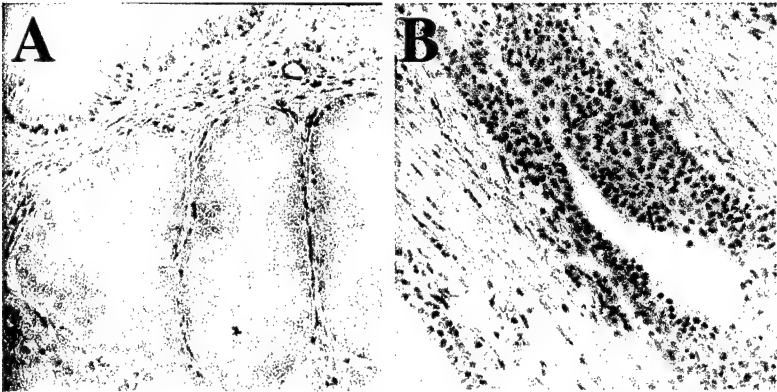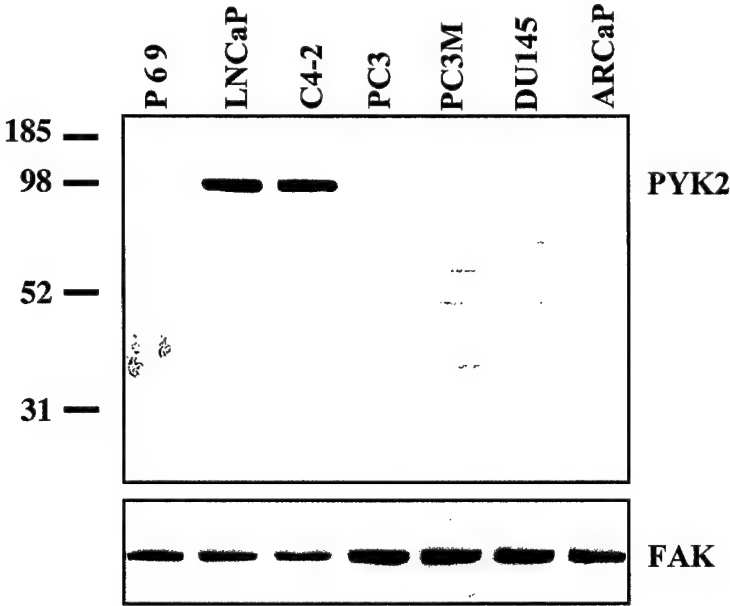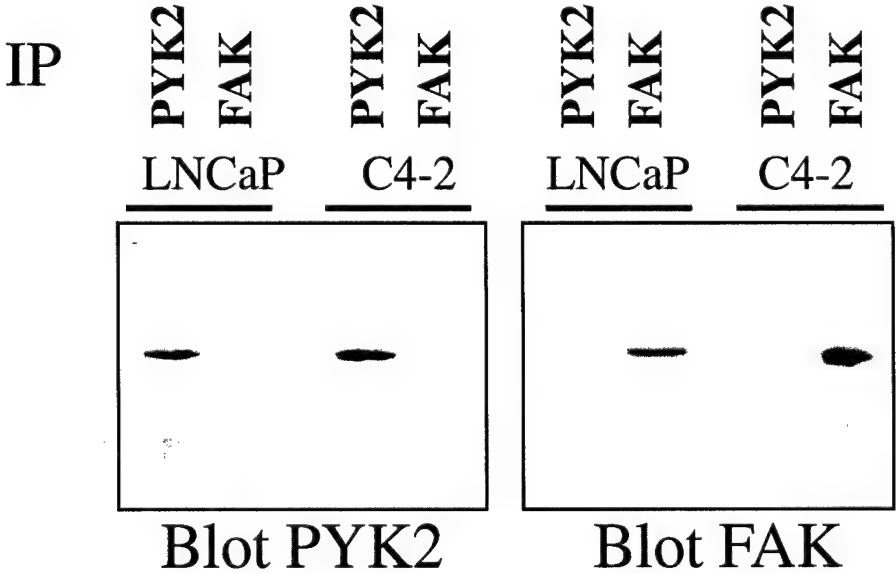
Figure 1.

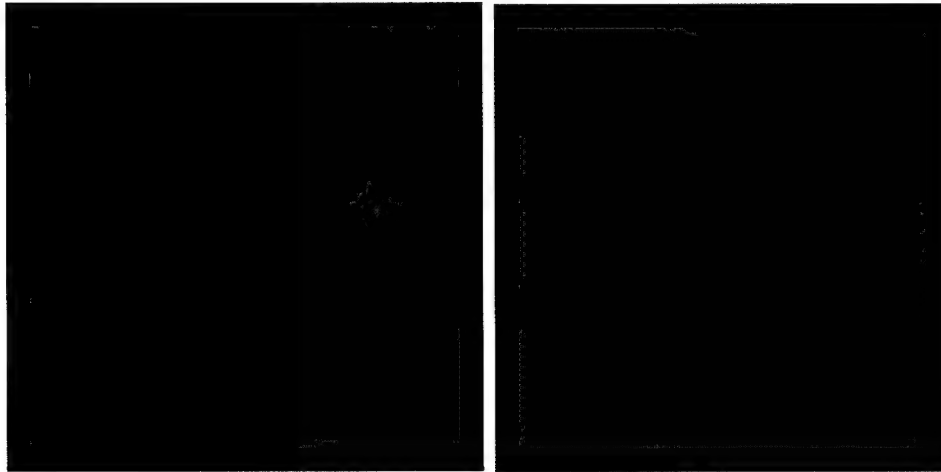Figure 2.

Figure 3.

PYK2-GFP in C4-2 cells

Figure 4.
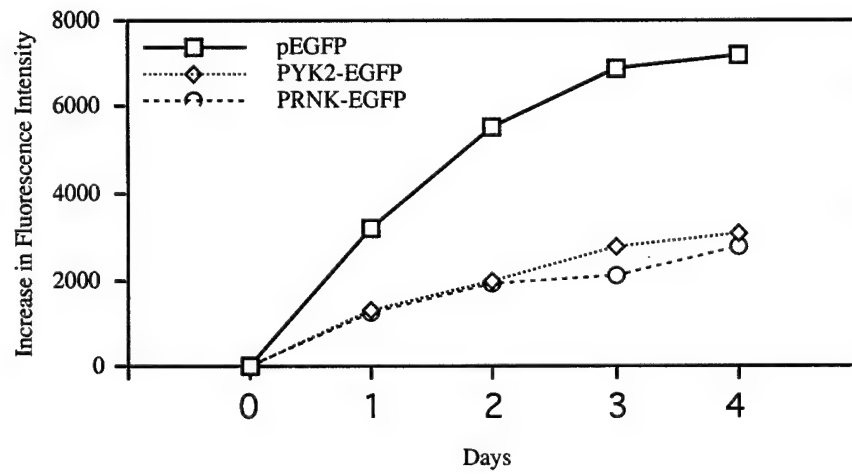
Figure 5.

Figure 6A.

Figure 6B.

LNCaP

PSA level ng/ml vs Days after transfection
- EGFP Control
- PYK2-EGFP
- PRNK-EGFP

C4-2

PSA level ng/ml vs Days after transfection
- EGFP Control
- PYK2-EGFP
- PRNK-EGFP
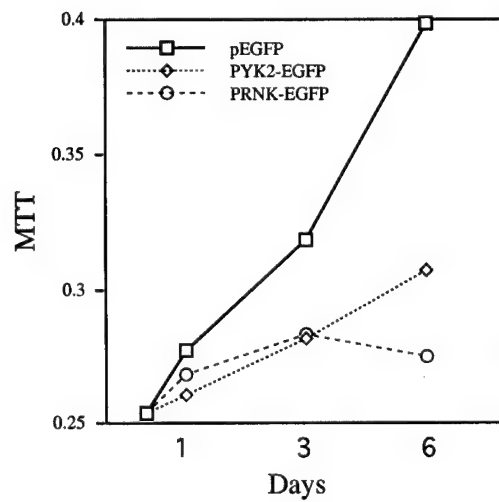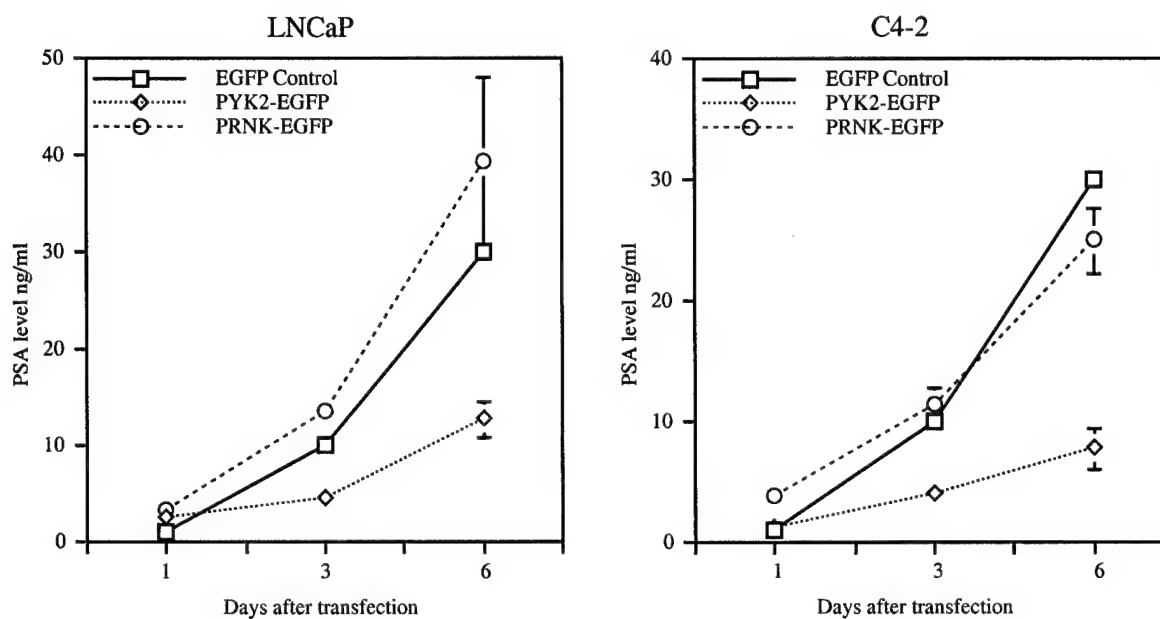
Figure 7.

Expression of Integrins by FACS Analysis

	P69	LNCaP	C4	C4-2	C4-2B	ARCaP
α1	3.1 (0.6)	1.7 (1.0)	1.2 (0.4)	1.8 (0.2)	1.1 (0.2)	28.2 (0.4)
α2	183.6 (21.1)	7.7(1.2)	9.4 (0.4)	13.7 (0.4)	13.0 (3.2)	281.2 (44.4)
α3	166.9 (5.6)	4.4 (0.6)	4.6 (3.2)	3.4 (1.2)	3.2 (0.0)	49.5 (8.2)
α4	25.2 (7.6)	2.8 (0.0)	3.6 (0.7)	2.1 (0.2)	2.5 (1.8)	13.9 (0.6)
α5	20.6 (6.0)	6.2 (0.4)	12.0 (2.4)	6.4 (0.4)	3.2 (0.0)	26.8 (2.8)
α6	16.0 (4.4)	9.8 (0.4)	11.6 (2.2)	10.8 (0.8)	9.5 (0.2)	27.2 (0.6)
αv	32.4 (6.4)	15.8 (0.8)	15.6 (0.4)	14.4 (1.4)	12.8 (0.8)	22.6 (1.2)
αIIb	1.2 (0.2)	1.3 (0.6)	1.2 (0.8)	1.4 (0.4)	1.1 (0.6)	1.1 (0.0)
β1	39.8 (2.4)	17.2 (3.2)	17.7 (4.8)	15.5 (2.8)	13.6 (6.4)	97.2(10.0)
β2	1.0 (0.0)	0.8 (0.4)	0.8 (0.0)	0.8 (0.0)	1.4 (0.6)	1.3 (0.2)
β3	11.2 (0.4)	2.4 (0.8)	3.8 (0.4)	2.6 (0.4)	1.5 (0.0)	21.0 (0.4)
β4	19.0 (3.2)	1.7 (0.6)	2.6 (0.0)	1.3 (0.2)	1.2 (0.8)	48.8 (4.8)
β5	2.3 (0.2)	2.6 (0.2)	6.6 (0.5)	7.4 (2.7)	8.6 (3.4)	2.8 (0.3)
β6	13.0 (1.6)	1.2 (0.4)	1.0 (0.0)	1.2 (0.4)	0.9 (0.0)	1.6 (0.8)
αvβ3		2.1 (0.4)		1.6 (0.4)		6.9 (0.4)
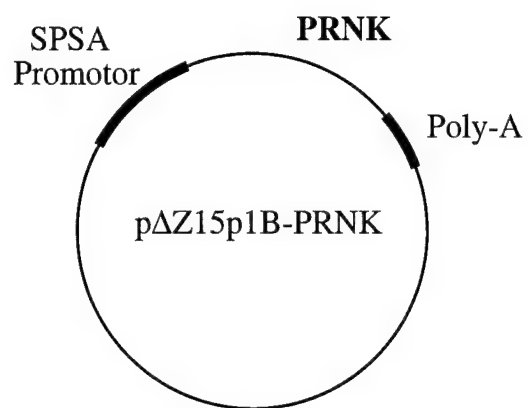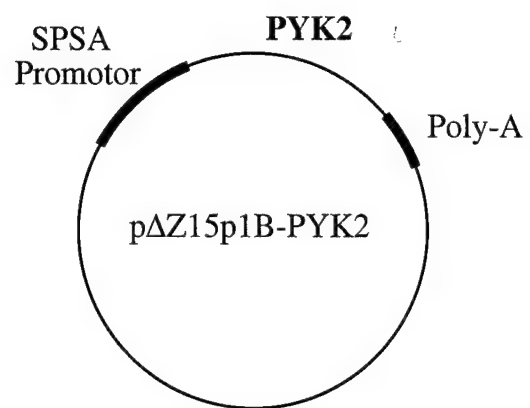
Figure 8.

Integrin Expression and Usage by Prostate Cancer Cell Lines on Laminin Substrata[1]

Magnus Edlund,[2] Tadayuki Miyamoto,[2]
Robert A. Sikes, Roy Ogle, Gordon W. Laurie,
Mary C. Farach-Carson, Carol A. Otey,
Haiyen E. Zhau, and Leland W. K. Chung[3]

Departments of Urology [M. E., T. M., R. A. S., H. E. Z., L. W. K. C.] and
Cell Biology [R. O., G. W. L., L. W. K. C.], University of Virginia Health
System, Charlottesville, Virginia 22908; Cell and Molecular Physiology,
University of North Carolina at Chapel Hill, Chapel Hill, North Carolina
27599-7545 [C. A. O.]; and Department of Biological Sciences,
University of Delaware, Newark, Delaware 19716 [M. C. F-C.]

Abstract

**During prostate cancer progression, invasive glandular
epithelial cells move out of the ductal-acinar
architecture and through the surrounding basement
membrane. Extracellular matrix proteins and
associated soluble factors in the basal lamina and
underlying stroma are known to be important
regulators of prostate cell behaviors in both normal
and malignant tissues. In this study, we assessed cell
interactions with extracellular matrix and stromal
factors during disease progression by characterizing
integrin usage and expression in a series of parental
and lineage-derived LNCaP human prostate cancer cell
lines. Although few shifts in integrin expression were
found to accompany disease progression, integrin
heterodimer usage did change significantly. The more
metastatic sublines were distinct in their use of $\alpha_v\beta_3$
and, when compared with parental LNCaP cells,
showed a shift in α_6 heterodimerization, a subunit
critical not only for interaction with prostate basal
lamina but also for interaction with the bone matrix, a
favored site of prostate cancer metastases.**

Introduction

Cancerous prostate cells are regulated in their differentiation,
growth, and metastasis by interactions with the surrounding
cells and ECMs[4] (1–3). Cell behavior decisions, such as
decreasing cell-cell and cell-substrate attachment, and in-
creasing cell motility are accompanied by changes in the
expression and/or usage of adhesion receptors, including
those of the integrin family (2, 3). Past studies in prostate
cancer have focused on quantitation as well as cell surface
distribution of integrins (4–8) and on correlating changes in
integrin expression with invasive cell behavior (9, 10). The
expression level studies have taken two forms: (*a*) cell lines
with different metastatic potential have been found to ex-
press different levels and subtypes of integrins; and (*b*) within
a given cell line, metastatic potential has been experimentally
correlated with increases or decreases in levels of integrin
expression (9, 11, 12).

Integrin molecular structure, heterodimerization, and intra-
and extracellular interactions of integrins with cytoplasmic
regulatory proteins and ECM ligands provide tremendous
potential for variation among cell types, well beyond that
available through quantitative variation in integrin expression
level alone. Integrins are themselves heterodimeric mole-
cules, consisting of one α and one β subunit, with at least 20
different combinations already described, many of which
differ in their extra- and intracellular binding specificities (13,
14). "Inside-out" regulation of integrin heterodimer activity
and subunit partner choices are thought to depend on
unique cytoplasmic regulatory protein repertoires, which dif-
fer among host cell types (Refs. 15–17 and Ref. 18 and
references within). "Outside-in" regulation by integrins, in
response to extracellular cues, has also been well studied
and has revealed shifts in integrin gene expression as well as
changing integrin associations with numerous signaling mol-
ecules, including protein tyrosine kinases (focal adhesion
kinase and pp60src), serine kinases (protein kinase C, extra-
cellular signal-regulated kinase, c-Jun-NH$_2$-terminal kinase,
and integrin-linked kinase), and lipid intermediates (phos-
phatidylinositol 3′-kinase and phosphatidylinositol 4,5-ki-
nase; Refs. 14 and 19–21 and the references within). Hence,
integrin activity within a given cell is tightly coordinated with
its cell cycle, gene expression profiles, differentiation, and
cell survival (13). The stroma is a source of key extracellular
cues (including soluble growth factors and insoluble matrix
proteins) known to modulate integrin-dependent cell func-
tions (22, 23). Although a number of integrin variations during
prostate cancer cell progression have been described (5–12),
neither modulation of these variations by external factors nor
integrin heterodimer usage regulation is well understood.

The LNCaP lineage cell model of prostate cancer progres-
sion (24–26) has given us an opportunity to follow coordi-
nated changes in integrin expression, usage, and cell behav-
ior of prostate cancer cells when exposed to different ECM
substrata and stromally secreted soluble factors. LNCaP and
LNCaP-derived cell lines are unique in that they vary in
metastatic potential but share a common genetic back-
ground. Previous phenotypic (26) and genotypic (27) char-
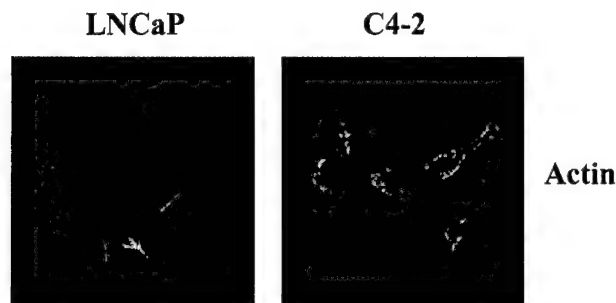
LNCaP   **C4-2**

Actin

Fig. 1. Actin staining in LNCaP and C4-2 cell lines. Both LNCaP and C4-2 cells show diffuse actin staining and small actin fibers when grown on laminin substrata labeled with phalloidin.

acterizations of these cell lines have revealed their remarkable resemblance to progressing clinical human prostate cancer. We focus here on characterizing interactions between these cancerous prostate cells and their ECM microenvironments, particularly on the ability of cell lines of different metastatic potential to attach, spread, and migrate on laminin, a key protein in both the basement membrane surrounding the acini and in tumors themselves (28). We also examine cell line behaviors on several other matrix components found in bone, a favorite destination for prostate cancer cells following a metastatic cascade (Ref. 29 and the references within). Human prostate tumors disseminated to the bone have been shown to have altered integrin expression, particularly laminin-binding integrin expression, when compared with hyperplastic, benign tumors (11, 12, 30, 31). One integrin heterodimer thought to bind laminin along with VN is $\alpha_v\beta_3$, an integrin that is not expressed in normal prostate tissue but is up-regulated in prostatic adenocarcinoma (11, 32). Likewise, in primary prostate carcinomas, shifts in α_6 integrin subunit expression (and heterodimerization with its β subunit partner) were observed during prostate cancer progression (8). In other tumor cell types, the laminin-binding integrins $\alpha_6\beta_4$ and $\alpha_6\beta_1$ have also been linked to acquisition of invasive behaviors (6, 12).

Results
LNCaP Parental and Lineaged Cell Lines Attach to Laminin Using Different Integrin Subunits.
Nonmetastatic LNCaP human prostate cancer epithelial cells and their derivative metastatic sublines (C4, C4-2, and C4-2B) readily attached to a common laminin substrate, and all displayed focal contacts and some poorly developed stress fibers, as seen by staining for filamentous actin. The poor development of stress fibers is characteristic of all LNCaP lineage-related cell lines and is not substrate dependent. Representative actin staining in attached LNCaP and C4-2 cells is shown in Fig. 1; C4 and C4-2B cells stained similarly (data not shown).

To identify the integrins used for attachment by the different cell types, parental LNCaP and its derivative C4, C4-2, and C4-2B cell lines were selected (26), and specific, function-blocking integrin antibodies were added to the attachment assays. Although the antibody staining suggested the formation of focal adhesion structures in all cell lines (data

not shown), the cells responded differently to the function-blocking antibodies (Fig. 2). Attachment of parental LNCaP cells was best blocked by antibodies against subunits α_6 and β_4, whereas antibodies against these subunits did not effectively block attachment of C4, C4-2, or C4-2B cells, whose attachments were best blocked by antibodies against the intact $\alpha_v\beta_3$ integrin and the subunits α_3 and β_1. Attachments of all four cell lines were also somewhat reduced by antibodies against the subunit α_2.

The Differences in LNCaP and C4-2 Cell Attachment Are Not Likely to Be Due to Differential Expression of Integrin Subunits.
FACS analyses were used to determine integrin subunit (α_2, α_3, α_v, β_1, β_3, and β_4) expression levels in LNCaP and C4-2 cell lines (Table 1). Characterization of potential laminin-binding integrin levels by flow cytometry revealed only one difference in expression level (*i.e.*, the α_2 subunit) among the four cell types. Although the expression of the integrin α_2 subunit in C4-2 cells was approximately double that in LNCaP cells, all other integrin receptors were found to remain fairly constant in expression level across all cell lines (Table 1; including C4 and C4-2B; data not shown).

Cell surface expression data were verified by immunoprecipitation of integrin subunits α_3, α_6, $\alpha_v\beta_3$, and β_1 from biotinylated cells of different cell lines (Fig. 3). Similar levels of the α_3 and β_1 subunit were precipitated in all cell lines. The α_3 subunit dimerizes most readily with the β_1 subunit, as seen by immunoprecipitation with either α_3-specific or β_1-specific antibodies (Fig. 3A). Although immunoprecipitation with an α_6 antibody coprecipitated β_1 and β_4 subunits from both LNCaP and C4 cells (Fig. 3B), the $\alpha_6\beta_1$ heterodimer is not likely to be used for laminin attachment in LNCaP cells because very little inhibition of cell attachment is seen by the β_1 antibody in LNCaP competition experiments (Fig. 2). In comparison with LNCaP, very little β_4 subunit appears to be used for laminin attachment in the C4-2 and C4-2B sublines; the α_6 antibody did not immunoprecipitate as much of the β_4 subunit from the latter two cell lines (Fig. 3B), and a function-blocking antibody against β_4 did not inhibit their attachment to a laminin substrate (Fig. 2), as it does for LNCaP. Ratio comparisons, using band intensities on Western blots of α_6-immunoprecipitated β_1 and β_4, reveal a 1:1 ratio of β_1:β_4 in LNCaP cells but show a ratio of 1:0.8 in C4 and 1:0.2 in C4-2 and C4-2B cells.

Although FACS analyses detected both α_v and β_3 subunits in all cell lines, at equivalent surface expression levels, immunoprecipitation with antibody to the $\alpha_v\beta_3$ heterodimer revealed nearly undetectable levels of $\alpha_v\beta_3$ in LNCaP cells while readily detecting the heterodimer in all three derived sublines (Fig. 3C). Use of the $\alpha_v\beta_3$ heterodimer does appear to be important for laminin attachment in the three metastatic sublines (but not LNCaP cells) because function-blocking antibody was able to inhibit cell attachment in the sublines (Fig. 2).

The $\alpha_v\beta_3$ Subunit Is Necessary for C4-2, but not LNCaP, Cell Attachment and Migration.
Because prostate cancer cells metastasize preferentially to bone, we were particularly interested in the integrin heterodimers known to interact with VN and OPN, two noncollagenous bone matrix proteins. The integrin $\alpha_v\beta_3$ was chosen for attachment and
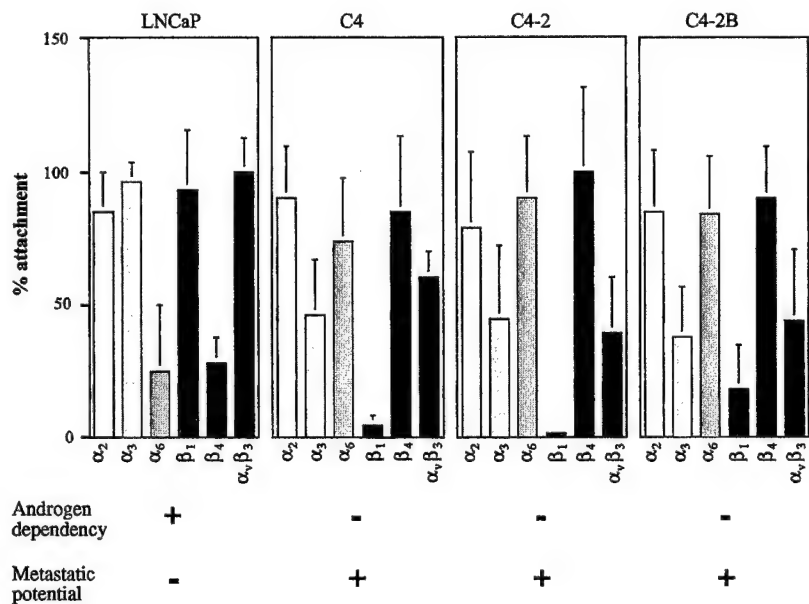
Fig. 2. Inhibition of cell attachment to a laminin substrate using integrin subunit-specific antibodies. LNCaP and the derived sublines C4, C4-2, and C4-2B were preincubated with function-blocking antibodies as indicated. Experimental attachment is shown as a percentage of control, untreated cell attachment, and results are presented as the mean of representative triplicate experiments, with SDs shown as *error bars*.

Table 1   Expression of integrins by FACS analysis

Integrin expression in LNCaP and its more metastatic, derived C4-2 cell line. Values for integrin expression are presented as the mean of two individual duplicate experiments, with the range given in parentheses. An isotype nonspecific antibody was used for control. All experimental fluorescence values are reported as the ratio of the control and specific fluorescence values. Relative values of integrin expression can only be compared for the same antibody on different cells due to differences of antibody affinities for their ligands.

	LNCaP	C4-2
α_2	7.7 (2.6)	13.7 (0.4)
α_3	4.4 (0.6)	3.4 (1.2)
α_6	9.8 (0.4)	10.8 (0.8)
α_v	15.8 (0.8)	14.4 (1.4)
β_1	17.2 (3.2)	15.5 (2.8)
β_3	2.4 (0.8)	2.6 (0.4)
β_4	1.7 (0.6)	1.3 (0.2)

Fig. 3. Immunoprecipitation of biotinylated cell surface integrin isotypes using α_3 and β_1 (*A*), α_6 (*B*), and $\alpha_v\beta_3$ (*C*). Retrieved complexes from each LNCaP, C4, C4-2, or C4-2B cell line were separated by PAGE under reducing conditions, blotted, and visualized with peroxidase-conjugated streptavidin.

migration assays because it is known to interact not only with these two bone matrix proteins but also with laminin (33). LNCaP and C4-2 cells adhered to all three substrata, but only C4-2 attachment could be inhibited with increasing concentrations of antibodies against $\alpha_v\beta_3$ integrin (Fig. 4). At high antibody concentrations of 10 μg/ml, attachments of the metastatic C4-2 cells to all three substrata were reduced by approximately 60%, but no attachment effect was seen for the nonmetastatic LNCaP cells. However, LNCaP attachment could be decreased by using a $\alpha_v\beta_5$ function-blocking antibody (data not shown). The role of the $\alpha_v\beta_3$ heterodimer in cell migration was evaluated using modified Boyden chambers, and the haptotactic responses of each cell line were quantified on laminin, VN, and OPN. Fig. 5 shows the cell migratory behaviors of C4-2 cells on these three bone matrix proteins and that C4-2 cell migration could be inhibited by an $\alpha_v\beta_3$ isotype-specific integrin antibody. LNCaP cells migrated at very low levels on both laminin and VN but did not migrate at all on OPN (data not shown).
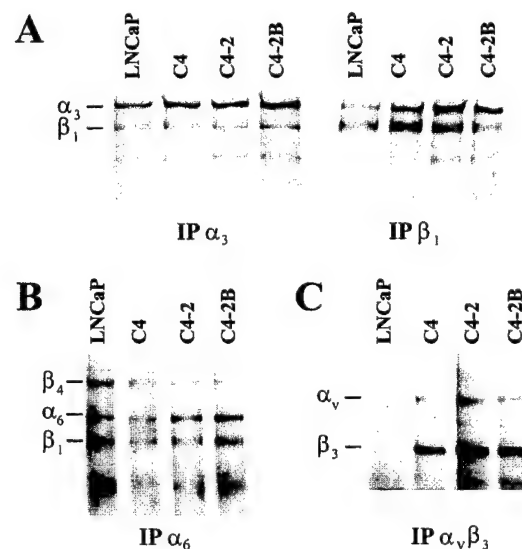
Soluble Stromal Factors Induce C4-2, but not LNCaP, Cells to Attach to Laminin. To begin identifying possible regulators of integrin subunit usage and cell behavior in LNCaP and C4-2 cell lines, we tested the effect of stromal factors on cell line interactions with laminin substrata. Cells were treated with conditioned media from primary cultures of the transition or peripheral zone stromal cells of the prostate gland from four different patients with prostatic adenocarcinoma and allowed to adhere for 90 min. Cell spreading was quantified as indicated in "Materials and Methods." Fig. 6A shows the differential effects of this soluble paracrine factor on the spread of LNCaP and C4-2 cells. Although all condi-
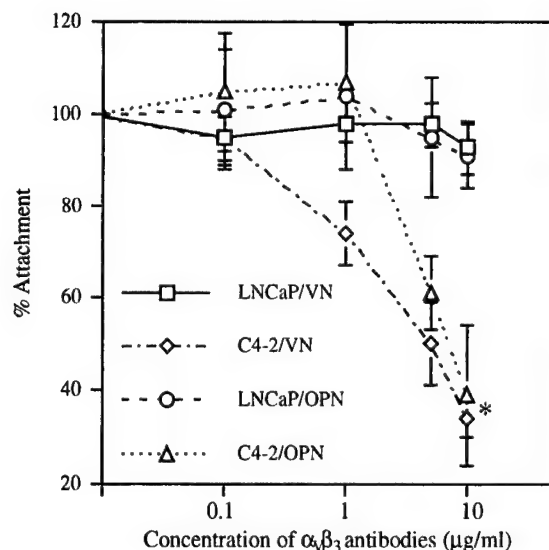
Fig. 4. Antibody-mediated attachment inhibition of LNCaP and C4-2 cells on VN or OPN substrata. Inhibition of attachment is shown with increasing $\alpha_v\beta_3$ antibody concentration expressed as a percentage of control, untreated cell attachment. Values are the mean of two experiments ($n = 6$), and *error bars* represent SDs. Statistically significant differences from the control were at $P < 0.001$ (*).
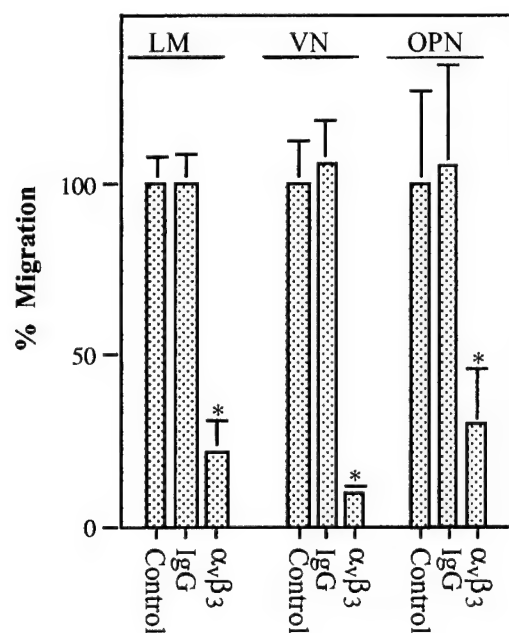

Fig. 5. Migration of C4-2 cells on laminin, VN, or OPN substrata in the presence and absence of 10 μg/ml control or $\alpha_v\beta_3$ function-blocking integrin antibody. Boyden chambers were used for haptotactic assays, and values shown are the average of two experiments ($n = 6$). *Error bars* represent SDs. Statistically significant differences between $\alpha_v\beta_3$ and the control were at $P < 0.001$ (*).

tioned media caused C4-2 cells to spread more rapidly on laminin, none had any noticeable effect on the spreading of LNCaP cells. No increase in spreading was seen for either cell line when treated with conditioned media from mouse fibroblastic cells (Sw3T3 cells; data not shown).
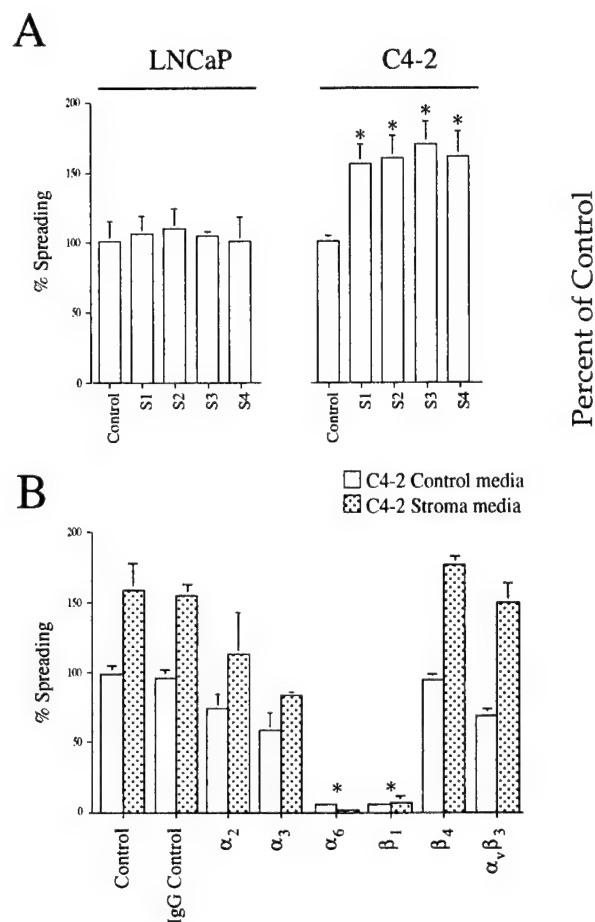

Fig. 6. LNCaP and C4-2 cell attachment to laminin substrata after treatment with stromal cell-conditioned media and/or integrin isotype-specific antibodies. *A,* LNCaP and C4-2 cell attachment responses to conditioned media from four primary prostate stromal cell cultures (three different patients). All percentage attachment values are normalized to the behavior of control, LNCaP, and C4-2 cells that were not treated with conditioned media (after 90 min, 25% of C4-2 untreated control cells had attached, compared with only 6% of LNCaP untreated control cells). *B,* comparison of C4-2 cell attachment percentages after treatment with stromal cell-conditioned media in the presence or absence of function-blocking, integrin isotype-specific antibodies. All experiments were repeated six times. Statistically significant differences between treated and untreated cells were at $P < 0.001$ (*).

The effects of conditioned media could be reversed using integrin isotype-specific, function-blocking antibodies. Fig. 6B shows that function-blocking antibodies to both α_6 and β_1 inhibit cell spreading in both control and stromal cell-conditioned media-treated cells. Function-blocking antibodies against the α_2, α_3, and $\alpha_v\beta_3$ integrins also were able to block 20–50% of the increase in cell spreading induced by conditioned media. Quantification of integrin cell surface expression by FACS analyses (Fig. 7) did not reveal any change in receptor availability between control and stromal cell-conditioned media-treated cells, thus the observed variation in cell response to external regulation is unlikely to be based on changing integrin profiles but instead appears to be based on the improved efficiency of C4-2 cells in use of specific integrin isotypes for cell spreading in the presence of prostate stromal cell-conditioned media.

Fig. 7. FACS analysis of cells treated with stromal cell-conditioned media. Surface expression of integrin subtypes after 90 min of treatment with stromal cell-conditioned media is shown. No change in the integrin surface expression is evident.
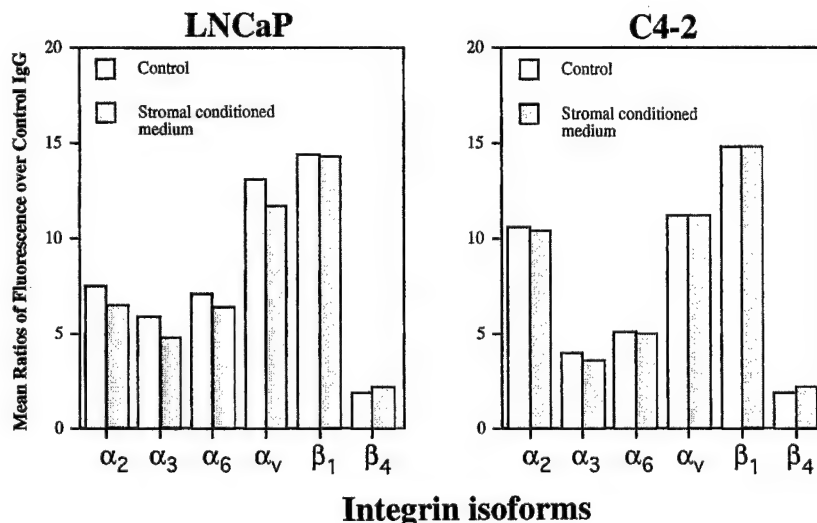
Table 2 Comparison of previously reported integrin usage during prostate cancer progression and the usage found in the LNCaP progression model.

Integrin heterodimer	LNCaP	C4-2	Normal to carcinoma (Ref. no.)
$\alpha_3\beta_1$	+	++	Stable (8, 34)
$\alpha_6\beta_1$	+	++	Stable (5, 6, 8, 34)
$\alpha_6\beta_4$	++	−	Decreases (5, 7, 33)
$\alpha_v\beta_3$	−	+	Increases (11)

Discussion

During prostate cancer progression, changes occur not only in the microenvironments of cells but in the cells' reception and interpretation of cues from these environments. We have focused here on shifts in integrin receptor expression and usage accompanying cancerous progression in the prostate and occurring in response to cues, such as stromally secreted factors. Although we did find expression levels of the integrin subunit α_2 to be elevated in metastatic cell lines, overall, the usage of integrin subunits varied more strikingly than did expression level between cell lines and varied in response to exposure to stromal factors. The integrin usage we detected in the LNCaP model system correlated well with previously published immunohistochemical staining for integrin expression in patient specimens (Table 2; Refs. 5–8, 33, and 34) and added to a number of past *in vitro* studies showing differences in integrin heterodimer expression among cultured normal, neoplastic, and prostate carcinoma cells (10, 34–37). Our results may also help clarify previous studies of integrin expression in various epithelial carcinomas, whose results have conflicted with one another, and may have implications in prostate cancer cell homing to the skeleton, along with preferential survival and proliferation in the bone microenvironment.

Integrin subunit partner choice repeatedly appeared to affect cell migratory and adhesive behaviors in the absence of shifts in subunit expression levels. For example, the partner choice of the integrin α_6 subunit varied between cell lines, whereas the integrin β_1 and β_4 subunit expression levels

remained constant among lines of very different invasive behaviors. LNCaP cells attached to laminin primarily with $\alpha_6\beta_4$, whereas cells in the more invasive C4-2 subline attached with $\alpha_3\beta_1$ and $\alpha_v\beta_3$ (Figs. 2 and 3). This shift in α_6 usage fits with previous studies, in which $\alpha_6\beta_1$ and $\alpha_6\beta_4$ were both found in normal prostate cells, but β_4 subunit expression was lost in carcinomas (5, 6, 8). Because the α_6 integrin subunit preferentially associates with β_4, it is believed that a reduction in β_4 subunit expression results in a relative increase in the formation of the $\alpha_6\beta_1$ heterodimer (38). The varied pattern of integrin heterodimerization in these cell lines could be due in part to differential expression of α_6 subunit isoforms. The integrin α_6 subunit exists as two isoforms, α_{6A} and α_{6B} (34, 38–42), both of which are expressed in LNCaP cells (34). Although we do not yet know the specific α_6 isoform expressed by C4-2 cells, overexpression of the α_{6A} isoform is known to increase $\alpha_6\beta_1$ heterodimerization as well as overall cell motility, tumorigenicity, and invasion (12).

$\alpha_6\beta_4$ use declined in C4-2 cells, in conjunction with an increased use of $\alpha_6\beta_1$, $\alpha_v\beta_3$, and $\alpha_3\beta_1$ (Fig. 2). Unlike $\alpha_6\beta_4$, which is associated with stable, hemidesmosomal cell attachment sites and appears to restrict cell migration, $\alpha_6\beta_1$ and $\alpha_3\beta_1$ are both involved in the formation of dynamic focal contacts important for cell locomotion (12). Prostate cell lines able to form invasive tumors in immunocompromised mice have previously been shown to have increased expression of the $\alpha_6\beta_1$ heterodimer (10, 12, 36, 43), and antibodies against $\alpha_6\beta_1$ are able to inhibit invasion. Like Vafa *et al.* (36), we too found the $\alpha_6\beta_1$ heterodimer to be more involved in cell spreading than static cell attachment (Figs. 2 and 6), but the role of this heterodimer in metastatic cell interpretation of environmental cues, such as matrix and secreted factors, requires further study. The $\alpha_3\beta_1$ integrin is likely to have both direct and indirect effects on cell motility because of its bidirectional interactions with the matrix. The ability of $\alpha_3\beta_1$ to alter laminin chains and overall basement membrane architecture (44, 45) is particularly suggestive, given that proteolytic cleavage of laminin can drive cells from static adhesion to active migration (46, 47). It is interesting to note in this

context that oncogene-transformed rat prostate cells express elevated levels of both laminin type I and the $\alpha_6\beta_1$ integrin (36, 43).

An additional integrin heterodimer implicated in increased metastatic potential and tumorigenicity is $\alpha_v\beta_3$ (48–50). Although not frequently found in epithelial cells, $\alpha_v\beta_3$ is common to a number of bone-receding metastases, including prostate and breast carcinomas (10, 11, 51). In the LNCaP model system, $\alpha_v\beta_3$ was similar to $\alpha_3\beta_1$ in that its individual subunits were expressed at all stages of cancerous progression (that is, in all cell lines), but the assembled, functional heterodimers were only detectable in the more metastatic cell lines C4, C4-2, and C4-2B (Table 1; Fig. 3). Although such differences in integrin usage have been noted before between very different cell lines with different metastatic potentials, this is the first study we know of that reveals such shifts in integrin usage between cells with common genetic backgrounds but different *in vivo* metastatic potentials.

Two possible consequences of $\alpha_v\beta_3$ heterodimer usage in the metastatic LNCaP sublines are (*a*) preferential relocation to the bone and (*b*) increased cell survival/suppressed cell death. Integrins are likely to be involved in both the establishment of prostate cell anchorage to the bone endothelium and its surrounding matrix and the transmission of multiple cues from the cells' microenvironments supporting cell survival and proliferation. Not only do C4-2 cells, cells known to preferentially relocate to bone (26), increase their use of the $\alpha_v\beta_3$, but we show here that they use this integrin to migrate on OPN, a key component of bone matrix. $\alpha_v\beta_3$ has also previously been shown to support migration on VN, another dominant component of bone matrix (52, 53). Regardless of the role of $\alpha_v\beta_3$ in binding metastatic cells to the bone matrix, this integrin heterodimer is a good candidate regulator of cell survival in the absence of cell adhesion. Although loss of appropriate adhesion is normally a cue for apoptosis, human breast cancer cells are able to use $\alpha_v\beta_3$ to inhibit p53 activity and suppress the bax death pathway (54). Likewise, $\alpha_v\beta_3$ has been shown to regulate cell proliferation in prostate epithelia (55).

Integrin regulation of prostate epithelial proliferation is likely to involve interactions between integrins and growth factor receptors. Such receptors are used by cells to interpret positive and negative growth factor and cytokine signals from surrounding stromal cells (Refs. 1 and 56 and the references within), and they do so through common signaling cascade components (for example the small GTPases), which are also important for integrin signaling and activation. There is evidence that the two types of surface proteins may associate directly and preferentially with one another (55). In the context of changing integrin usage [such as that observed between LNCaP and C4-2 cells or reported previously *in vivo* (see Table 2)], preferential associations between the growth factor receptors and the changing integrin heterodimers could have serious consequences for the cells' responses to environmental cues. Indeed, Fig. 6 shows that C4-2 and LNCaP cells do respond differently to soluble factors in media from prostate stromal cells, with only C4-2 cells showing increased spreading on laminin substrates after stromal media treatment.

We investigated the roles of $\alpha_6\beta_1$ and $\alpha_v\beta_3$ integrins in response to stromal cues by adding function-blocking antibodies against these integrins to C4-2 cell cultures before and after treatment with prostate stromal cell-derived conditioned media. The dramatic increase in C4-2 laminin spreading after treatment with such conditioned media was relatively unaffected by $\alpha_v\beta_3$ function-blocking antibodies, whereas antibodies against either α_6 or β_1 completely obliterated spreading on laminin both before and after stromal cell-conditioned media treatment (Fig. 7), a result in agreement with the work of Vafa *et al.* (36) on c-erb B2/neu-transformed rat prostate epithelial cells. The identities of the responsible soluble factors (cytokines, growth factors, or others) behind the $\alpha_6\beta_1$-specific response remain to be determined, although one candidate growth factor, which is found in the conditioned media, is the HGF/SF.[5] Although purified HGF/SF has the ability to stimulate prostate cancer cell spreading and migration when placed on ECM substrata, HGF/SF is only one of many such factors secreted by the prostate stromal cells. Whether growth factor receptors on the C4-2 cells interact directly with nearby $\alpha_6\beta_1$ integrins after stimulation by a stromally secreted growth factor is also unknown. Stimulated receptors could also signal the integrins indirectly through intracellular cofactors, such as focal adhesion kinase (62).

In summary, use of a lineage-derived LNCaP cancer cell progression model has allowed us to compare the integrin expression levels, heterodimer usage, and cell behaviors in cells sharing a common genetic background but differing in their metastatic potentials on different matrices and in the presence or absence of stromal factors. We have found that although integrin expression levels do not change markedly among the cell lines (with the exception of an increase in collagen binding α_2 expression), integrin heterodimer usage does change. In particular, the androgen-independent and invasive LNCaP derivative C4-2 subline shows marked differences in its use of $\alpha_3\beta_1$, $\alpha_6\beta_1$, $\alpha_6\beta_4$, and $\alpha_v\beta_3$ when compared with that of the androgen-dependent and noninvasive parental LNCaP cells. Although all cells attached to laminin, VN, and OPN matrices, only the more invasive and metastatic C4-2 cells were able to migrate on OPN. C4-2 cells were also unique because of their response to prostate stromal cell-derived factors. The striking increase in the spreading of C4-2 cells on laminin after treatment with stromal factors could be completely obliterated by the addition of function-blocking antibodies against α_6 or β_1, but not against α_2, α_3, β_4, or $\alpha_v\beta_3$. Because C4-2 cells were found to increase usage of $\alpha_6\beta_1$ but decrease usage of the $\alpha_6\beta_4$ heterodimer, additional studies are called for to characterize this shift in heterodimer usage and its direct and/or indirect effects on cell behavioral and survival responses to matrix and stromal environmental cues. Such future studies promise to have profound implications for control of metastatic human

---

[5] M. Edlund, T. Miyamoto, R. A. Sikes, R. Ogle, G. W. Laurie, M. C. Farach-Carson, C. A. Otey, H. E. Zhau, and L. W. K. Chung. Regulation of cell adhesion in prostate cancer cell lines by hepatocyte growth factor, manuscript in preparation.

prostate cancer cell dissemination, proliferation, and survival in the skeleton.

Materials and Methods

Cell Culture, Antibodies, and ECMs. LNCaP cells and their more metastatic sublines, C4, C4-2, and C4-2B (25), were grown in T-media (Life Technologies, Inc., Rockville, MD) supplemented with 5% fetal bovine serum. Primary cultures of prostate stromal cells were derived from the tissue surrounding prostatic adenocarcinomas, as described by Ozen *et al.* (57). Conditioned media were prepared by adding fresh media without serum when cells reached 80% confluence and removing it 48 h later. Laminin-1 was purified from Engelbreth-Holme-Swarm tumors according to Davis *et al.* (58), based on the protocol of Kleinman *et al.* (59). OPN-2 was purified as described by Devoll *et al.* (60). VN was purchased from Promega (Madison, WI). Antibodies to integrin subunits α_2, α_3, α_6, $\alpha_v\beta_3$, β_1, β_3, and β_4 were all obtained from Chemicon (Emecula, CA). Vinculin antibody (V9131) was obtained from Sigma (St. Louis, MO), and all secondary-conjugated antibodies were obtained from Jackson Immunochemicals (West Grove, PA).

Immunofluorescent Confocal Microscopy. Cells were seeded onto glass coverslips coated with 50 μg/ml laminin-1. For immunocytochemistry, cells were allowed to spread, fixed in 3% formaldehyde, permeabilized in 0.2% Triton X-100, and stained using either FITC-labeled phalloidin to label filamentous actin or antivinculin antibody (V9131) to detect focal adhesions. Texas Red-conjugated goat antimouse secondary antibodies were obtained from Jackson Immuno Research (Bar Harbor, ME). Cells were mounted on glass coverslips with gel-Mount (Biomedia Corp.), and images were acquired using a laser-scan confocal microscope 410 (Carl Zeiss, Minneapolis, MN).

Flow Cytometry Analysis. Cells below 70% confluence were detached from tissue culture plates and suspended as single cells using a brief treatment of 10 mM EDTA and 20 mM HEPES buffer (pH 7.4) in T-media. The EDTA was neutralized with $CaCl_2$ and $MgSO_4$, and the cells were washed again with T-media containing 0.1% BSA. A total of 2.5×10^5 cells were used for each preparation. Cells and primary antibodies (30 μg/ml) were incubated for 60 min at 4°C, washed, and further incubated with secondary FITC-labeled goat antimouse (30 μg/ml) antibody for an additional 60 min at 4°C. After three brief washes, 1×10^4 cells were analyzed for fluorescence using a FACScan (Becton Dickinson, San Jose, CA). Cells treated with isotype-specific immunoglobulins served as controls. For both cell types, the relative fluorescence intensity was expressed as the increase over background fluorescence. Data points were presented as the mean of two independent experiments, with a range in parentheses (Table 1).

Substrate Adhesion, Attachment, and Migration Assays. Cell attachment and competition assays were performed as described by Vafa *et al.* (36). Assay plates were precoated with laminin, VN, or OPN by overnight incubation at 4°C and subsequently blocked with heat-inactivated BSA for an additional 4 h at room temperature. For adhesion assays, cells were trypsinized with 0.2% trypsin/2% EDTA in

PBS (pH 7.2), suspended in T-media for titration to single cell suspension, and centrifuged briefly. Resuspended cells were then held in adhesion media [T-media with 20 mM HEPES (pH 7.4), 7 mM EDTA, and 0.1% BSA] for 5 h at 37°C and 5% CO_2 to ensure reexpression of integrins on the cell surface. After preincubation, $CaCl_2$ and $MgSO_4$ were added to neutralize EDTA. Cells (5×10^3) in 100 μl of serum-free media were added to each well and allowed to attach for 6 h at 37°C. Triplicate cultures were prepared for each condition. After culture, cells were washed twice in PBS and stained using 3-(4,5-dimethylthiazol-2-yl)-2,5-diphenyltetrazolium bromide (61, 62) or visually counted.

For the attachment assay with or without stromal cell-conditioned media, cell lines were grown to confluence, trypsinized, and replated (1:8) on tissue culture dishes, where they were allowed to grow for another 2 days before being lifted and treated briefly with 10 mM EDTA and 20 mM HEPES buffer in T-media. After neutralizing the EDTA with $CaCl_2$ and $MgSO_4$, the cells were washed with T-media containing 0.1% BSA. Cells were finally held in unconditioned or stromally conditioned media for 10 min, placed on laminin-coated dishes, allowed to adhere for 90 min, and then fixed in formaldehyde. Visible lamelopodia or fillopodia categorized a cell as positively spread. Each cell line was scored for the percentage of spread cells, and all values were normalized to that of control cells that had not been subjected to treatment with conditioned media. At 90 min, untreated LNCaP cells spread on laminin and VN at percentages of 5–10% and 45%, respectively, while at the same time point, untreated C4-2 cells spread on laminin and VN at percentages of 25–35% and 40%, respectively.

Haptotaxis was assayed in triplicate using modified Boyden chambers with an 8 μm pore size [Becton Dickinson (Bedford, MA) or Corning (Acton, MA)]. PBS (100 μl) containing laminin (50 μg/ml), VN (50 μg/ml), or OPN (20 μg/ml) was placed on the underside of the porous membrane and chambers were pre-incubated at 4°C overnight. PBS (100 μl) alone served as a negative control. On the second day, chambers were assembled with serum-free T-media containing 0.1% BSA. Cells (5×10^4) were added to the upper chambers and incubated at 37°C, 5% CO_2 for 16 h. Cells were then fixed with 2% parafomaldehyde and stained with crystal violet. Cells remaining in the upper chamber were removed with a cotton swab. Cells that had migrated were counted using light microscopy; for each condition, 10 randomly chosen fields of cells were counted, and the results were presented as an average ± SD. Migrated control cells were counted at densities of approximately 100 cells/mm^2.

Cell Surface Biotinylation. Integrins on cells surfaces were biotinylated as described previously (63). Briefly, cells were washed in PBS and incubated with 500 μg/ml sulfo-NHS-LC-biotin (Pierce, Rockford, IL) for 30 min at room temperature. Cells were then washed in 50 mM glycine and PBS before they were lysed [20 mM HEPES (pH 7.4), 150 mM NaCl, 1% NP40, 2 mM phenylmethylsulfonyl fluoride, 20 μg/ml aprotinin, and 20 μg/ml leupeptin]. Cell extracts were precleared with protein A/G-agarose beads (Oncogen Science, Cambridge, MA) for 1 h at 4°C and spun at 10,000 rpm for 30 min. Integrin subunits were retrieved by immunopre-

cipitation. Integrin subunit-specific antibodies (200–500 μg/ml) were incubated with the cell lysate for 1 h at 4°C, and immunocomplexes recovered using protein A/G-coated agarose beads. Complexes were analyzed by nondenaturing 7.5% PAGE and electroblotting. After transfer, filters were blocked in 5% milk for 1 h at room temperature. Filters were then incubated with horseradish peroxidase-streptavidin, and proteins were detected using enhanced chemiluminescence (Amersham, Piscataway, NJ).

Statistical Analyses. Where applicable, data were analyzed using Excell or QuickTTest, for determination of mean, SD, and parametric statistics (paired *t* test).

References

1. Chung, L. W., and Davies, R. Prostate epithelial differentiation is dictated by its surrounding stroma. Mol. Biol. Rep., *23:* 13–19, 1996.

2. Varner, J. A., and Cheresh, D. A. Integrins and cancer. Curr. Opin. Cell Biol., *8:* 724–730, 1996.

3. Albelda, S. M. Role of integrin and other cell adhesion molecules in tumor progression and metastasis. Lab. Investig., *68:* 4–16, 1993.

4. Murant, S. J., Handley, J., Stower, M., Reid, N., Cussenot, O., and Maitland, N. J. Co-ordinated changes in expression of cell adhesion molecules in prostate cancer. Eur. J. Cancer, *33:* 263–271, 1997.

5. Knox, J. D., Cress, A. E., Clark, V., Manriquez, L., Affinito, K-S., Dalkin, B. L., and Nagle, R. B. Differential expression of extracellular matrix molecules and the α_6 integrins in the normal and neoplastic prostate. Am. J. Pathol., *145:* 167–174, 1994.

6. Bonkhoff, H., Stein, U., and Remberger, K. Differential expression of α_6 and α_2 very late antigen integrins in the normal, hyperplastic, and neoplastic prostate: simultaneous demonstration of cell surface receptors and their extracellular ligands. Hum. Pathol., *24:* 243–248, 1993.

7. Nagle, R. B., Knox, J. D., Wolf, C., Bowden, G. T., and Cress, A. E. Adhesion molecules, extracellular matrix, and proteases in prostate carcinoma. J. Cell. Biochem. Suppl., *19:* 232–237, 1994.

8. Nagle, R. B., Hao, J., Knox, J. D., Dalkin, B. L., Clark, V., and Cress, A. E. Expression of hemidesmosomal and extracellular matrix proteins by normal and malignant human prostate tissue. Am. J. Pathol., *146:* 1498–1507, 1995.

9. Dedhar, S., Saulnier, R., Nagel, R., and Overall, C. M. Specific alterations in the expression of $\alpha_3\beta_1$ and $\alpha_6\beta_4$ integrins in highly invasive and metastatic variants of human prostate carcinoma cells selected by *in vitro* invasion through reconstituted basment membrane. Clin. Exp. Metastasis, *11:* 391–400, 1993.

10. Witkowski, C. M., Rabinovitz, I., Nagle, R. B., Affinito, K-S. D., and Cress, A. E. Characterization of integrin subunits, cellular adhesion and tumorgenicity of four human prostate cell lines. J. Cancer Res. Clin. Oncol., *119:* 637–644, 1993.

11. Zheng, D-Q., Woodward, A. S., Fornaro, M., Tallini, G., and Languino, L. R. Prostatic carcinoma cell migration via $\alpha_v\beta_3$ integrin is modulated by a focal adhesion kinase pathway. Cancer Res., *59:* 1655–1664, 1999.

12. Rabinovitz, I., Nagle, R. B., and Cress, A. E. Integrin α_6 expression in human prostate carcinoma cells is associated with a migratory and invasive phenotype *in vitro* and *in vivo*. Clin. Exp. Metastasis, *13:* 481–491, 1995.

13. Aplin, A. E., Howe, A., Alahari, S. K. amd Juliano, R. L. Signal transduction and signal modulation by cell adhesion receptors: the role of integrins, cadherins, immunoglobulin-cell adhesion molecules, and selectins. Pharmacol. Rev., *50:* 197–263, 1998.

14. Schwartz, M. A., Schaller, M. D., and Ginsberg, G. H. Integrin emerging paradigms of signal transduction. Annu. Rev. Cell Biol., *11:* 549–599, 1995.

15. Hughes, P. E., and Pfaff, M. Integrin affinity modulation. Trends Cell Biol., *8:* 359–364, 1998.

16. Elices, M. J., and Hemler, M. E. The human integrin VLA-2 is a collagen receptor on some cells and a collagen/laminin receptor on others. Proc. Natl. Acad. Sci. USA, *86:* 9906–9910, 1989.

17. O'Toole, T. E., Mandelman, D., Forsyth, J., Shattil, S. J., Plow, E. F., and Ginsberg, M. H. Modulation of the affinity of integrin $\alpha_{IIb}\beta_3$ (GPIIb-IIIa) by the cytoplasmic domain of α_{IIb}. Science (Washington DC), *254:* 845–847, 1991.

18. Sims, P. J., Ginsberg, M. H., Plow, E. F., and Shattil, S. J. Effect of platelet activation on the conformation of the plasma membrane glycoprotein IIb-IIIa complex. J. Biol. Chem., *266:* 7345–7352, 1991.

19. Clark, E. A., and Brugge, J. S. Integrin and signal transduction pathways: the road taken. Science (Washington DC), *268:* 233–239, 1995.

20. Burridge, K., and Chrzanowska-Wodnicka, M. Focal adhesions, contractility and signaling. Annu. Rev. Cell Biol., *12:* 463–519, 1996.

21. Schoenwaelder, S. M., and Burridge, K. Bidirectional signaling between the cytoskeleton and integrin. Curr. Opin. Cell Biol., *11:* 274–286, 1999.

22. Ridley, A. J., and Hall, A. The small GTP-binding protein rho regulates the assembly of focal adhesions and actin stress fibers in response to growth factors. Cell, *70:* 389–399, 1992.

23. Mainiero, F., Pepe, A., Yeon, M., Ren, Y., and Giancotti, F. G. The intracellular functions of $\alpha_6\beta_4$ integrin are regulated by EGF. J. Cell Biol., *134:* 241–253, 1996.

24. Chung, L. W. K., Zhau, H. E., and Wu, T. T. Development of human prostate cancer models for chemoprevention and experimental therapeutics studies. J. Cell. Biochem. Suppl., *28/29:* 174–181, 1997.

25. Wu, H. C., Hsieh, J. T., Gleave, M. E., Brown, N. M., Pathak, S., and Chung, L. W. Derivation of androgen-independent human LNCaP prostatic cancer cell sublines: role of bone stromal cells. Int. J. Cancer, *57:* 406–412, 1994.

26. Thalmann, G. N., Anezinis, P. E., Chang, S. M., Zhau, H. E., Kim, E. E., Hopwood, V. L., Pathak, S., von Eschenbach, A. C., and Chung, L. W. Androgen-independent cancer progression and bone metastasis in the LNCaP model of human prostate cancer. Cancer Res., *54:* 2577–2581, 1994 [published erratum appears in Cancer Res., *54:* 3953, 1994].

27. Hyytinen, E. R., Thalmann, G. N., Zhau, H. E., Karhu, R., Kallioniemi, O. P., Chung, L. W., and Visakorpi, T. Genetic changes associated with the acquisition of androgen-independent growth, tumorigenicity and metastatic potential in a prostate cancer model. Br. J. Cancer, *75:* 190–195, 1997.

28. Bonkhoff, H. Analytical molecular pathology of epithelial-stromal interactions in the normal and neoplastic prostate. Anal. Quant. Cytol. Histol., *20:* 437–442, 1998.

29. Koeneman, K. S., Yeung, F., and Chung, L. W. Osteomimetic properties of prostate cancer cells: a hypothesis supporting the predilection of prostate cancer metastasis and growth in the bone environment. Prostate, *39:* 246–261, 1999.

30. Rabinovitz, I., and Mercurio, A. M. The integrin $\alpha_6\beta_4$ functions in carcinoma cell migration on laminin-1 by mediating the formation and stabilization of actin-containing motility structures. J. Cell Biol., *139:* 1873–1884, 1997.

31. Kitazawa, S., and Maeda, S. Development of skeletal metastases. Clin. Orthop. Relat. Res., *312:* 45–50, 1995.

32. Schulze, B., Mann, K., Poschl, E., Yamada, Y., and Timpl, R. Structural and functional analysis of the globular domain IVa of the laminin α_1 chain and its impact on an adjacent RGD site. Biochem. J., *314:* 847–851, 1996.

33. Allen, M. V., Smith, G. J., Juliano, R., Maygarden, S. J., and Mohler, J. L. Down-regulation of the β_4 integrin subunit in prostatic carcinoma and prostatic intraepithelial neoplasia. Hum. Pathol., *29:* 311–318, 1998.

34. Cress, A. E., Rabinovitz, I., Zhu, W., and Nagel, R. B. The $\alpha_6\beta_1$ and $\alpha_6\beta_4$ integrins in human prostate cancer progression. Cancer Metastasis Rev., *14:* 219–228, 1995.

35. Rokhlin, O. W., and Cohen, M. B. Expression of cellular adhesion molecules on human prostate tumor cell lines. Prostate, *26:* 205–212, 1995.

36. Vafa, A., Zhang, Y., Sikes, R. A., and Marengo, S. R. Overexpression of p185erbB2/neu in the NbE prostatic epithelial cell line increases cellular spreading and the expression of integrin $\alpha_6\beta_1$. Int. J. Oncol., *13:* 1191–1197, 1998.

37. Hullinger, T. G., McCauley, L. K., DeJoode, M. L., and Somerman, M. J. Effect of bone proteins on human prostate cancer cell lines *in vitro*. Prostate, *36:* 14–22, 1998.

38. Hemler, M. E., Crouse, C., and Sonnenberg, A. Association of the VLA α_6 subunit with a novel protein. A possible alternative to the common VLA β_1 subunit on certain cell lines. J. Biol. Chem., *264:* 6529–6535, 1989.

39. Cooper, H. M., Tamura, R. N., and Quaranta, V. The major laminin receptor of mouse embryonic stem cells is a novel isoform of the $\alpha_6\beta_1$ integrin. J. Cell Biol., *115:* 843–850, 1991.

40. Hogervorst, F., Admirall, L. G., Niessen, C., Kuikman, I., Janssen, H., Daams, S., and Sonnenberg, A. Biochemical characterization and tissue distribution of the A and B variants of the integrin α_6 subunit. J. Cell Biol., *121:* 179–191, 1993.

41. Hogervorst, F., Kuikman, I., van Kessel, A. G., and Sonnenberg, A. Molecular cloning of the human α_6 integrin subunit. Alternative splicing of α_6 mRNA and chromosomal localization of the α_6 and β_4 genes. Eur. J. Biochem., *199:* 425–433, 1991.

42. Shaw, L. M., and Mercurio, A. M. Regulation of $\alpha_6\beta_1$ integrin laminin receptor function by the cytoplasmic domain of the α_6 32 subunit. J. Cell Biol., *123:* 1017–1025, 1993.

43. Marengo, S. R., Sikes, R. A., Anezinis, P., Chang, S. M., and Chung, L. W. Metastasis induced by overexpression of p185neu-T after orthotopic injection into a prostatic epithelial cell line (NbE). Mol. Carcinog., *19:* 165–175, 1997.

44. DiPersio, C. M., Hodivala-Dilke, K. M., Jaenisch, R., Kreidberg, J. A., and R. O Hynes. $\alpha_3\beta_1$ integrin is required for normal development of the epidermal basement membrane. J. Cell Biol., *137:* 729–742, 1997.

45. Rabinovitz, I., Cress, A. E., and Nagle, R. B. Biosynthesis and secretion of laminin and S-laminin by human prostate carcinoma cell lines. Prostate, *25:* 97–107, 1994.

46. Calof, A. L., Campanero, M. R., O'Rear, J. J., Yurchenco, P. D., and Lander, A. D. Domain-specific activation of neuronal migration and neurite outgrowth-promoting activities of laminin. Neuron, *13:* 117–130, 1994.

47. Giannelli, G., Falk-Marzillier, J., Schiraldi, O., Stetler-Stevenson, W. G., and Quaranta, V. Induction of cell migration by matrix metalloprotease-2 cleavage of laminin-5. Science (Washington DC), *277:* 225–228, 1997.

48. Felding-Habermann, B., Mueller, B. M., Romerdahl, C. A., and Cheresh, D. A. Involvement of integrin α_V gene expression in human melanoma tumorigenicity. J. Clin. Investig., *89:* 2018–2022, 1992.

49. Albelda, S. M., Mette, S. A., Elder, D. E., Stewart, R., Damjanovich, L., Herlyn, M., and Buck, C. A. Integrin distribution in malignant melanoma: association of the β_3 subunit with tumor progression. Cancer Res., *50:* 6757–6764, 1990.

50. Gehlsen, K. R., Davis, G. E., and Sriramarao, P. Integrin expression in human melanoma cells with differing invasive and metastatic properties. Clin. Exp. Metastasis, *10:* 111–120, 1992.

51. Liapis, H., Adler, L. M., Wick, M. R., and Rader, J. S. Expression of $\alpha_V\beta_3$ integrin is less frequent in ovarian epithelial tumors of low malignant potential in contrast to ovarian carcinomas. Hum. Pathol., *28:* 443–449, 1997.

52. Seiffert, D. Detection of vitronectin in mineralized bone matrix. J. Histochem. Cytochem., *44:* 2275–2280, 1996.

53. Liaw, L., Skinner, M. P., Raines, E. W., Ross, R., Cheresh, D. A., Schwartz, S. M., and Giachelli, C. M. The adhesive and migratory effects of osteopontin are mediated by distinct cell surface integrin. J. Clin. Investig., *95:* 713–724, 1995.

54. Stromblad, S., Becker, J. C., Yebra, M., Brooks, P. C., and Cheresh, D. A. Suppression of p53 activity and p21$^{\text{WAF1/CIP1}}$ expression by vascular cell integrin $\alpha_V\beta_3$ during angiogenesis. J. Clin. Investig., *98:* 426–433, 1996.

55. Elgavish, A., Prince, C., Chang, P. L., Lloyd, K., Lindsey, R., and Reed, R. Osteopontin stimulates a subpopulation of quiescent human prostate epithelial cells with high proliferative potential to divide *in vitro*. Prostate, *35:* 83–94, 1998.

56. Giancotti, F. G., and Ruoslahti, E. Integrin signaling. Science (Washington DC), *285:* 1028–1032, 1999.

57. Ozen M., Multani, A. S., Chang, S-M., Von Eschenbach., Chung, L. W. K., and Pathak, S. Establishment of an *in vitro* cell model system to study human prostate carcinogenesis: involvement of chromosome 5 in early stages of neoplastic transformation. Int. J. Oncol., *8:* 883–888, 1996.

58. Davis, L. A., Ogle, R. C., and Little, C. D. Embryonic heart mesenchymal cell migration in laminin. Dev. Biol., *133:* 37–43, 1989.

59. Kleinman, H. K., McGravey, M. L., Hassell, J. R., and Martin, G. R. Formation of a supramolecular complex involved in the reconstitution of basement membrane components. Biochemistry, *22:* 4969–4974, 1983.

60. Devoll, R. E., Pinero, G. J., Appelbaum, E. R., Dul, E., Troncoso, P., Butler, W. T., and Farach-Carson, M. C. Improved immunohistochemical staining of osteopontin (OPN) in paraffin-embedded archival bone specimens following antigen retrieval: anti-human OPN antibody recognizes multiple molecular forms. Calcified Tissue Int., *60:* 380–386, 1997.

61. Carmichael, J., DeGraff, W. G., Gazdar, A. F., Minna, J. D., and Mitchell, J. B. Evaluation of a tetrazolium-based semiautomated colorimetric assay: assessment of chemosensitivity testing. Cancer Res., *47:* 936–942, 1987.

62. Romijn, J. C., Verkoelen, C. F., and Schroeder, F. H. Application of the MTT assay to human prostate cancer cell lines *in vitro*: establishment of test conditions and assessment of hormone-stimulated growth and drug-induced cytostatic and cytotoxic effects. Prostate, *12:* 99–110, 1988.

63. Schuberth, H. J., Kroell. A., and Leibold, W. Biotinylation of cell surface MHC molecules: a complementary tool for the study of MHC class II polymorphism in cattle. J. Immunol. Methods, *189:* 89–98, 1996.

CELL MOTILITY
AND THE CYTOSKELETON

This journal is online
WILEY InterScience®
www.interscience.wiley.com

Dynamics of α-Actinin in Focal Adhesions and Stress Fibers Visualized With α-Actinin-Green Fluorescent Protein

Magnus Edlund,[1] Marc A. Lotano,[2] and Carol A. Otey[2]*

[1]*Department of Cell Biology, University of Virginia, Charlottesville*
[2]*Department of Cell and Molecular Physiology, University of North Carolina at Chapel Hill, Chapel Hill*

Motile cells undergo changes in cell adhesion, behavior, and shape that are mediated by small-scale cytoskeletal rearrangements. These rearrangements have proven difficult to follow quantitatively in living cells, without disrupting the very structures and delicate protein balances under study. We have expressed a prominent cytoskeletal protein, α-actinin, as a fusion with green fluorescent protein (αAGFP), and have followed this construct's movements within transfected mouse Swiss 3T3 and BALB/c fibroblasts. αAGFP was expressed at low levels to avoid overexpression artifacts. αAGFP localized to cellular structures, including stress fibers, focal adhesions, microspikes, and lamellipodia. High-resolution video-microscopy revealed that the αAGFP construct could be seen relocating to focal adhesions early in their formation and shortly thereafter to stress-fiber dense bodies. By Fluorescent Recovery After Photo-bleaching (FRAP) techniques, αAGFP was found to have similar exchange rates and protein stability in focal adhesions and stress fibers (despite the known differences in protein composition in these two structures). This raises the possibility that the two structures share common key regulatory factors and may not be as affected by protein-protein binding interactions as previously suggested. Additionally, the exchange rates revealed by video-microscopy and FRAP analysis of αAGFP are more rapid than those reported previously, which were obtained using microinjection of large excesses of fluorescently-tagged protein. Cell Motil. Cytoskeleton 48:190–200, 2001.   © 2001 Wiley-Liss, Inc.

INTRODUCTION

At focal adhesions, bundles of internal actin filaments are linked to the extracellular matrix via the transmembrane proteins called integrins and a large complex of cytoplasmic components. Shifts in the balance of cytoskeletal anchorage and cell attachment proteins have been found to affect not only the strength of adhesion, but also the signaling cascades that regulate cell death, proliferation, and metastatic behavior [Giancotti and Ruoslahti, 1999]. However, following the dynamics of such protein shifts in living, motile cells has proven difficult. Microinjection of fluorochrome-labeled proteins has provided valuable information about protein localizations [Feramisco, 1979; Geiger et al., 1984a,b; Pavalko et al., 1995], but the necessarily large amounts

of protein injected in past studies may have disrupted the very structures and subtle protein balances and rearrangements under study. We report here the use of a new fusion protein of a focal adhesion and stress fiber component, α-actinin, made with Green Fluorescent Protein (GFP), which, when expressed at very low levels, has

allowed high-resolution video microscopy of normal protein rearrangement during processes such as focal adhesion and stress fiber assembly.

To date, over 30 proteins have been found to localize to focal adhesion sites [Giancotti and Ruoslahti, 1999, Yamada and Geiger, 1997]; of these, only a few are believed to interact directly with the transmembrane integrins. These integrin-binding partners include both classical signaling molecules and protein adaptors that bind along the cytoplasmic face of the cell membrane [reviewed in Hemler, 1998]. Two proteins, talin and α-actinin, are known to bind directly to both integrin and actin. The highly conserved α-actinin protein, the subject of these studies, cross-links actin filaments in muscle and non-muscle cells, and binds a number of focal adhesion components, including three different β subunits of integrins [Otey et al., 1990, 1993; Pavalko and LaRoche, 1993; Lewis and Schwartz, 1995] and the intracellular structural proteins zyxin and vinculin [Critchley et al., 1999]. α-actinin also appears to be involved in cell-cell anchorage, as it binds to α-catenin [Knudsen et al., 1995], a protein that interacts directly with the cytoplasmic domains of cell-cell adhesion molecules [Balzar et al., 1998]. Although four α-actinin isoforms have been identified in humans [Youssoufian et al., 1990; Beggs et al., 1992; Honda et al., 1998], we focus here on the major non-muscle isoform, α-actinin-1. Micro-injection and antibody staining show α-actinin distributed along the stress fibers of non-muscle cells in a distinctive, periodic array [Lazarides and Burridge, 1975]. It also localizes to regions of dynamic membrane activity, such as the lamellipodia at the leading edges of migrating cells [Pavalko et al., 1995; Knudsen et al., 1995]. Because of α-actinin's diverse roles in both actin-filament and integrin binding, the protein's expression levels have been correlated with many cell functions, including adhesive strength, cell motility, and cell growth rate, as well as metastatic transformation [Glück et al., 1993; Glück and Ben-Ze'ev, 1994].

Like α-actinin, a number of proteins are common to both stress fiber and focal adhesion structures; however, not all of α-actinin's known binding partners and potential regulators are found evenly distributed between both structures. For example, α-actinin binds to integrin, vinculin, and zyxin in vitro, but these three proteins are concentrated in the focal adhesions and not along the stress fibers. If α-actinin dynamics do differ in the two locales, do the transmembrane integrins, unique to focal adhesions, stabilize the α-actinin found at these sites, relative to the α-actinin found elsewhere in the cytoskeleton? This possibility is supported first by in vitro studies showing direct binding between integrins and α-actinin, including differential affinities between the β subunit isoforms [Belkin et al., 1997] and second by micro-

injections of large excesses of fluorescently-labeled α-actinin, followed by Fluorescent Recovery After Photobleaching (FRAP) studies, which suggest differences between the two structures [McKenna et al., 1985]. To avoid disrupting endogenous protein balances when addressing this question, we made use of jellyfish green fluorescent protein [Chalfie, 1995; Ludin and Matus, 1998] to construct a chimeric protein of α-actinin, (α-actinin-GFP, denoted αAGFP), enabling us to express the fusion protein in fibroblasts at known low levels (compared to endogenous levels of α-actinin). We then followed αAGFP movements during cytoskeletal and focal adhesion rearrangements in living cells, using video microscopy and FRAP [Swaminathan et al., 1997]. We report here that, despite the protein composition (and postulated binding-partner) differences between focal adhesions and stress fibers, α-actinin turnover rates are similar in the two structures, and more rapid than previously reported.

MATERIALS AND METHODS

Expression of the Plasmid Construct

Non-muscle α-actinin cDNA (gift of Dr. D. J. Kwiatkowski, Harvard Medical school) was used as a PCR template to generate a fragment of α-actinin sequence, containing a deleted stop codon. Forward and backward primers 5'-ACGGTACCCATCATGGAC-CATTATGATTCT-3' and 5'-TGGAAGCTTAGGTC-CGAGGTCACTCTCGCCGTACAG -3' were used. The PCR product was subcloned to the 5' end of the humanized S65T version of green fluorescent protein (hGFP, Clontech, Palo Alto, CA), inside the Kpn1 and Xba1 sites of the mammalian expression vector pcDNA3 (Invitrogen, Carlsbad, CA).

Cell Culture and Transfection

Swiss 3T3 fibroblast cells from the American Type Culture Collection were maintained at 37°C in Dulbecco's Modified Eagle's Media (DMEM), with 10% fetal bovine serum, 100 U/ml penicillin, and 100 mg/ml streptomycin. Cells were transfected using the Lipofectamine plus reagent (GIBCO, Life Technologies, Inc., Gaithersburg, MD), according to the manufacturer's instructions. Transfected cells were selected in G418 gentamycin-containing growth medium (GIBCO BRL, Gaithersburg, MD).

Immunoprecipitation

GFP-transfected Swiss 3T3 cells were rinsed three times in ice-cold phosphate buffered saline (PBS), and solubilized in lysis buffer (1% NP-40, 50 mM Tris-HCl, 150 mM NaCl, 2 mM EDTA, 50 mg/ml leupeptin, 0.5%

aprotinin, 1 mM sodium orthovanadate, 1 mM PMSF). For each immunoprecipitation, ten 150-mm culture dishes of confluent cells were scraped, using a siliconized spatula and 2 ml of ice-cold lysis buffer. Insoluble material was removed by centrifugation for 30–40 min at 10,000 or 100, 000g, at 4°C. Polyclonal anti-GFP antibody (Clontech, Palo Alto, CA) was used to precipitate αAGFP. Protein-A sepharose beads (Pharmacia, Piscataway, NJ) were pre-incubated with the anti-GFP antibody and then incubated for 2 h with the cell lysate. The beads were washed five times with lysis buffer and resuspended in SDS-PAGE loading buffer. Samples were resolved on 7.5% polyacrylamide gels and electro-blotted. After transfer, the filters were blocked in 5% milk overnight, at 4°C. Filters were incubated with primary and secondary antibodies for 1 h each, at room temperature. Peroxidase-conjugated secondary antibodies were diluted 1:5,000 (Jackson Immunoresearch Labs, Bar Harbor, ME). Membranes were probed with secondary antibody and the proteins detected with Enhanced Chemi-Luminescence (ECL). Quantification was performed on a Molecular Dynamics densitometer.

Immunofluorescence, Imaging, and Photo-Bleaching

Cells of similar fluorescent intensities were isolated by fluorescent cell sorting and either lysed immediately for analyses, or re-plated and allowed to recover in growth media. For fluorescent imaging, sorted cells were seeded onto clean glass coverslips or onto glass coverslips coated with 50 µg/ml human plasma fibronectin (Sigma, St. Louis, MO). For immuno-cytochemistry, cells were allowed to spread, fixed in 3% formaldehyde, permeabilized in 0.2% Triton X-100, and stained with the following antibodies (from Sigma): anti-α-actinin (A 5044) or anti-vinculin (V9131). TRITC-phalloidin was used to label filamentous actin. Texas-red conjugated, goat-anti-mouse secondary antibodies were from Jackson Immuno Research (Bar Harbor, ME). Images were acquired using an Olympus inverted microscope (IX-70), with a water-immersion 60× Olympus objective. Images from a cooled PXL CCD camera (Photometrix, Tucson, AZ) were processed on a Silicon Graphics workstation with Isee software (Inovision, Raleigh, NC).

Photobleaching was performed on a Leica TCS-NT Confocal system. Transfected cells were maintained on the confocal microscope stage, under constant 5% CO_2 flow, in a PDMI-2 micro-incubator, with a TC-202 temperature-control unit (Medical Systems, Harvard Apparatus, Holliston, MA). The 488-nm line of a 25-mW Argon laser was used in bleach pulses of 50–100 msec. Fluorescent recovery was assayed up to 60 min by measuring the average intensity of the bleached areas, and normalizing the values to an unbleached reference point

within the same cell. The number of samples in either focal adhesions or stress fibers at each time is 9 from at least 3 different cells. Since movement of the cell, or of the subcellular focal adhesions or stress fibers, would complicate interpretation of the data, only stationary structures in stable, non-migrating cells were photobleached. Grouped data is presented as the mean + standard deviation (SD). Assessment of differences in recovery was performed using analysis of variance (ANOVA) models, which were fit using maximum likelihood techniques. A natural logarithmic variance-stabilizing transformation, as well as a variance-weighting scheme, was needed to help meet assumptions of a linear model (constant variance and normally distributed error terms). The variance-weighting scheme involved weighting variances at each time point by a function proportional to the time at which the measurement took place [Neter et al., 1990]. The logarithmic transformation facilitates the use of the anti-logarithm of pair-wise differences to compare the ratio of two quantities (fold change). Confidence intervals for pair-wise differences were generated by Fisher's Least Significant Difference method with a comparison type I error rate of 0.05 [Hsu., 1996]. A 95% confidence interval, which does not contain 1, implies statistical significance at the 5% level.

RESULTS

Characterization of α-Actinin-GFP

We fused GFP to the carboxyl-terminus of α-actinin, as illustrated in Figure 1A, in order to follow the protein's localization in living cells. The GFP-fused form of α-actinin (αAGFP) was expressed in Swiss 3T3 and BALB/c mouse fibroblasts, and the properties of αAGFP were investigated by immunoprecipitation of the fusion protein from cultures of stably-transfected cells. Because the results were identical in the two cell lines, only data acquired from Sw3T3 fibroblasts are presented here. As shown in Figure 1B, the apparent molecular mass of αAGFP was 130 kDa, consistent with the predicted mass of the two fused proteins (100 kDa for α-actinin and 27 kDa for GFP). It is well established that overexpression of cytoskeletal proteins can alter the behavior of transfected cells. To determine if we were significantly altering the level of expression of α-actinin by transfecting the cells with the αAGFP construct, we used Fluorescent Automated Cell Sorting (FACS) to sort transfected cells according to their fluorescent intensity, and compared the levels of endogenous vs. transfected proteins. The amount of GFP construct, even in the highest expressers, was found to be very small relative to the amount of native α-actinin. Quantification of Western blot bands, using anti-α-actinin antibodies, revealed that approxi-
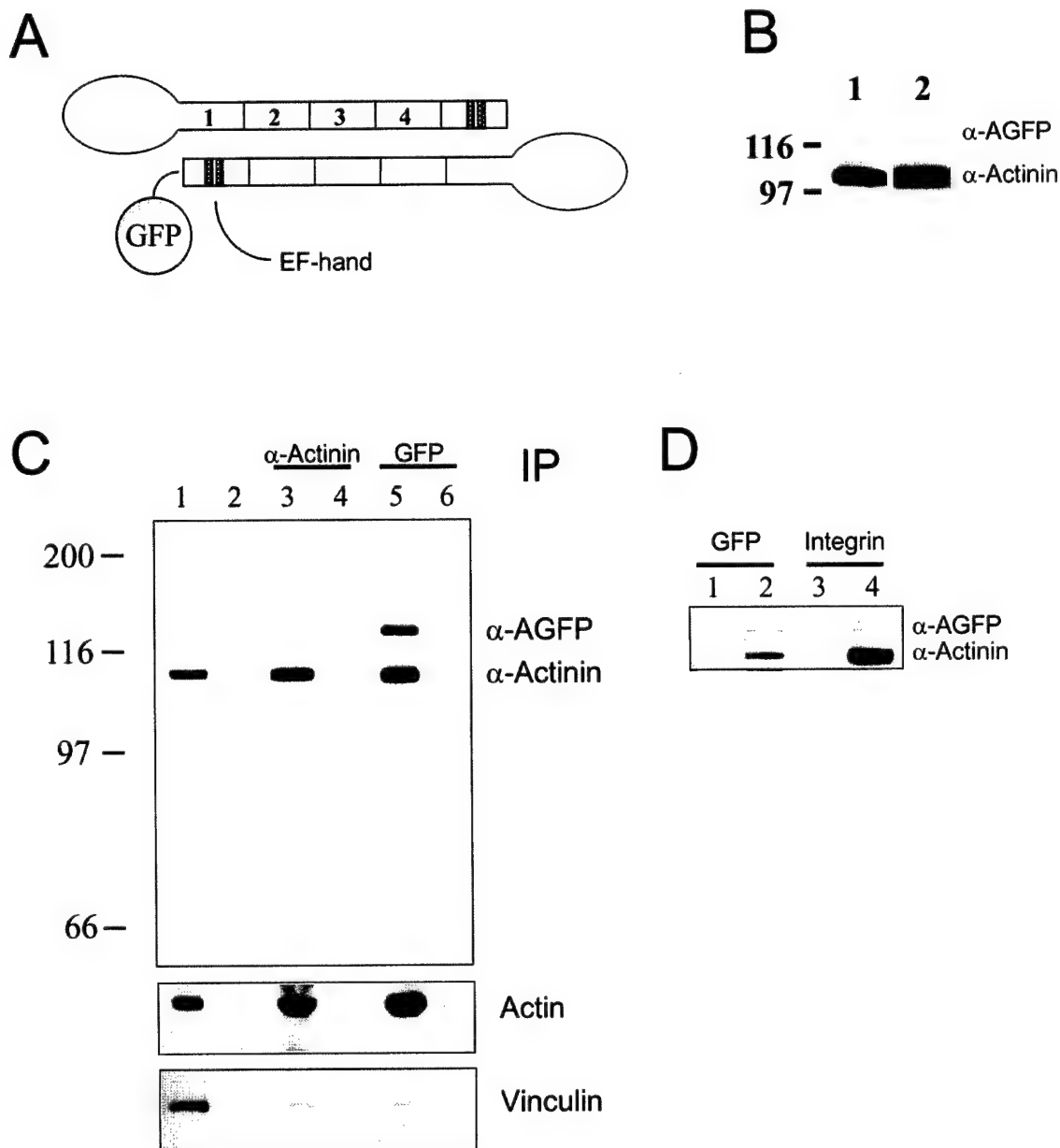
Fig. 1. **A:** Schematic diagram of the α-actinin-GFP (αAGFP) fusion construct, with head and rod domains indicated. **B:** Relative levels of endogenous and transfected α-actinin. Control, untransfected Swiss 3T3 cells (**lane 1**), and αAGFP-expressing cells (**lane 2**), were sorted according to fluorescence intensity and lysed. Western blots of equal amounts of cell lysate were quantified with anti-α-actinin antibody, revealing that approximately 1% of all α-actinin within the cells is fused to GFP. **C:** Actin and vinculin co-immunoprecipitate with both endogenous α-actinin and with GFP-α-actinin. After extraction, immunoprecipitation was performed using sepharose beads alone (**lane 2**), anti α-actinin antibody (**lanes 3** and **4**) and anti-GFP antibody (**lanes 5** and **6**). The blot was stained for actin, then stripped and re-probed for vinculin. Total cell lysate was loaded in **lane 1** as a positive control for antibody detection of actin and vinculin. Lanes 4 and 6 were loaded with the last wash from the sepharose beads prior to elution of the immunoprecipitated product from lanes 3 and 5, respectively. **D:** α-actinin was co-immunoprecipitated with either GFP or an integrin antibody. **Lanes** 1 and **3** were loaded with the last wash from the sepharose beads prior to elution of the immunoprecipitated product from **lanes 2** and **4**, respectively. The integrin antibody brought down similar levels of endogenous α-actinin and fusion protein to those seen in the total cell lysate (B, lane 2).

mately 1% of all α-actinin in the cells is fused to GFP (Fig. 1B). No noticeable difference in growth rate between populations of parental and transfected cells was detectable, nor were any phenotypic changes in cell shape or behavior observed.

To determine if αAGFP was capable of forming dimers with endogenous α-actinin, and interacting with known binding partners, we immunoprecipitated endogenous α-actinin and αAGFP, and used Western blot analysis to detect co-precipitated proteins. We were concerned that long F-actin filaments might contaminate these precipitations, and carry both endogenous and GFP-fused α-actinin with them, so we pre-cleared the lysates with a high-speed centrifugation step (40 min at 100,000g) prior to the immunoprecipitation. Subsequent immunoprecipitation from the cleared lysates with anti-GFP antibody and immunoblotting for α-actinin revealed that the GFP fusion protein co-precipitated in a roughly 1:1 ratio with endogenous α-actinin (Fig. 1C, lane 5), suggesting that αAGFP is able to form dimers with the endogenous protein. Additionally, as shown in Figure 1C, similar amounts of vinculin and actin were precipitated with antibodies for either endogenous α-actinin or αAGFP (compare lanes 3 and 5 in Fig. 1C, bottom panel). We interpret this to indicate that αAGFP is not inhibited from binding to either vinculin or to the short F-actin filaments that remain in the pre-cleared lysate. We also asked if αAGFP was able to bind to β1 integrins, as has been reported for α-actinin previously [Otey et al., 1990]. When integrin was immunoprecipitated and blotted for α-actinin, the ratio of αAGFP to endogenous α-actinin (shown in Fig. 1D, lane 4) was the same as the ratio seen in whole-cell lysates (Fig. 1B, lane 2), indicating that β1 integrin binds equally well to endogenous and GFP-fused α-actinin.

Cellular Localization of αAGFP

In order to monitor the subcellular localization of αAGFP, transfected cells were fixed and double-labeled with anti-vinculin or rhodamine-phalloidin. As shown in Figure 2, αAGFP localized to all structures previously reported to contain endogenous α-actinin [Lazarides and Burridge, 1975; Pavalko et al., 1995]. αAGFP distributed to the ruffling edge of cellular protrusions, to focal adhesions (where αAGFP co-localized with vinculin; Fig. 2C,D) and in a punctate, periodic pattern along stress fibers (Fi. 2A). In addition, αAGFP was also concentrated in cell-cell junctions, both in fibroblast and epithelial cells (data not shown), as has previously been described [Knudsen et al., 1995; Ozawa, 1998].

Time-Lapse Video-Microscopy

αAGFP allowed time-lapse video-microscopy of changing protein distributions in living cells. Figure 3

shows six movie frames, covering 35 min of subcellular activity in a transfected Sw3T3, during which time membrane ruffles and focal adhesions were seen forming and rearranging rapidly. At Time 0, a focal adhesion first appeared as a bright spot in a diffusely fluorescent lamellipodia. Over the next 30 min, the focal adhesion enlarged and elongated, as an αAGFP-containing tail radiated inward from the site. When cells were fixed and stained, more details of newly formed focal adhesions were visible than could be seen in live cells. In many cases, a fan-shaped arrangement of actin filaments radiated outward from a newly-formed focal adhesion (Fig. 3B). These nascent stress fibers did not display the punctate distribution of α-actinin that is seen in mature stress fibers, but instead were stained evenly with αAGFP.

Quantification of αAGFP Dynamics in Stress Fibers and Focal Adhesions

Data accumulated from biochemical studies of α-actinin suggest that α-actinin may have different binding partners in different subcellular structures. To question whether the greater known number of α-actinin binding partners within focal adhesions constrains protein turnover in these structures, we used FRAP, and measured the rate at which bleached molecules of αAGFP were replaced with unbleached molecules, within both focal adhesions and stress fibers. To ensure that energy absorption during the laser pulses did not disrupt structural integrity, cells were fixed immediately after laser illumination, stained with rhodamine-phalloidin or an antibody to vinculin, and examined by conventional microscopy. Stress fibers appeared unaffected throughout the bleached area, and focal adhesions were uniform and normal for vinculin staining (data not shown).

Figure 4 shows the recovery time-course of bleached αAGFP along stress fibers. Four time points during recovery are detailed in Figure 4B. Dense bodies along the stress fiber were bleached, and the recoveries of typical dense bodies during the 15 min are shown with their respective intensity profiles in Figure 4C. By the same technique, the turnover of αAGFP was investigated within round (2-μm diameter) spots in focal adhesions. Strikingly, these bleached spots recovered at similar rates to those in stress fiber dense bodies. Figure 5 shows three time-points during the recovery of a focal adhesion. Rapid diffusion within 5 min of bleaching results in an even redistribution of protein. This is followed by a phase of fluorescence intensity increase. Fluorescence was completely re-established by approximately 15 min post bleaching in both structures, with 90% recovery after 10 min, and a half-time of recovery (T1/2) of approximately 5 min. The biphasic character of recovery was also common to both stress fibers and focal adhe-
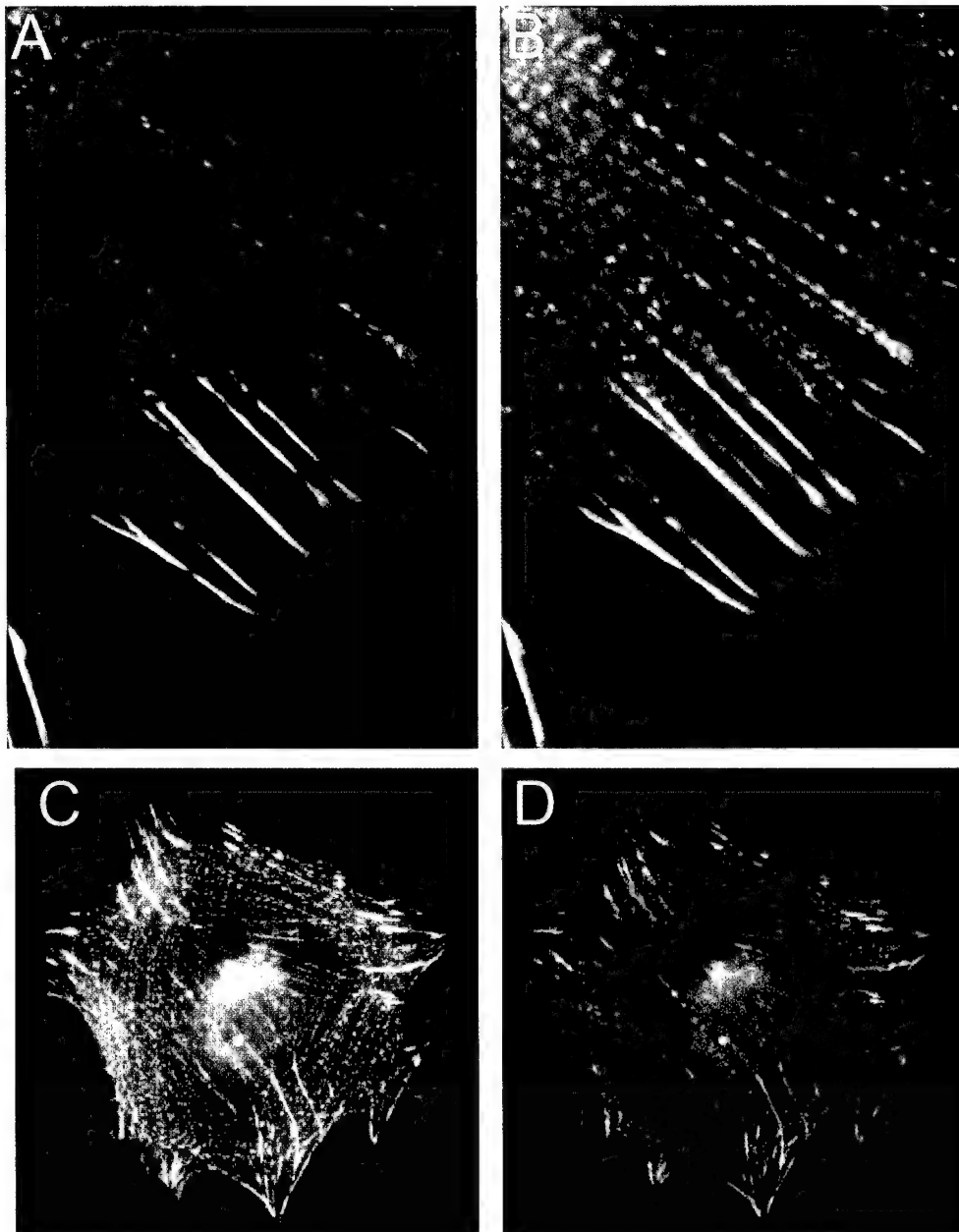
Fig. 2.   Co-localization of αAGFP construct with actin and vinculin in transfected Swiss 3T3 fibroblasts. Cells expressing αAGFP were fixed and labeled with rhodamine-phalloidin to detect actin filaments (B), or with anti-vinculin to detect focal adhesions (D). **A,C:** αAGFP alone. **B,D:** Merged images. Scale bar = 5 μm.

sions, as can be seen in the graphical representation of fluorescence recovery presented in Figure 6A. All data points are the averages from nine structures, taken from at least three different cells. Error bars show standard deviation. Figure 6B shows the statistical analysis of similarities in recovery dynamics between the two structures, which differ by less than 10% at 15 min (95% confidence interval).

Recoveries in stress fibers and focal adhesions were compared statistically using analysis of variance (ANOVA) models, which were fit using maximum likelihood techniques, in combination with Fisher's Least Significance Difference methods, for establishing the confidence intervals in pair-wise differences (see Materials and Methods). ANOVA models lend themselves to easy interpretation and ease of making pair-wise com-
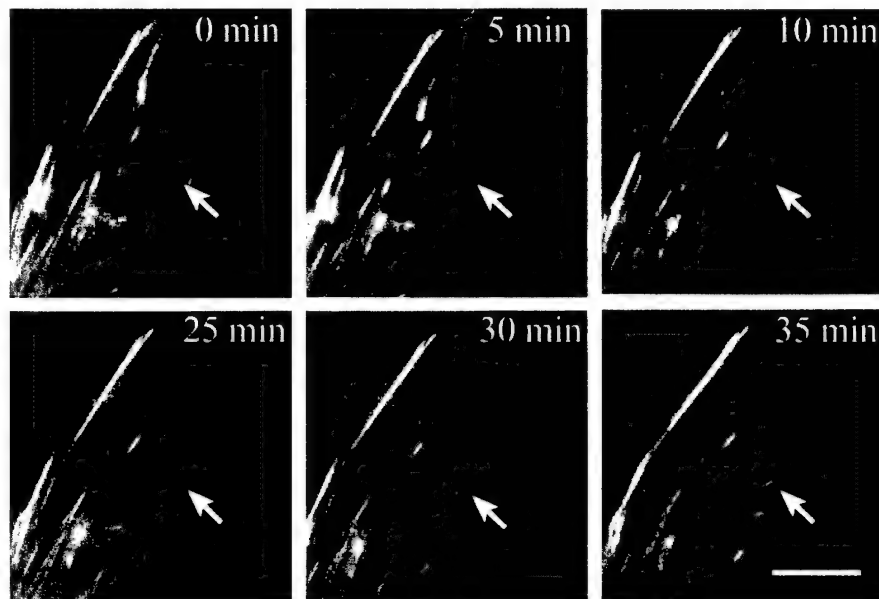
A

B

Fig. 3.   αAGFP movements during focal adhesion formation in a Swiss 3T3 fibroblast, as recorded by high-resolution camera, with intervals and exposure times chosen to minimize photo-toxicity. **A:** In 6 frames taken during a 30-min time interval, a new young focal adhesion is first visible as a small fluorescent spot (time 0), but enlarges and elongates over time. **B:** αAGFP detected in a fixed cell, photographed at high magnification. In a focal adhesion near the edge of the cell (apparently a nascent focal adhesion), filaments were observed to converge in a fan-shaped array at the adhesion site. Scale bar = 10 μm.

parisons. The method generates a global test for whether any differences exist with respect to time and method as well as a test for the time effect being differential between methods. All tests were significant at the 5% level, which led us to investigate method comparisons for each time point using Fisher's LSD method. This method tests each comparison at the 5% level using a pooled estimate of variance based upon the entire experiment. By these tests, a ratio of one would indicate that both structures had fully recovered. Those time-points with statistical significance ($P < 0.05$) are marked in Figure 6B with a line. Both structures appear fully recovered after 15 min. Even if the recoveries fell outside the 95% probability window, no stress fiber recovery was more than 10% below focal adhesion recovery.

DISCUSSION

Until recently, localization studies of cytoskeletal components have relied upon antibody staining of fixed cells, or microinjection of fluorescently-labeled proteins into living cells. Limitations to microinjection techniques include the risk of protein denaturation following fluorochrome conjugation, fluorophore disruption of normal protein function, and primarily the risk of overloading cells with excess injected protein. Although recent flu-
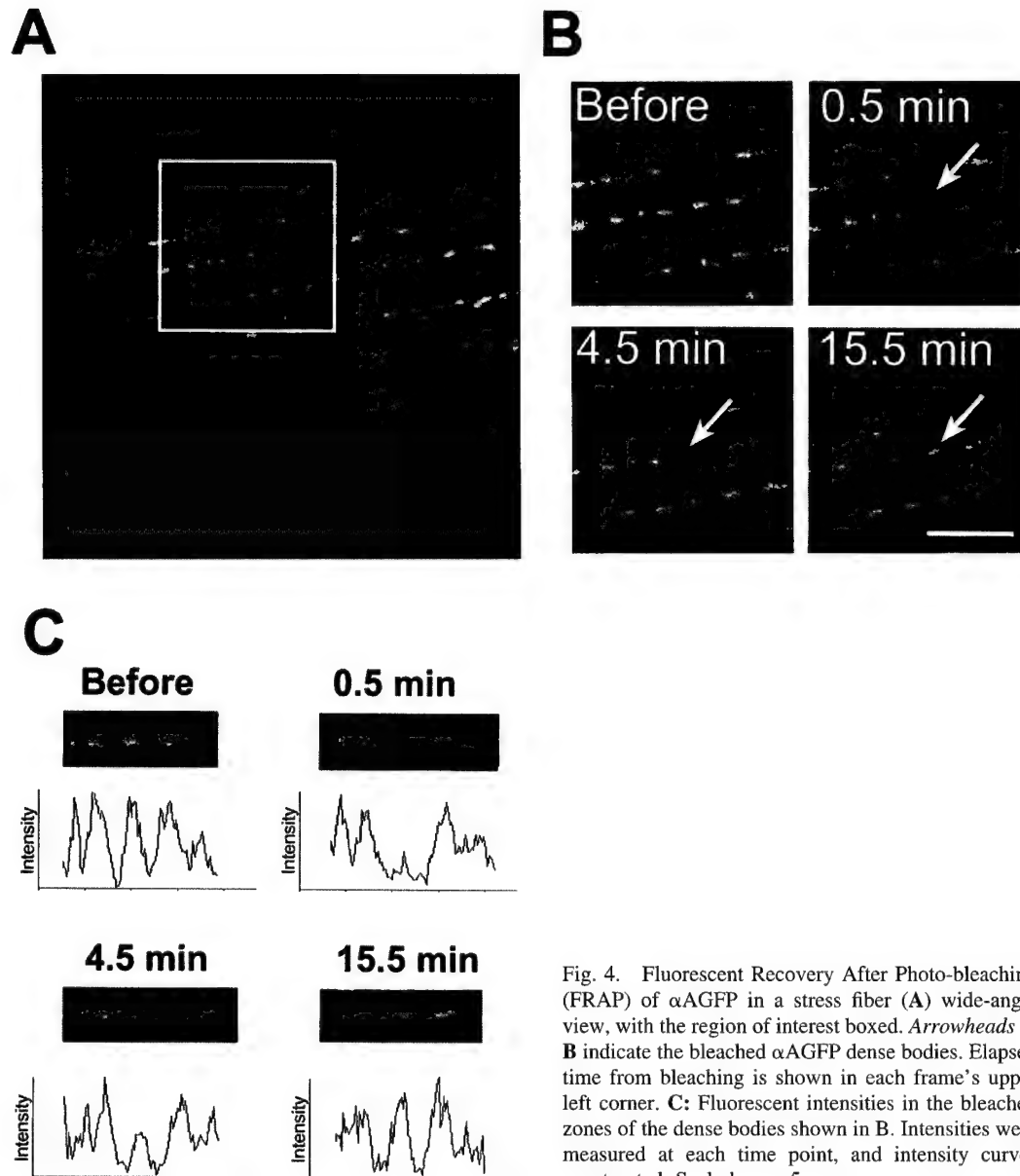
Fig. 4. Fluorescent Recovery After Photo-bleaching (FRAP) of αAGFP in a stress fiber (**A**) wide-angle view, with the region of interest boxed. *Arrowheads* in **B** indicate the bleached αAGFP dense bodies. Elapsed time from bleaching is shown in each frame's upper left corner. **C:** Fluorescent intensities in the bleached zones of the dense bodies shown in B. Intensities were measured at each time point, and intensity curves constructed. Scale bar = 5 μm.

orophore and detector innovations improve the sensitivity of such microinjections, fusing Green Fluorescent Protein (GFP) to a protein and transfecting cells with the construct provides a less invasive means for studying protein rearrangements in living cells. We fused GFP to α-actinin (αAGFP) and used the construct together with videomicroscopy and Fluorescence Recovery After Photobleaching (FRAP) to qualitatively and quantitatively follow α-actinin's dynamics in the focal adhesions and stress fibers of living cells.

The recruitment order of the many structural and regulatory proteins within focal adhesions has been debated in past years. In 1992, Nuckolls et al. used microinjection of anti-talin antibodies to demonstrate that talin is a required component of newly-forming focal adhesions [Nuckolls et al., 1992]. At that time, it was postulated that talin could form the initial linkage between cytoskeletal actin and transmembrane integrins, with α-actinin joining this linkage only in more mature focal adhesions. However, in 1995, Miyamoto et al. used coated beads to form artificial focal adhesions and demonstrated that α-actinin was recruited to sites of integrin clustering at the same time as both talin and vinculin [Miyamoto et al., 1995]. Although our experiments do not provide a direct comparison of the rate at which protein components are recruited to the focal adhesions, the αAGFP localization patterns in time-lapse images of newly spread cells do provide compelling visual evi-
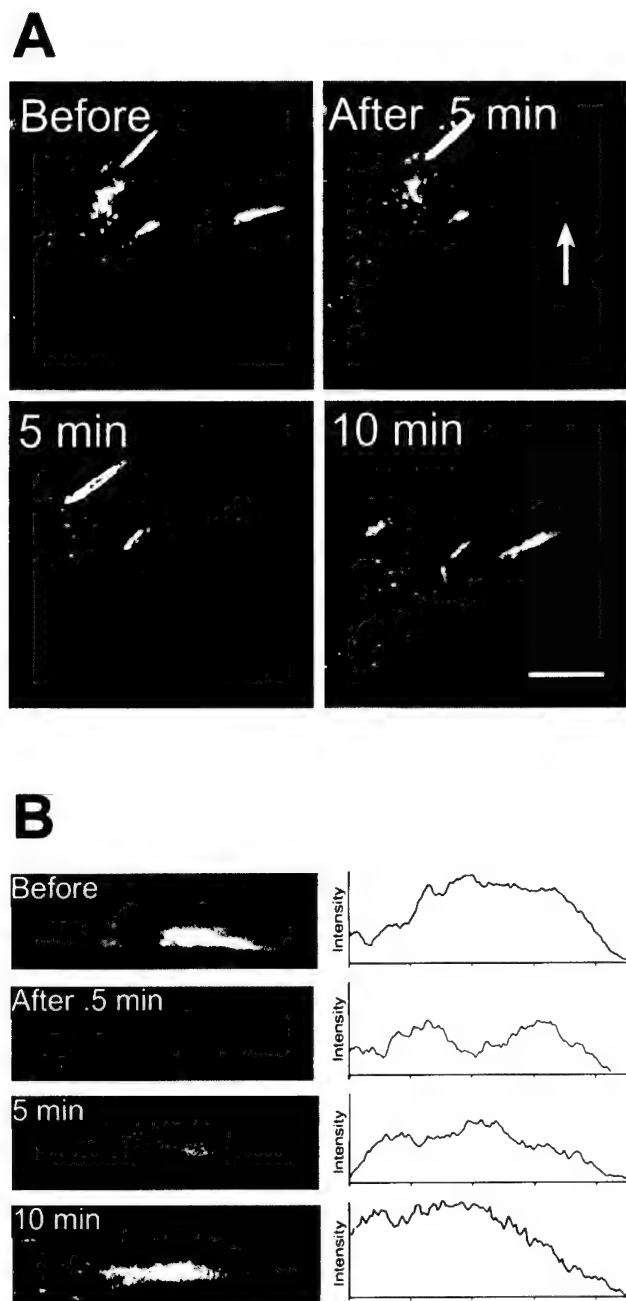
A

B

Fig. 5.   Fluorescent Recovery After Photo-bleaching (FRAP) assay of a focal adhesion within an αAGFP-transfected fibroblast. **A:** Fluorescence recovery in a focal adhesion. *Arrow* indicates the bleached area. Elapsed time from bleaching is shown in each frame's upper left corner. **B:** The average fluorescent intensities in the focal adhesion were measured, and intensity profiles for each time point are shown to the right of each focal adhesion. Scale bar = 5 μm.

Fig. 6.   αAGFP replacement rates in focal adhesion and dense bodies along stress fibers. **A:** Both stress fiber dense bodies (*circles, solid lines*) and focal adhesions (*diamonds, dotted lines*) recovered their fluorescence completely within 15 min of photo-bleaching. All points are the average of nine individual structures with Standard Deviations shown as error bars. αAGFP replacement rates in focal adhesion and dense bodies along stress fibers. **B:** Statistical comparison of the recovery of the two α-actinin containing structures at each time point. Using the Analysis of Variance (ANOVA) models, a ratio of 1 indicates that fluorescence intensity in both of the two structures (focal adhesions vs. stress fibers) is fully recovered. Both structures were fully recovered by 15 min. The regions indicated for each time point represent the 5% confidence window.

dence that α-actinin is present in recently formed focal adhesions. The fan-shaped arrays of αAGFP-coated actin fibers that we found radiating from many focal adhesions suggest that integrins are attached to small bundles of actin microfil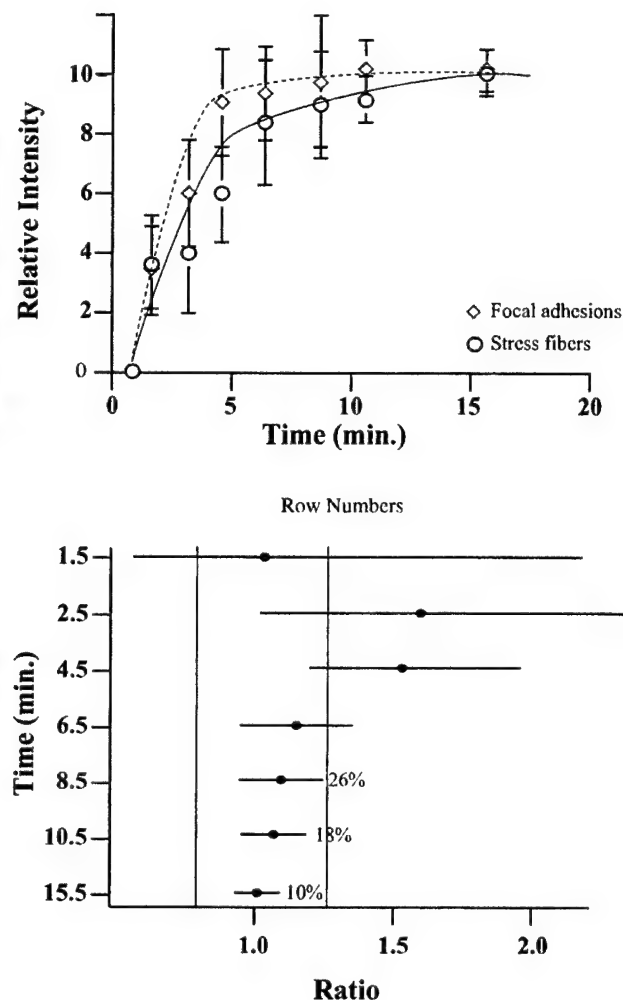aments at the time that a focal adhesion forms, and that lateral associations between the small bundles may subsequently produce the larger stress fibers. When a muscle-specific isoform of α-actinin was expressed as a GFP fusion in cardiac myocytes, in order to monitor the formation of myofibrils in living cells, myofibrils were also seen to form from the lateral coalescence of small pre-myofibrils [Dabiri et al., 1997]. Furthermore, the even distribution of our αAGFP construct on the fanning actin filaments suggests that con-

densation of α-actinin into periodic dense bodies along the stress fibers is subsequent to the re-localization of α-actinin to the actin fiber. The assembly of the α-actinin-containing periodic dense bodies is thought to follow the formation of flanking myosin structures along the small actin filaments [Verkhovsky et al., 1995]. One model suggests that activation of myosin light chain kinase (MLCK) may be responsible for collecting small actin filaments into stress fibers, and for the clustering of integrins to form focal adhesions [Chrzanowska-Wodnicka and Burridge, 1996]. Focal adhesion stability has also been suggested to depend upon acto-myosin driven contractions [Zamir et al., 1999]. Consistent with models of myosin involvement, we also witnessed focal adhesions forming in response to cell contraction, as well as the recruitment of αAGFP from lamellipodia to new focal adhesion sites (data not shown).

FRAP quantification of αAGFP exchange rates in stress-fiber dense bodies and focal adhesions revealed no significant difference between the two structures. Thus, despite known differences in protein compositions, key rate determining or regulatory factors may be common to both structures. Actin itself is notably found in both structures and has been argued to be α-actinin's primary binding partner, using comparative Resonance Energy Transfer analysis [Kam et al., 1995]. Our finding of rate similarities rather than differences is in agreement with one past microinjection study [Glück and Ben-Ze'ev, 1994], but differs from another [McKenna et al., 1985]. Recent evidence that there are at least three different forms of focal adhesions [Zamir et al., 1999], could clarify the issue, as by this model the focal adhesions we bleached were "classical" Focal Contacts (FC), while McKenna et al. [1985] may have studied "mosaic" FC. Moreover, cell-line specific variations in the compositions of focal adhesions and stress fibers could affect fluorescence recovery rates for the α-actinin interacting with these components. Recovery appeared biphasic in both structures, reaching ~80% at approximately 6 min, before continuing more slowly to completion by 10–15 min, a property that may be attributable to the initially rapid rearrangements of labeled proteins within the structures themselves, followed by a slow exchange with the cytosolic protein pool.

In both stress fibers and focal adhesions, αAGFP redistribution was complete by 15 min post-bleach. This result is similar to McKenna et al.'s results [1985] but unlike Geiger et al.'s data [1984a] which reported 40% final fluorescence recovery in focal adhesions, obtained by using microinjection of fluorescently-tagged α-actinin. In addition, the rate of recovery in our experiments was twice as rapid as that measured by Geiger et al. using microinjection. Two unresolved possibilities are that the GFP fusion to α-actinin could change the protein's binding interactions with some untested binding partner and that access to the focal adhesion and stress fiber structures could be decreased by fusion of α-actinin to GFP. Since steric interference would be expected to occur with both kinds of labeled proteins (GFP and other fluorophores), this second possibility seems unlikely. Notably, our immunoprecipitations provide evidence that αAGFP-s access to focal adhesion proteins such as vinculin and integrin is not impaired in vivo.

αAGFP has proven to be a useful tool for visual exploration of the living cytoskeleton and for quantification of the molecular dynamics within discrete cytoskeletal structures. Recent advances in GFP technology offer the possibility of expressing additional cytoskeletal proteins with blue or yellow forms of GFP, thus allowing simultaneous imaging of interacting elements.

ACKNOWLEDGMENTS

REFERENCES

Balzar M, Bakker HA, Briaire-de-Bruijn IH, Fleuren GJ, Warnaar SO, Litvinov SV. 1998. Cytoplasmic tail regulates the intercellular adhesion function of the epithelial cell adhesion molecule. Mol Cell Biol 18:4833–4843.

Beggs AH, Byers T J, Knoll JHM, Boyce FM, Bruns GAP, Kunkel LM. 1992. Cloning and characterization of two human skeletal muscle α-actinin genes located on chromosomes 1 and 11. J Biol Chem 267:9281–9288.

Belkin AM, Retta SF, Pletjushkina OY, Balzac F, Silengo L, Fassler R, Koteliansky VE, Burridge K, Tarone G. 1997. Muscle beta1D integrin reinforces the cytoskeleton-matrix link: modulation of integrin adhesive function by alternative splicing. J Cell Biol 139:1583–1595.

Chalfie M. 1995. Green fluorescent protein. Photochem Photobiol 62:651–656.

Chrzanowska-Wodnicka M, Burridge K. 1996. Rho-stimulated contractility drives the formation of stress fibers and focal adhesions. J Cell Biol 133:1403–1415.

Critchley DR, Holt MR, Barry ST, Priddle H, Hemmings L, Norman J. 1999. Integrin-mediated cell adhesion: the cytoskeletal connection. Biochem Soc Symp 65:79–99.

Dabiri GA, Turnacioglu KK, Sanger JM, Sanger JW. 1997. Myofibrillogenesis visualized in living embryonic cardiomyocytes. Proc Natl Acad Sci USA 94:9493–9498.

Feramisco JR. 1979. Microinjection of fluorescently labeled α-actinin into living fibroblasts. Proc Natl Acad Sci 76:3967–3971.

Geiger B, Avnur Z, Kreis TE, Schlessinger J. 1984a. The dynamics of cytoskeletal organization in areas of cell contact. Cell Muscle Motil 5:195–234.

Geiger B, Avnur Z, Rinnerthaler G, Hinssen H, Small VJ. 1984b. Microfilament-organizing centers in areas of cell contact: cytoskeletal interactions during cell attachment and locomotion. J Cell Biol 99:83–91.

Giancotti FG, Ruoslahti E. 1999. Integrin signaling. Science 285:1028–1032.

Glück U, Ben-Ze'ev A. 1994. Modulation of α-actinin levels affect cell motility and confers tumorigenicity on 3T3 cells. J Cell Sci 107:1773–1782.

Glück U, Kwiatkowski DJ, Ben-Ze'ev, A. 1993. Suppression of tumorigenicity in simian virus 40-transformed 3T3 cells transfected with α-actinin cDNA. Proc Natl Acad Sci 90:383–387.

Hemler ME. 1998. Integrin associated proteins. Curr Opin Cell Biol 10:578–585.

Honda K yamada T, Endo R, Ino Y, Gotoh M, Tsuda H, Yamada Y, Chiba H, Hirohashi S. 1998. Actinin-4, a novel actinin-bundling protein associated with cell motility and cancer invasion. J Cell Biol 140:1383–1393.

Hsu JC. 1996. Multiple comparisons: theory and methods. London: Chapman and Hall.

Kam Z, Volberg T, Geiger B. 1995. Mapping of adherens junction components using microscopic resonance energy transfer imaging. J Cell Sci 108:1051–1062.

Knudsen KA, Soler AP, Johnson KR, Wheelock, MJ. 1995. Interaction of α-actinin with the cadherin/catenin cell-cell adhesion complex via α-catenin. J Cell Biol 130:67–77.

Lazarides E, Burridge K. 1975. α-actinin: immunofluorescent localization of a muscle structural protein in nonmuscle cells. Cell 6:289–298.

Lewis JM, Schwartz MA. 1995. Mapping in vivo associations of cytoplasmic proteins with integrin beta 1 cytoplasmic domain mutants. Mol Biol Cell 6:151–160.

Ludin B, Matus A. 1998. GFP illuminates the cytoskeleton. Trends Cell Biol 8:72–77.

McKenna MN, Meigs JB, Wang Y-L. 1985. Exchangeability of α-actinin in living cardiac fibroblasts and muscle cells. J Cell Biol 101:2223–2232.

Miyamoto S, Teramoto H, Coso OA, Gutkind JS, Burbelo PD, Akiyama SK, Yamada KM. 1995. Integrin function: hierarchies of cytoskeletal and signaling molecules. J Cell Biol 131:791–805.

Neter J, Wasserman W, Kunter MH. 1990. Applied linear statistical models. Burr Ridge, IL: Burr Ridge, pp 420.

Nuckolls G H, Romer LH, Burridge K. 1992. Microinjection of antibodies against talin inhibits spreading and migration of fibroblasts. J Cell Sci 102:753–762.

Ozawa M. 1998. Identification of the region of alpha-catenin that plays an essential role in cadherin-mediated cell adhesion. J Biol Chem 273:29524–2959.

Otey CA, Pavalko FM, Burridge K. 1990. An interaction between α-actinin and the beta 1 integrin subunit in vitro. J Cell Biol 111:721–729.

Otey CA, Vasquez GB, Burridge K, Erickson B W. 1993. Mapping of the α-actinin binding site within the beta 1 integrin cytoplasmic domain. J Biol Chem 268:21193–2119.

Pavalko FM, LaRoche SM. 1993. Activation of human neutrophils induces an interaction between the integrin β_2-subunit (CD18) and the actin binding protein α-actinin. J Immunol 151:3795–3807.

Pavalko FM, Schneider G, Burridge K, Lim S-S. 1995. Immunodetection of α-actinin in focal adhesions is limited by antibody inaccessibility. Exp Cell Res 217:534–540.

Swaminathan R, Hoang CP, Verkman AS. 1997. Photobleaching recovery and anisotropy decay of green fluorescent protein GFP-S65T in solution and cells: cytoplasmic viscosity probed by green fluorescent protein translational and rotational diffusion. Biophys J 72:1900–1907.

Verkhovsky AB, Svitkina TM, Borisy GG. 1995. Myosin II filaments assemblies in the active lamella of fibroblasts: their morphogenesis and role in the formation of filament bundles. J Cell Biol 131:989–1002.

Yamada KM, Geiger B. 1997. Molecular interactions in cell adhesion complexes. Curr Opin Cell Biol 9:76–85.

Youssoufian H, McAfee M, Kwiatkowski DJ. 1990. Cloning and chromosomal localization of the human cytoskeletal α-actinin gene reveals linkage to the α-spectrin gene. Am J Hum Genet 47:62–72.

Zamir E, Katz BZ, Aota S, Yamada KM, Geiger B, Kam Z. 1999. Molecular diversity of cell-matrix adhesions. J Cell Sci 112:1655–1669.

CELL MOTILITY

AND CYTOSKELETON
THE

Volume 48, Number 3, March 2001

Articles

Cover image: A Swiss 3T3 fibroblast transiently transfected with α-actinin-GFP construct and co-stained with phalloidin, seen in contact with neighboring fibroblasts that are not transfected. See the accompanying article by Edlund et al., on pages 190–200 in this issue.

WILEY   This journal is online
InterScience®
www.interscience.wiley.com

met Independent Hepatocyte Growth Factor regulation of cell adhesion in prostate cancer cell lines

Magnus Edlund[1], Michael J. Bradley[2], Robert A. Sikes[2], and Leland W.K. Chung[1]

[1] Department of Urology, Emory University, Winship Cancer Institute, Atlanta, GA 30322, [2]Department of Urology, University of Virginia Health System, Charlottesville, Virginia, 22908 USA.

Author for Correspondence: Leland W.K. Chung, Department of Urology, Emory University, B3108 Winship Cancer Institute, 1365-B Clifton Rd., N.E., Atlanta, GA 30322. Phone: (404) 778 2538. Fax: (404) 778 5016 E-mail: Chung@emory.edu

Abstract

Cell behaviors in prostate epithelia and the surrounding stroma are reciprocally regulated, with each tissue secreting factors for interpretation by the other. Changes in either stromal signals or epithelial signal reception can result in cancerous progression in the prostate, affecting cell-matrix adhesion, in concert with the cell motility and invasive behaviors based upon this adhesion. We find that treatment of prostate cancer cells with secreted factors from the stroma results in variation in cell-matrix attachment behaviors, and have sought candidate regulators of these behaviors, using prostate cancer cell lines of different metastatic potential (PC3, PC3M, DU145, LNCaP, and C4-2), along with blocking antibodies against specific stromal factors and integrin cell adhesion molecules. We have identified Hepatocyte Growth Factor (HGF) as a major signaling component of prostate stromal-conditioned media. Its "removal" from conditioned media via blocking antibodies also removes the adhesion-stimulatory effects of the media. Likewise, addition of purified HGF to control media mimics stromal conditioning. The prostate cancer cell line C4-2 responds to HGF in a concentration-dependent manner, by increasing its adhesion and reducing its migration on laminin substrata. HGF's effects are not due to shifts in the expression levels of laminin-binding integrins, nor strikingly, can they be linked to expression of HGF's known receptor met, as neither LNCaP nor clonally-derived C4-2 sublines contains any detectable met protein. Even in the absence of met, however, the response to HGF treatment by C4-2 prostate cells does include Focal Adhesion Kinase (FAK) phosphorylation, similar to that seen in met-containing cell lines following their exposure to HGF. Finally, co-immunoprecipitation and sequencing have identified the membrane-bound form of the protein Nucleolin as a major binding partner of HGF in C4-2 cells. This finding further supports previous suggestions that both nuclear and membrane-localized nucleolin could support cell reception of heparin-binding growth factors.

2

Introduction

In the prostate, cell-matrix adhesion, cell motility and invasive behaviors are regulated by an interplay of signals between the epithelia and surrounding stroma. When adhesion-based behaviors are altered by changes in the signals, their reception, or the intracellular interpretation of their meaning, tumor formation and cancer progression can result. Signal reciprocity ensures that prostate stromal fibroblasts can control epithelial cell proliferation (Nemeth and Lee 1996), while epithelial cells control stromal smooth muscle maturation (Cunha et al. 1992), and when cancerous, signal to optimize their own stromal growth environment (Law et al., in preparation). The list of established prostate regulatory factors is exceptionally long, containing representatives of many growth factor families, among them, Hepatocyte Growth Factor (HGF; (Liotta et al. 1986), a subject of this study.

HGF regulates cell behaviors in development, regeneration and cancer (Santos et al. 1993; Schmidt et al. 1995; Thery et al. 1995; Andermarcher et al. 1996; Gohda et al. 1998; Ohmichi et al. 1998) and is heavily studied in many systems, but the growth factor's source, reception by, and effects on prostate cancer cells have proven difficult to define. Expression of met, the known HGF receptor, correlates with cancerous transformation in numerous cancers (Di Renzo et al. 1992; Jucker et al. 1994; Pisters et al. 1995; D'Errico et al. 1996; Hiscox et al. 1997; Inoue et al. 1998; de Luca et al. 1999; Helou et al. 1999; Ferracini et al. 2000)), although not all prostate cancers. met is found by immunostaining in 90% of high grade prostatic intraepithelial neoplasia (PIN), and 75 - 100% of lymph node and bone secondary tumors (Humphrey et al. 1995; Pisters et al. 1995), but overall, is expressed in only 45% of prostatic carcinomas (Humphrey et al. 1995). Thus, cancer progression models that call on HGF to act as a paracrine factor for cancer progression via the met receptor must take into account the lack of met in some cancerous prostate cells and the possibility of a met-independent response to HGF.

Further complicating our understanding of HGF's roles in prostate cancer are the factor's multiple, sometimes contradictory, effects on cell behavior. Also called Scatter Factor (SF), HGF is known to stimulate motility in both endothelial and epithelial metastatic cancers (Birchmeier et al. 1997; Meiners et al. 1998; Nishimura et al. 1998; Nishimura et al. 1999)), and has a number of similarities to the invasion promoting factor plasminogen (Nakamura et al. 1989; Bottaro et al. 1991; Kim et al. 1998). It is not surprising, then, that HGF levels affect the function of prostate cell lines' integrin molecules (Nishimura et al. 1998; Nishimura et al. 1999), molecules involved in cell adhesion and motility. However, multiple past studies have credited HGF with both apoptotic and proapoptotic activities (**refs**), discrepancies which could be attributed to the multiple splice variants that exist for both HGF and its receptor met, or to differences in cell signalling machinery contained by each experimental system. Variants of met that differ in the splicing of their cytoplasmic domains do appear to change intracellular binding partners (**ref**), but the possibility that HGF acts through multiple receptors and/or signalling cascades to bring about a plethora of cell responses should not be dismissed.

3

Using blocking antibodies and purified protein, we have identified HGF as a major secreted factor responsible for the changes in cell spreading we previously observed in prostate cancer cell lines treated with stromal-conditioned media. Earlier work from our laboratory showed that stromal-conditioned media increased cell spreading of metastatic C4-2 cells, while having little effect on attachment of the lineage-related, but less metastatic LNCaP cell line (Edlund et al. 2001). We have now extended this comparison, focusing on these cell lines' integrin-based responses to HGF, in particular, their HGF-regulated shifts in cell attachment, cell motility, integrin expression and use, and Focal Adhesion Kinase (FAK) phosphorylation. After assaying the expression levels of the met HGF receptor in LNCaP, C4-2 and other prostate cancer cell lines, and finding met to be lacking in both LNCaP and C4-2 lines, despite their concentration dependent response to HGF, we have searched for novel HGF ligands in these cells, and have identified the protein nucleolin as an HGF binding partner. Nucleolin, an abundant nuclear protein (Ginisty et al. 1999; Srivastava and Pollard 1999) is also found on the cell surface, where it has been shown to interact with heparin-bound growth factors (Callebaut et al. 2001), just as HGF's known receptor met does **(Ref)**.

Materials and Methods

Cell Culture, Antibodies, Extracellular Matrix and Growth Factors

Prostate and stromal cell lines were maintained at 37°C, in T-media with 5% fetal bovine serum, 100 U/ml penicillin and 100 mg/ml streptomycin. Conditioned media were prepared by adding fresh media to cell cultures at 80% confluency, and removing it for use after 48 hours exposure to the cells. Laminin-1 (a kind gift of Roy Ogle at University of Virginia) was purified from Engelbreth-Holme-Swarm (EHS) tumors according to Davis et al., 1989, based on the protocol of Kleinman et al., 1983. Hepatocyte Growth Factor (HGF) was from Sigma (St. Louis, MO). Function-blocking antibodies to integrin subunits were all obtained from Chemicon (Emecula, CA). Anti-FAK and HGF antibodies were from Sigma (St. Louis, MO). Antibodies to nucleolin were purchased from Santa Cruz Biotechnology (Santa Cruz,CA) and received as a gift from Dr. Deng at Pittsburgh Medical Center. met antibodies were purchased from both UpState Biotechnology (Lake Placid, NY) and Transduction Laboratories (Lexington, KY). Phosphotyrosine antibodies were from Transduction Laboratory (Lexington, KY), and all secondary-conjugated antibodies were from Jackson Immunochemicals (West Grove, PA).

Reverse Transcription.

Total cellular RNA was isolated with RNA-STAT (BioTec-X, Houston, TX), a protocol using chaotropic salts followed by organic extraction, essentially as described by Chomczynski and Sacchi (Chomczynski and Sacchi 1987), RNA was resuspended in DEPC-treated sterile water and its concentration determined spectrophotometrically at 260 nm, using a Beckman DU650 spectrophotometer (Beckman Coulter Inc., Fullerton, CA). 5 μg of total cellular RNA was reverse transcribed using the OmniScript RT Kit (Qiagen, Inc., Valencia, CA), according to manufactures instructions. In brief, RNA was combined with 1X Omni-RT buffer, 10 μg/μl of each oligo $d(T)_{12}$ and random hexamer primer $pd(N)_6$ (Amersham Pharmacia, Piscataway, NJ), 0.25 U/μl RNasin RNAse inhibitor (LifeTechnologies Inc., Gaithersburg, MD), and sterile water to 16.5 μl. The reaction mixture was heated to 90°C for 3 minutes, then cooled on ice. 0.25 U/μl RNasin, 1 μl OmniScript RT, and dNTPs (0.5 mM final) were then added, and the transcription reaction allowed to proceed for 1 hour at 37°C.

Polymerase Chain Reaction.

Two microliters of the cDNA reaction (corresponding to 0.25 μg of total RNA) were used in the PCR reaction. The forward met primer (F-met) was 5'-GGTTGCTGATTTTGGTCAT-3' and the reverse primer (B-met) was 5'-TTCGGGTTGTGGAGTCTT-3'. These were used at 50 pmoles per reaction with 0.25 mM dNTPs, 7.5 mM $MgCl_2$, 1X platinum Taq buffer (LifeTechnologies, Inc.), 0.5% DMSO (Sigma Chemical Co., St. Louis, MO) and 0.3 μl of platinum taq DNA polymerase, in a reaction volume of 50 μl. The thermalcycle parameters were 1hr.45min. at 95°C, followed by 35 cycles of 30 min. at 94°C; 30 min. at 58°C and 30 min. at 72°C. A final extension of 7 hr. at 72°C was added to complete elongation. 20% of the PCR reaction was separated electrophoretically, using 2% agarose (LifeTechnologies)/0.5x TAE (40 mM Tris-acetate, 5 mM EDTA) to determine relative production of met product in the prostate cell lines.

Immunoprecipitation

Cells were serum starved for 48 hours and allowed to grow to 80% confluency. Plates were rinsed twice in ice-cold phosphate buffered saline (PBS), and solubilized in lysis buffer (1% NP-40, 50 mM Tris-HCl, 150 mM NaCl, 2 mM EDTA, 50 mg/ml leupeptin, 0.5% aprotinin, 1 mM sodium orthovanadate, 1 mM PMSF). Insoluble material was removed by centrifugation for 30'' at 10,000 x g, at 4°C. Protein concentration was determined by BRC assay (BioRad, Hercules, CA), and 1-2 mg of protein used for each immunoprecipitation condition. Antibodies were incubated with the cell lysate for 2 hrs at 4°C, and an additional 30 min. with Protein A/G-sepharose beads (Sigma). The beads were washed three times with lysis buffer and resuspended in SDS-PAGE loading buffer. Samples were resolved on gradient (4-12%) or 10% polyacrylamide gels (Novex) and electro-blotted. After transfer, the filters were blocked in BSA (5%) overnight, at 4°C. Filters were incubated with primary antibodies for 1 hr, at room temperature. Membranes were then probed for 1 hr with peroxidase-conjugated secondary antibody (diluted 1:5000; Jackson Immunoresearch Labs, Bar Harbor, ME) and the proteins detected with Enhanced Chemi-Luminescence (ECL).

Substrate Adhesion and Growth Assay

Attachment assays were performed as previously described in Edlund et al., 2001, and Vafa et al., 1998. Cell lines were grown to confluence, trypsinized, and re-plated (1:8) on tissue culture dishes, where they were allowed to grow for another two days, before being lifted after a brief treatment with 10 mM EDTA, 20 mM Hepes buffer in T-media. After neutralizing the EDTA with $CaCl_2$ and $MgSO_4$, the cells were washed with T-media containing 0.1% BSA. Cells were placed on laminin-coated dishes (laminin from EHS tumors), allowed to adhere for 30 to 90 minutes with or with out addition of either HGF or function blocking integrin antibodies, and then fixed in formaldehyde. The percentage of spread cells was scored for each cell line, and all values were normalized to control cells treated identically only without being subjected to conditioned media or growth factors. Cell growth was quantified using MTT (Carmichael et al., 1987; Romijn et al., 1988).

Flow Cytometry Analysis

Cell cultures below 70% confluence were detached from tissue culture plates and suspended as single cells using a brief treatment of 10 mM EDTA, 20 mM Hepes buffer (pH 7.4) in T-media. The EDTA was neutralized with $CaCl_2$ and $MgSO_4$, and the cells washed again with T-media containing 0.1% BSA. 2.5×10^5 cells were used for each condition. Cells and primary antibodies (30µg/ml) were incubated for 60 min. at 4°C, washed, and further incubated with secondary FITC-labeled goat anti-mouse (30µg/ml) antibody for an additional 60 min., at 4°C. Following three brief washes, 1×10^4 cells were analyzed for fluorescence, using a FACS scan (Becton Dickinson, San Jose, CA). Cells treated with isotype-specific immuoglobulins served as controls. For both cell types, the relative fluorescence intensity was expressed as the increase over background fluorescence. Data points are presented as the mean of two independent experiments, with a range in parentheses.

ELISA Detection of HGF

ELISAs were performed as suggested in Pharmigen Research Products Catalog, 1999. Briefly, rabbit anti-human HGF antibodies (gift of Dr XXXX, Osaka University Medical School) were diluted to a concentration of 1μg/ml in 0.1M Na_2HPO_4 and 0.1M NaH_2PO, pH 9.0. Wells of a 96 well ELISA plate (Costar) were filled with 50 μl, sealed with parafilm, and incubated overnight at 4°C. Plates were then brought to room temperature and antibodies captured and removed. 200 μl of blocking buffer (10% FBS in PBS) was added to each well and incubated at room temperature for 2 hours. The plate was washed three times with PBS/Tween 20 (0.05%) (Sigma, St. Louis, MO). 100 μl of standard or sample diluted in blocking buffer/Tween 20 (0.05%) was added to each plate, which was then sealed with parafilm, and incubated at 4°C overnight. On day 3, the plate was washed four times with PBS/Tween. 100ul of the detection antibody, Goat anti-human HGF antibody (Sigma, St. Louis, MO), diluted to a concentration of 0.01μg/ml in blocking buffer/Tween 20, was added to each well, incubated at room temperature for one hour, and washed four times in PBS/Tween 20. 100 μl of Avidin-Horseradish Peroxidase conjugated mouse anti-goat IgG (Jackson ImmunoReseach, West Grove, PA) diluted 1:1000 in blocking buffer/Tween 20 was added to each well. After 30 minutes incubation at room temperature and five washes with PBS/Tween 20, 200 μl of Sigma Fast OPD solution (Sigma, St. Louis, MO) was added to each well. After 20 minutes, the plate was read at a wavelength of 405nm using a microplate reader (Molecular Devices, Sunnyvale, CA); data was analyzed using the Molecular Devices SOFTmax program.

Cell Migration

Cell migration assays were preformed according to product instructions (CSM Inc. Phoenix, AZ). Chilled cell manifolds were placed on Teflon-printed, precoated microscope slides, subdivided into 10 wells, and filled with cold media. 1 ul of cell suspension (2500 cells) was added to each chamber and allowed to precipitate by gravity and adhere to the coverslip. After two hours, the manifold was moved to a cell incubator (37°C under 5% CO_2) and allowed to reach growth temperature for four hours, at which point the cell sedimentation manifold was removed and the coverslip submerged in media, to which HFG was added. The area covered by cells was recorded at 2 hrs and subsequently every 24 hours. The 2 hr area was used as a reference point for all succeeding measurements. Results are presented as increases relative to this area.

Protein sequencing

The HGF and major co-immunoprecipitated product from C4-2 cell lysates were excised from the gel and transferred to a siliconized tube, washed and destained in 50% methanol overnight. The gel pieces were dehydrated in aceto-nitrile, rehydrated in 10 mM Dithiolthreitol (DTT) in 0.1 M Ammonium bicarbonate, and reduced at room temperature for 30 minutes. The DTT solution was removed and the samples alkylated in 50 mM iodoacetamide, in 0.1 M ammonium bicarbonate, for 30 minutes at room temperature. Samples were then dehydrated again in aceto-nitrile, rehydrated in 0.1 M Ammonium bicarbonate, dehydrated in acento-nitrile and completely dried by vacuum

7

centrifugation. Finally, samples were he rehydrated for 10 minutes in 20ng/ml trypsin in 50 mM Ammonium bicarbonate, on ice. Any excess trypsin solution was removed, and 50 mM ammonium bicarbonate added. Samples were digested overnight at 37 C.

Statistical analyses
Results were analyzed for statistical significance using the nonparametric Mann-Whitney U test, with significance at $P < 0.05$.

Results

In this study, we have identified Hepatocyte Growth Factor (HGF) as a major signalling component of prostate stromal-conditioned media. Its "removal" from conditioned media via blocking antibodies also removes the adhesion-stimulatory effects of the media. Likewise, addition of purified HGF to control media mimics stromal conditioning. The prostate cancer cell line C4-2 responds to HGF in a concentration-dependent manner, by increasing its adhesion and reducing its migration on laminin substrata. HGF's effects are not due to shifts in the expression levels of laminin-binding integrins, nor strikingly, can they be linked to expression of HGF's known receptor met, as neither LNCaP nor clonally-derived C4-2 sublines contains any detectable met protein. Even in the absence of met, however, the response to HGF treatment by C4-2 prostate cells does include Focal Adhesion Kinase phosphorylation, similar to that seen in met-containing cell lines following exposure to HGF. Finally, co-immunoprecipitation has identified the protein Nucleolin as a major binding partner of HGF in C4-2 cells.

Stromal-conditioned media affect attachment of all prostate cancer cell lines tested, except LNCaP

Stromal-conditioned media was recently found to increase spreading of the metastatic cell line C4-2, while having little effect on attachment of the lineage-related, but less metastatic LNCaP cell line (Edlund et al. 2001); Figure 1). We therefore sought the regulators of these attachment behaviors using blocking antibodies against soluble paracrine factors and human prostate epithelial cells with different tumorigenic ability. LNCaP, C4-2, DU145 and two PC3 cell lines were suspended in prostate stromal-conditioned media and allowed to adhere to laminin substrata. When the 25-40 % of cells that attach without treatment are set as 100% for normalization, all post-treatment cell attachments range from 150 to 200% except for that of the LNCaP cell line, which showed no increase in cell spreading under these conditions (Fig. 1).

HGF is naturally present in stromal-conditioned media, its effects blocked with antibodies, and mimicked by purified HGF

A host of growth factors have been shown to stimulate focal adhesion assembly. The concentration of HGF itself was identifiable in the stromal-conditioned media, at a concentration determined by Elisa to be between 15 and 25 ng/ml (Table 1). Addition of an antibody against Hepatocyte Growth Factor (HGF) markedly reduced stromal-conditioned media's ability to increase C4-2 cell adhesion (Fig. 2). Conditioned media were collected from five different primary cultures of human prostate stromal cells, from three different hosts, and were incubated with C4-2 cells in the presence or absence of an HGF antibody or an IgG control. A reduction of the stimulatory effect of the conditioned media on cell attachment was seen in all instances (Fig. 2).

Prostate cancer cell lines respond to HGF in a concentration-dependent manner

The increased cell spreading generated by HGF was concentration dependent for both the C4-2 and PC3 cell lines, with PC3 cells showing a greater increase in cell attachment than C4-2 at low HGF concentrations (Fig. 3). Both cell lines were stimulated maximally at HGF concentrations of 50 ng/ml. Strikingly, conditioned media containing only 7.5 and 12.5 ng/ml HGF, produced effects equivalent to those of much higher

9

concentrations of purified HGF, suggesting that the potency of the purified protein was compromised and/or that other stromal factors are involved.

Migratory behaviors are affected by HGF and are substrate dependent

In addition to increased attachment, C4-2 cells treated with HGF also displayed altered migratory behavior. While both a low and a high HGF concentration decreased cell migration on LM, we were surprised to notice that it had no affect on migration on FN substrata. C4-2 cells originally adhered in a round, confluent cell layer of known diameter. Cells were incubated in growth medium with 0, 10 or 100 ng/ml of HGF, and the increase in diameter of the confluent layer quantified. The change is presented as the fold increase over Day-0 diameter (Fig. 4). On laminin substrata both high and low HGF concentrations decreased migration, as predicted from the attachment experiments, while HGF had no visible effect on cell migration over FN substrata. The differences could not be explained by cell proliferation, because no change in C4-2 cell cycle was observed upon HGF stimulation (data not shown, manuscript in preparation). HGF did not stimulate adhesion on Fibronectin, Collagen (Col) or Vitronectin (VN) substrata either (Fig. 5).

HGF's effects are not due to shifts in integrin expression level

Blocking known laminin-binding integrin adhesion molecules could effectively reduce attachment in all cells, with or without conditioned-media treatment (Fig. 6). Just as C4-2 and LNCaP cells do not differ from one another in their expression of laminin-binding integrins (Edlund et al. 2001), but do differ in their attachment behaviors, so to does treatment with conditioned-media or purified HGF affect cell behavior without changing integrin expression (Table 2). Thus, it seems likely that integrin *affinity* rather than *expression level* are affected.

Variable responses of cell lines to HGF are not due to HGF's known receptor met

We measured transcript levels of the known HGF receptor met in LNCaP, C4-2, PC3 and DU145 prostate cancer cell lines using rtPCR. Levels of met transcript were 6 and 5 times higher respectively in PC3 and DU145 cells than they were in the LNCaP and C4-2 cell lines (Fig. 7). Because previous studies have not found mRNA and protein levels of met to be parallel (**ref**), we also determined the protein expression using antibodies for either the cytoplasmic or the extracellular domains of met. Although, expression was readily detected in DU145, PC3, PC3-M and HeLa cells, we did not detect met in LNCaP or C4-2 cells (Fig. 8). Immunoprecipitating total cell lysate in C4-2 and PC3 cells confirmed met's presence in HGF–stimulated PC3 cells and its absence in C4-2 cells (Fig. 9A).
Additional immunoprecipitation using HGF-conjugated agarose beads and subsequent staining with an antibody against the cytoplasmic domain of the met protein also confirmed met's presence in PC3 and absence in C4-2 cells (Fig. 10A). Note that control beads pulled down no detectable met protein from either PC3 or C4-2 lysates, as assayed by both silver staining and blotting. In C4-2 cells, two major band were visible upon silver staining, of approximate 60 kDa and 100 kDa sizes. The lower band represents HGF by itself, whereas the higher band was microsequenced and identified as Nucleolin, with an expected size of 98 kDa.

10

Phosphorylation of met and Focal Adhesion Kinase following HGF stimulation

Only in PC3, as previously shown, could met be seen to be tyrosine phosphorylated upon HGF stimulation (Fig. 9B, **ref**). The stimulation by HGF in C4-2 cells is further indicated by focal adhesion kinase (FAK) immunoprecipitation, which shows a decrease in phosphorylation at early time points, with a slow recovery and increase in phosphorylation after 30 minutes (Fig. 9C) in serum starved HGF stimulated attached cells. Such a response in C4-2 cells, taken together with the concentration-dependent adhesive and cell cycle responses noted above, suggests a met-independent pathway of HGF stimulation and integrin activation.

Nucleolin is an HGF binding partner in the C4-2 prostate cancer cell line

The higher band was identified as Nucleolin with an expected size of 98 kDA. A total 24 peptide was sequenced, approximately 30 % of the protein (Table 3). The identity of the 100 kDa protein was further confirmed by Western blotting to nucleolin (Fig. 10C). The sequence data showed a 100% match to the previously published protein sequence (NCBI#4885511). No other sequence homologies were found, suggesting that Nucleolin is the major protein in the 100 kDa band, and that Nucleolin is the major binding partner for HGF in the C4-2 cells.

Acknowledgements

References

Andermarcher, E., M. A. Surani and E. Gherardi (1996). "Co-expression of the HGF/SF and c-met genes during early mouse embryogenesis precedes reciprocal expression in adjacent tissues during organogenesis." Developmental Genetics **18**(3): 254-66.

Bellusci, S., G. Moens, J. P. Thiery and J. Jouanneau (1994). "A scatter factor-like factor is produced by a metastatic variant of a rat bladder carcinoma cell line." Journal of Cell Science **107**(Pt 5): 1277-87.

Birchmeier, W., V. Brinkmann, C. Niemann, S. Meiners, S. DiCesare, H. Naundorf and M. Sachs (1997). "Role of HGF/SF and c-Met in morphogenesis and metastasis of epithelial cells." Ciba Foundation Symposium **212**: 230-40; discussion 240-6.

Borer, R. A., C. F. Lehner, H. M. Eppenberger and E. A. Nigg (1989). "Major nucleolar proteins shuttle between nucleus and cytoplasm." Cell **56**(3): 379-90.

Bottaro, D. P., J. S. Rubin, D. L. Faletto, A. M. Chan, T. E. Kmiecik, G. F. Vande Woude and S. A. Aaronson (1991). "Identification of the hepatocyte growth factor receptor as the c-met proto-oncogene product." Science **251**(4995): 802-4.

Callebaut, C., S. Nisole, J. P. Briand, B. Krust and A. G. Hovanessian (2001). "Inhibition of HIV infection by the cytokine midkine." Virology **281**(2): 248-64.

Chan, A., J. Rubin, D. Bottaro, D. Hirschfield, M. Chedid and S. A. Aaronson (1993). "Isoforms of human HGF and their biological activities." EXS **65**: 67-79.

Chan, A. M., J. S. Rubin, D. P. Bottaro, D. W. Hirschfield, M. Chedid and S. A. Aaronson (1991). "Identification of a competitive HGF antagonist encoded by an alternative transcript." Science **254**(5036): 1382-5.

Chomczynski, P. and N. Sacchi (1987). "Single-step method of RNA isolation by acid guanidinium thiocyanate-phenol-chloroform extraction." Analytical Biochemistry **162**(1): 156-9.

Cunha, G. R., E. Battle, P. Young, J. Brody, A. Donjacour, N. Hayashi and H. Kinbara (1992). "Role of epithelial-mesenchymal interactions in the differentiation and spatial organization of visceral smooth muscle." Epithelial Cell Biology **1**(2): 76-83.

D'Errico, A., M. Fiorentino, A. Ponzetto, Y. Daikuhara, H. Tsubouchi, C. Brechot, J. Y. Scoazec and W. F. Grigioni (1996). "Liver hepatocyte growth factor does not always correlate with hepatocellular proliferation in human liver lesions: its specific receptor c-met does." Hepatology **24**(1): 60-4.

14

de Luca, A., N. Arena, L. M. Sena and E. Medico (1999). "Met overexpression confers HGF-dependent invasive phenotype to human thyroid carcinoma cells in vitro." Journal of Cellular Physiology **180**(3): 365-71.

Derenzini, M., V. Sirri, D. Trere and R. L. Ochs (1995). "The quantity of nucleolar proteins nucleolin and protein B23 is related to cell doubling time in human cancer cells." Laboratory Investigation **73**(4): 497-502.

Di Renzo, M. F., R. P. Narsimhan, M. Olivero, S. Bretti, S. Giordano, E. Medico, P. Gaglia, P. Zara and P. M. Comoglio (1991). "Expression of the Met/HGF receptor in normal and neoplastic human tissues." Oncogene **6**(11): 1997-2003.

Di Renzo, M. F., M. Olivero, S. Ferro, M. Prat, I. Bongarzone, S. Pilotti, A. Belfiore, A. Costantino, R. Vigneri and M. A. Pierotti (1992). "Overexpression of the c-MET/HGF receptor gene in human thyroid carcinomas." Oncogene **7**(12): 2549-53.

Edlund, M., T. Miyamoto, R. A. Sikes, R. Ogle, G. W. Laurie, M. C. Farach-Carson, C. A. Otey, H. E. Zhau and L. W. Chung (2001). "Integrin expression and usage by prostate cancer cell lines on laminin substrata." Cell Growth & Differentiation **12**(2): 99-107.

Ferracini, R., P. Longati, L. Naldini, E. Vigna and P. M. Comoglio (1991). "Identification of the major autophosphorylation site of the Met/hepatocyte growth factor receptor tyrosine kinase." Journal of Biological Chemistry **266**(29): 19558-64.

Ferracini, R., K. Scotlandi, E. Cagliero, F. Acquarone, M. Olivero, J. Wunder and N. Baldini (2000). "The expression of Met/hepatocyte growth factor receptor gene in giant cell tumors of bone and other benign musculoskeletal tumors." Journal of Cellular Physiology **184**(2): 191-6.

Gandino, L., P. Longati, E. Medico, M. Prat and P. M. Comoglio (1994). "Phosphorylation of serine 985 negatively regulates the hepatocyte growth factor receptor kinase." Journal of Biological Chemistry **269**(3): 1815-20.

Ginisty, H., H. Sicard, B. Roger and P. Bouvet (1999). "Structure and functions of nucleolin." Journal of Cell Science **112**(Pt 6): 761-72.

Gohda, E., H. Okauchi, M. Iwao and I. Yamamoto (1998). "Induction of apoptosis by hepatocyte growth factor/scatter factor and its augmentation by phorbol esters in Meth A cells." Biochemical & Biophysical Research Communications **245**(1): 278-83.

Helou, K., V. Wallenius, Y. Qiu, F. Ohman, F. Stahl, K. Klinga-Levan, L. G. Kindblom, N. Mandahl, J. O. Jansson and G. Levan (1999). "Amplification and overexpression of the hepatocyte growth factor receptor (HGFR/MET) in rat DMBA sarcomas." Oncogene **18**(21): 3226-34.

Hiscox, S. E., M. B. Hallett, M. C. Puntis, T. Nakamura and W. G. Jiang (1997). "Expression of the HGF/SF receptor, c-met, and its ligand in human colorectal cancers." Cancer Investigation 15(6): 513-21.

Humphrey, P. A., X. Zhu, R. Zarnegar, P. E. Swanson, T. L. Ratliff, R. T. Vollmer and M. L. Day (1995). "Hepatocyte growth factor and its receptor (c-MET) in prostatic carcinoma." American Journal of Pathology 147(2): 386-96.

Inoue, K., M. Chikazawa, T. Karashima, T. Iiyama, M. Kamada, T. Shuin, M. Furihata and Y. Ohtsuki (1998). "Overexpression of c-Met/hepatocyte growth factor receptors in human prostatic adenocarcinoma." Acta Medica Okayama 52(6): 305-10.

Jeffers, M., S. Rong and G. F. Woude (1996). "Hepatocyte growth factor/scatter factor-Met signaling in tumorigenicity and invasion/metastasis." Journal of Molecular Medicine 74(9): 505-13.

Jucker, M., A. Gunther, G. Gradl, C. Fonatsch, G. Krueger, V. Diehl and H. Tesch (1994). "The Met/hepatocyte growth factor receptor (HGFR) gene is overexpressed in some cases of human leukemia and lymphoma." Leukemia Research 18(1): 7-16.

Kim, S. J., E. Shiba, F. Tsukamoto, M. Izukura, T. Taguchi, K. Yoneda, Y. Tanji, Y. Kimoto and S. I. Takai (1998). "The expression of urokinase type plasminogen activator is a novel prognostic factor in dukes B and C colorectal cancer." Oncology Reports 5(2): 431-5.

Kurimoto, S., N. Moriyama, S. Horie, M. Sakai, S. Kameyama, Y. Akimoto, H. Hirano and K. Kawabe (1998). "Co-expression of hepatocyte growth factor and its receptor in human prostate cancer." Histochemical Journal 30(1): 27-32.

Liotta, L. A., R. Mandler, G. Murano, D. A. Katz, R. K. Gordon, P. K. Chiang and E. Schiffmann (1986). "Tumor cell autocrine motility factor." Proceedings of the National Academy of Sciences of the United States of America 83(10): 3302-6.

Maggiora, P., G. Gambarotta, M. Olivero, S. Giordano, M. F. Di Renzo and P. M. Comoglio (1997). "Control of invasive growth by the HGF receptor family." Journal of Cellular Physiology 173(2): 183-6.

Meiners, S., V. Brinkmann, H. Naundorf and W. Birchmeier (1998). "Role of morphogenetic factors in metastasis of mammary carcinoma cells." Oncogene 16(1): 9-20.

Nakamura, T., T. Nishizawa, M. Hagiya, T. Seki, M. Shimonishi, A. Sugimura, K. Tashiro and S. Shimizu (1989). "Molecular cloning and expression of human hepatocyte growth factor." Nature 342(6248): 440-3.

16

Naldini, L., E. Vigna, R. Ferracini, P. Longati, L. Gandino, M. Prat and P. M. Comoglio (1991). "The tyrosine kinase encoded by the MET proto-oncogene is activated by autophosphorylation." Molecular & Cellular Biology **11**(4): 1793-803.

Naldini, L., E. Vigna, R. P. Narsimhan, G. Gaudino, R. Zarnegar, G. K. Michalopoulos and P. M. Comoglio (1991). "Hepatocyte growth factor (HGF) stimulates the tyrosine kinase activity of the receptor encoded by the proto-oncogene c-MET." Oncogene **6**(4): 501-4.

Naldini, L., K. M. Weidner, E. Vigna, G. Gaudino, A. Bardelli, C. Ponzetto, R. P. Narsimhan, G. Hartmann, R. Zarnegar and G. K. Michalopoulos (1991). "Scatter factor and hepatocyte growth factor are indistinguishable ligands for the MET receptor." EMBO Journal **10**(10): 2867-78.

Nemeth, J. A. and C. Lee (1996). "Prostatic ductal system in rats: regional variation in stromal organization." Prostate **28**(2): 124-8.

Nishimura, K., M. Kitamura, H. Miura, N. Nonomura, S. Takada, S. Takahara, K. Matsumoto, T. Nakamura and K. Matsumiya (1999). "Prostate stromal cell-derived hepatocyte growth factor induces invasion of prostate cancer cell line DU145 through tumor-stromal interaction." Prostate **41**(3): 145-53.

Nishimura, K., M. Kitamura, S. Takada, N. Nonomura, A. Tsujimura, K. Matsumiya, T. Miki, K. Matsumoto and A. Okuyama (1998). "Regulation of invasive potential of human prostate cancer cell lines by hepatocyte growth factor." International Journal of Urology **5**(3): 276-81.

Ohmichi, H., U. Koshimizu, K. Matsumoto and T. Nakamura (1998). "Hepatocyte growth factor (HGF) acts as a mesenchyme-derived morphogenic factor during fetal lung development." Development **125**(7): 1315-24.

Orrick, L. R., M. O. Olson and H. Busch (1973). "Comparison of nucleolar proteins of normal rat liver and Novikoff hepatoma ascites cells by two-dimensional polyacrylamide gel electrophoresis." Proceedings of the National Academy of Sciences of the United States of America **70**(5): 1316-20.

Pisters, L. L., P. Troncoso, H. E. Zhau, W. Li, A. C. von Eschenbach and L. W. Chung (1995). "c-met proto-oncogene expression in benign and malignant human prostate tissues." Journal of Urology **154**(1): 293-8.

Prat, M., T. Crepaldi, L. Gandino, S. Giordano, P. Longati and P. Comoglio (1991). "C-terminal truncated forms of Met, the hepatocyte growth factor receptor." Molecular & Cellular Biology **11**(12): 5954-62.

Qadan, L. R., C. M. Perez-Stable, R. H. Schwall, K. L. Burnstein, R. C. Ostenson, G. A. Howard and B. A. Roos (2000). "Hepatocyte growth factor and vitamin D cooperatively inhibit androgen-unresponsive prostate cancer cell lines." Endocrinology **141**(7): 2567-73.

Rodrigues, G. A., M. A. Naujokas and M. Park (1991). "Alternative splicing generates isoforms of the met receptor tyrosine kinase which undergo differential processing." Molecular & Cellular Biology **11**(6): 2962-70.

Rodrigues, G. A. and M. Park (1993). "Isoforms of the met receptor tyrosine kinase." EXS **65**: 167-79.

Santos, O. F., L. A. Moura, E. M. Rosen and S. K. Nigam (1993). "Modulation of HGF-induced tubulogenesis and branching by multiple phosphorylation mechanisms." Developmental Biology **159**(2): 535-48.

Schmidt, C., F. Bladt, S. Goedecke, V. Brinkmann, W. Zschiesche, M. Sharpe, E. Gherardi and C. Birchmeier (1995). "Scatter factor/hepatocyte growth factor is essential for liver development." Nature **373**(6516): 699-702.

Srivastava, M. and H. B. Pollard (1999). "Molecular dissection of nucleolin's role in growth and cell proliferation: new insights." FASEB Journal **13**(14): 1911-22.

Thery, C., M. J. Sharpe, S. J. Batley, C. D. Stern and E. Gherardi (1995). "Expression of HGF/SF, HGF1/MSP, and c-met suggests new functions during early chick development." Developmental Genetics **17**(1): 90-101.

Tsuka, H., H. Mori, B. Li, H. Kanamaru, S. Matsukawa and K. Okada (1998a). "Enhanced hepatocyte growth factor level in human prostate cancer treated with endocrine therapy." International Journal of Oncology **13**(1): 169-76.

Tsuka, H., H. Mori, B. Li, H. Kanamaru, S. Matsukawa and K. Okada (1998b). "Expression of c-MET/HGF receptor mRNA and protein in human non-malignant and malignant prostate tissues." International Journal of Oncology **13**(5): 927-34.

Wordinger, R. J., A. F. Clark, R. Agarwal, W. Lambert and S. E. Wilson (1999). "Expression of alternatively spliced growth factor receptor isoforms in the human trabecular meshwork." Investigative Ophthalmology & Visual Science **40**(1): 242-7.

Figure Legends

Table 1. ELISA for Hepatocyte Growth Factor in conditioned media collected from normal prostate stromal cells.

Table 2. FACS analysis of cells treated with purified HGF or stromal-conditioned media for two hours. Integrin expression values are presented as the mean of two individual experiments with the range given in parentheses. An isotype non-specific antibody was used for control. All experimental fluorescence values are reported as the ratio of the control and specific fluorescence values. Relative values of integrin expression can only be compared for the same antibody on different cells, due to differences in antibody-ligand affinities.

Table 3. 24 peptides were sequenced from cell lysates, based on co-immunoprecipitation with purified HGF protein. All peptides showed 100% sequence homology to previously cloned nucleolin (NCBI#4885511). Numbers within the Table refer to the peptide's location within the published nucleolin sequence.

Figure 1. Prostate cancer cell lines compared for their cell attachment responses to treatment with stromal cell-conditioned media. All cell lines, except LNCaP, increased cell spreading on laminin following exposure to the conditioned media. Experimental attachment is shown as a percentage of control, untreated cell attachment, and results are presented as the mean of triplicate experiments, with standard deviation error bars. Statistically significant differences from the control in each group were at $P=<0.05$ (*).

Figure 2. C4-2 cell attachment to laminin following treatment with stroma-conditioned media or purified HGF. Cells were allowed to attach for 90 min., at which point ~25% of untreated C4-2 cells attached. Induction of cell spreading, as seen for both stroma-conditioned media and purified HGF, is reversible by addition of anti-HGF antibody. Conditioned media from three primary stromal cell lines gave similar results. Standard deviations shown as error bars (n=6). Statistically significant differences from the control in each group were at $P=<0.05$ (*).

Figure 3. Cell spreading behaviors of PC3 and C4-2 cells exposed to variable concentrations of purified HGF. Because the cells differ in control attachment speeds, experiments were terminated at 30 minutes for PC3 cells and 90 minutes for C4-2 cells. At these times, in high concentrations of HGF, filopodia and lamelipodia were visible in approximately 90% of PC3 cells and 65% of C4-2 cells. Both cell lines show a concentration dependent increase in cell spreading with increasing concentration of HGF

Figure 4. Time-course and quantification of C4-2 migratory behaviors. C4-2 cells were plated in a defined circlular area on lamin or fibronectin substrata, with different concentrations of HGF in the media. (A) Exemplar migration at 96 hr. time point, with 0 or 100 ng/ml of HGF in the medium. (B) Time-dependent migration, in the presence of HGF, on different matrices. All values are normalized to the cell area at 0 hr. time point.

Figure 5. HGF induction of C4-2 cell spreading is matrix dependent.

Figure 6. C4-2 cell attachment to laminin after 90 minutes of exposure to either purified HGF or stromal cell-conditioned media, in the presence or absence of function-blocking integrin isotype-specific antibodies. All values are presented as % attachment, normalized to control C4-2 cells, that were not treated with HGF or conditioned media (n=6).

Figure 7. met HGF receptor transcript in prostate cell lines detected by RTPCR. Amplified fragments of control μ-globulin and the cytoplasmic domain of human-met are shown on an ethidium-bromide stained agarose gel. The length of the h-met PCR product was 262 bp. Product levels close to undetectable in LNCaP and C4-2 samples.

Figure 8. Western blot analysis of total cell lysates from LNCaP, C4-2, PC3, PC3M, DU145 and HeLa cells. Equal amounts of cell lysate were separated and stained with antibodies against either the extracellular (A) or cytoplasmic (B) domains of the met receptor. Met was detected by characteristic double bands in all cell lines except LNCaP and C4-2.

Figure 9. Immunoprecipitation and FAK phosphorylation

Figure 10. Immunoprecipitation of nucleolin. Western and silver staining

Table 1. HGF concentrations in stromal conditioned media by ELISA (n=3)

Stroma	HGF ng/ml
Stroma 1	18.5 (4.6)
Stroma 2	24.1 (2.3)
Stroma 3	16.4 (2.0)
Stroma 4	13.9 (1.5)
Stroma 5	22.6 (3.2)

Table 1. Edlund et al.

Table 2. Integrin expression by FACS analyses

Integrin subunit	Control	Stroma	HGF
α_2	16.7 (2.3)	10.6 (0.5)	20.4 (1.6)
α_3	3.4 (1.2)	3.3 (0.6)	4.2 (0.3)
α_6	10.8 (0.8)	10.6 (1.5)	9.9 (0.2)
β_1	15.5 (2.8)	15.6 (2.5)	14.1 (0.4)
β_4	1.3 (0.2)	1.8 (0.5)	1.6 (0.4)
$\alpha_v\beta_3$	1.6 (0.4)	2.4 (0.9)	1.5 (0.2)

Table 2. Edlund et al.

Position	Sequence
72-79	VAVATPAK
72-80	VAVATPAKK
296-318	QKVEGTEPTTAFNLFVGNLNFNK
325-333	TGISDVFAK
334-342	NDLAVVDVR
348-362	KEGYVDFESAEDLEK
349-362	FGYVDFESAEDLEK
363-370	ALELTGLK
404-410	VTQDELK
404-420	VTQDELKEVFEDAAEIR
411-420	EVFEDAAEIR
428-437	SKGIAYIEFK
430-437	GIAYIEFK
438-449	TEADAEKTFEEK
450-457	QGTEIDGR
458-467	SISLYYTGEK
478-486	NSTWSGESK
522-537	SKGYAFIEFASFEDAK
525-537	GYAFIEFASFEDAK
555-561	LELQGPR
578-597	GLSEDTTEETLKESFDGSVR
611-624	GFGFVDFNSEEDAK
625-636	EAMEDGEIDGNK
625-645	EAMEDGEIDGNKVTLDWAKPK

Table 3. Edlund et al.
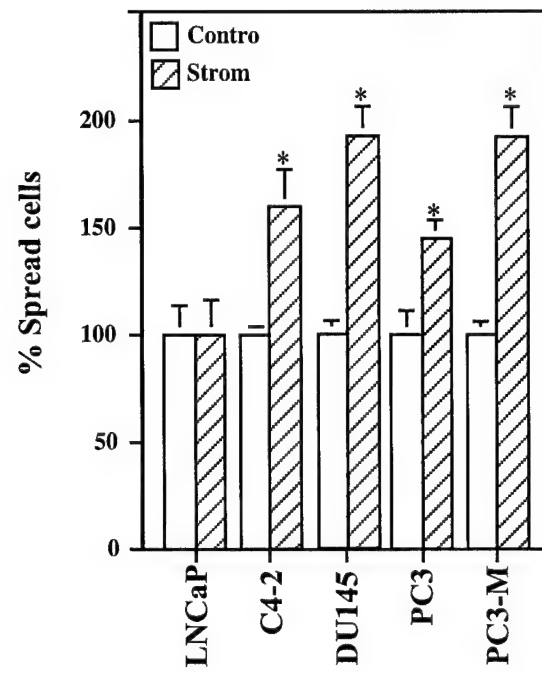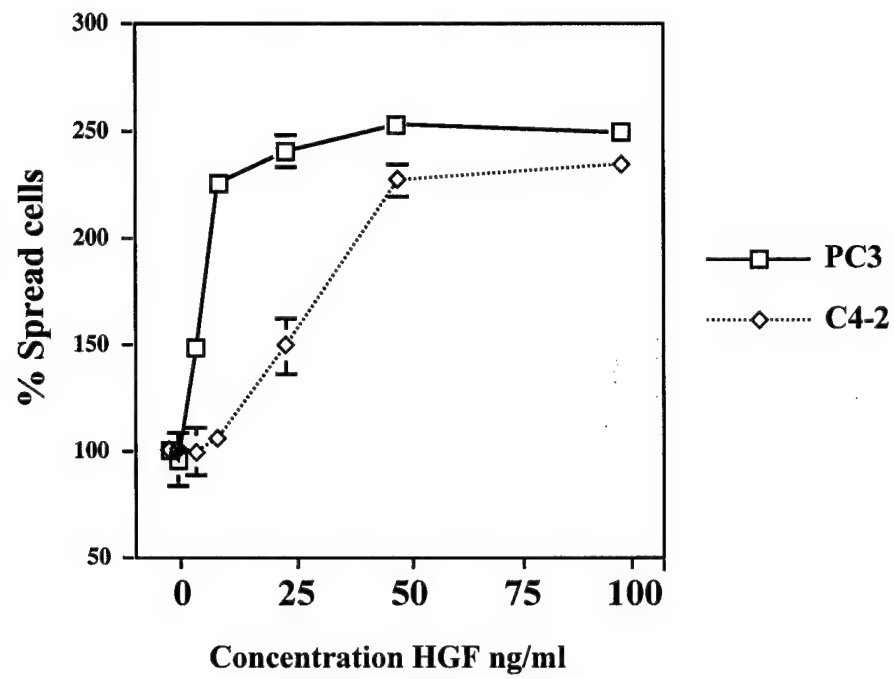
Figure 1. Edlund et al.
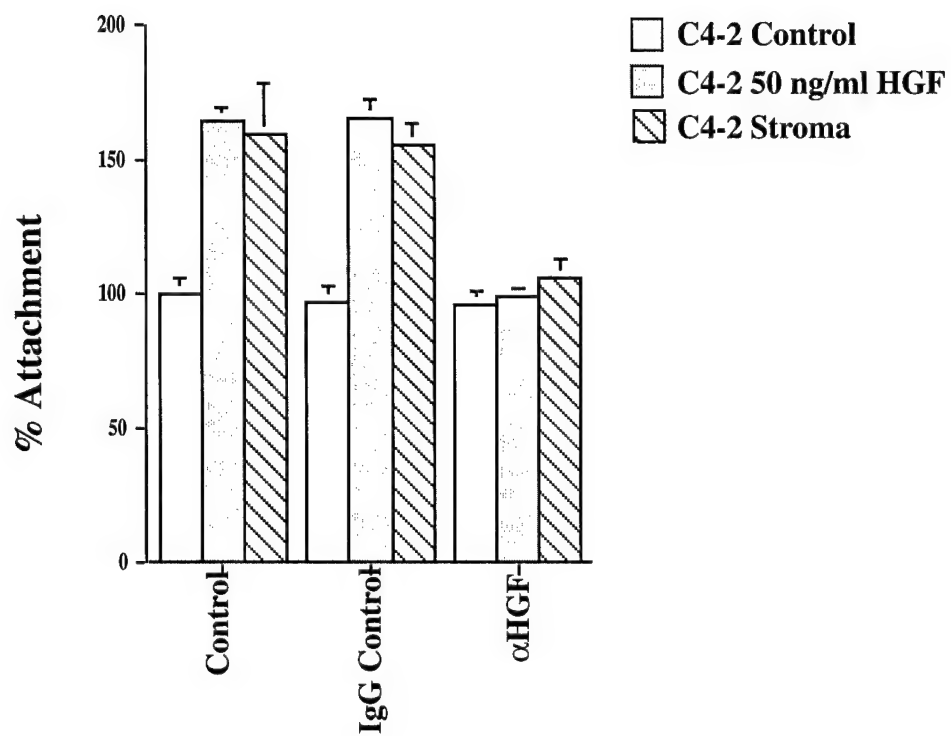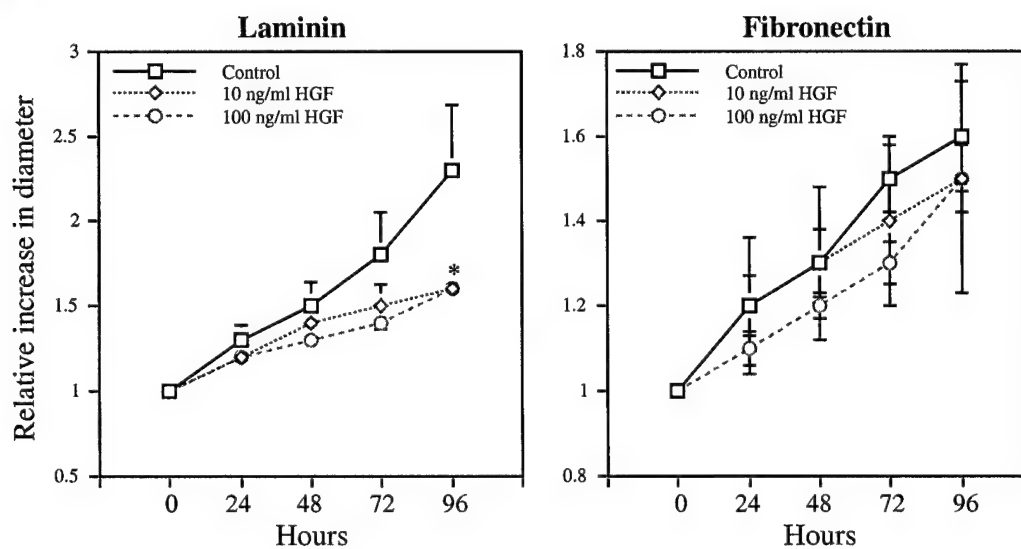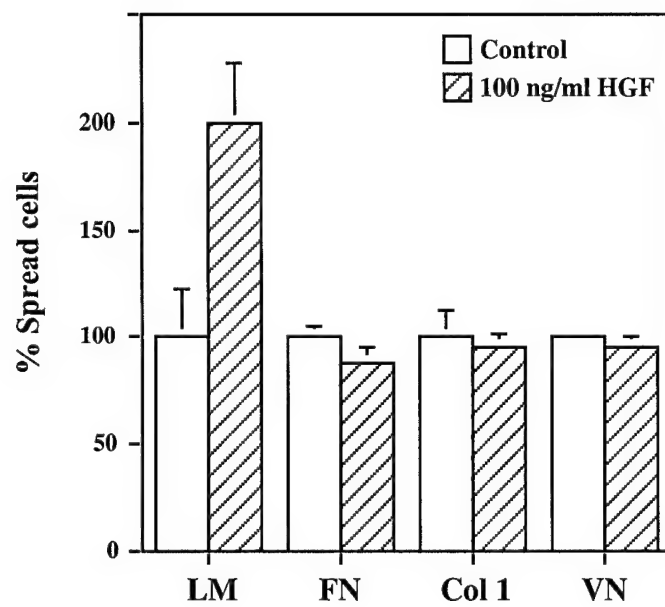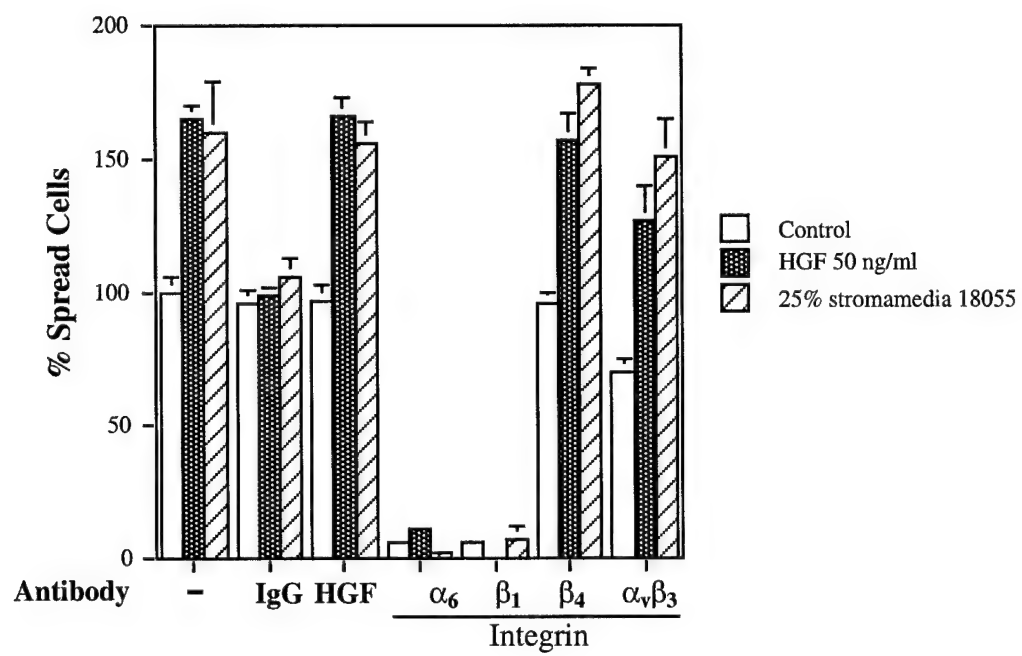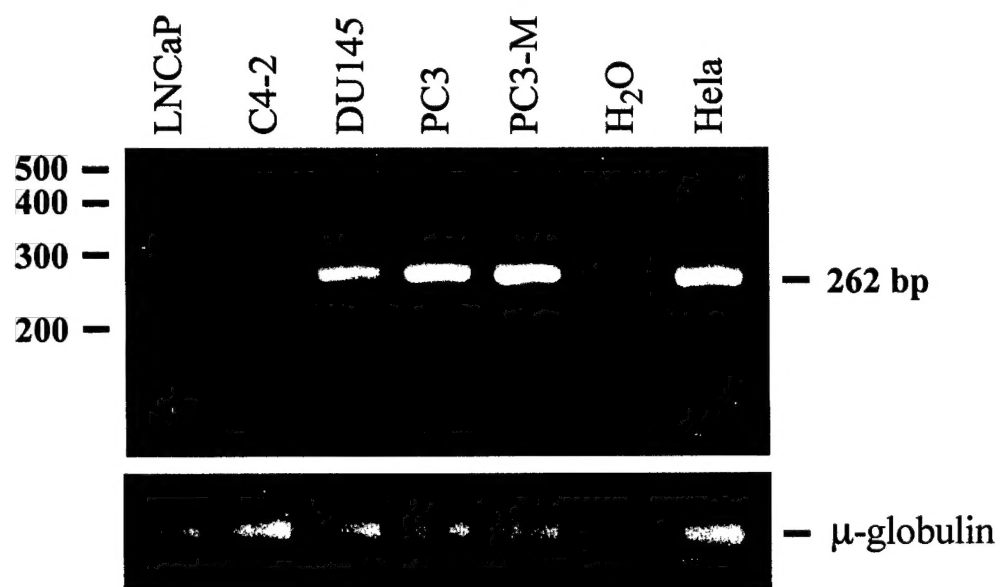
Figure 2. Edlund et al.

Figure 3. Edlund et al.

A

96 hours   96 hours

Control

100 ng/ml HGF

B

Figure 4. Edlund et al.

% Spread cells (y-axis)

Legend: Control, 100 ng/ml HGF

x-axis: LM, FN, Col 1, VN

Figure 5. Edlund et al.

% Spread Cells (y-axis, 0 to 200)

Legend:
- □ Control
- ■ HGF 50 ng/ml
- ▨ 25% stromamedia 18055

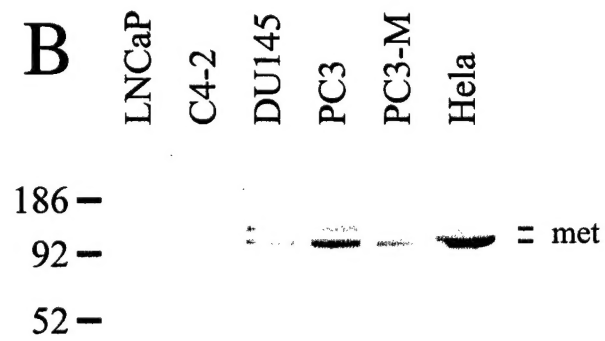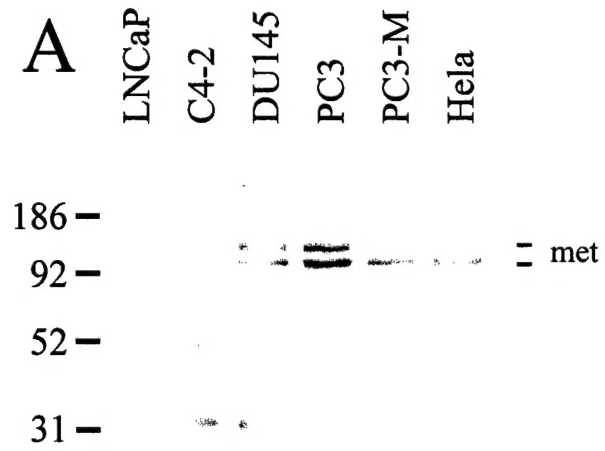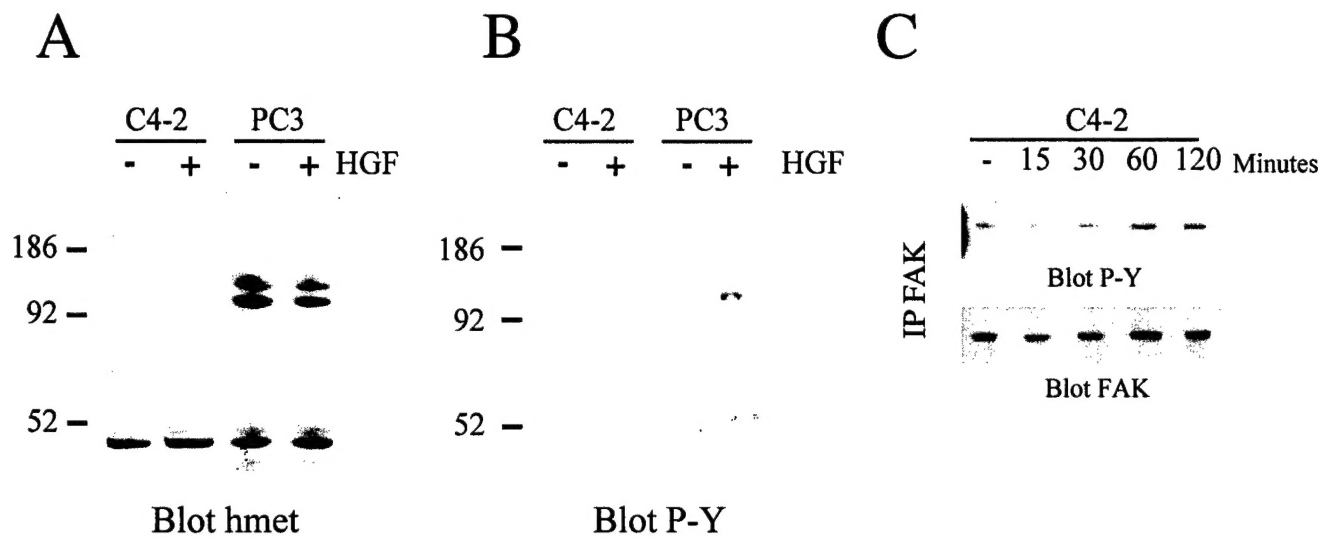**Antibody** — IgG HGF α6 β1 β4 αvβ3

Integrin

Figure 6. Edlund et al.

Figure 7. Edlund et al.

Figure 8. Edlund et al.

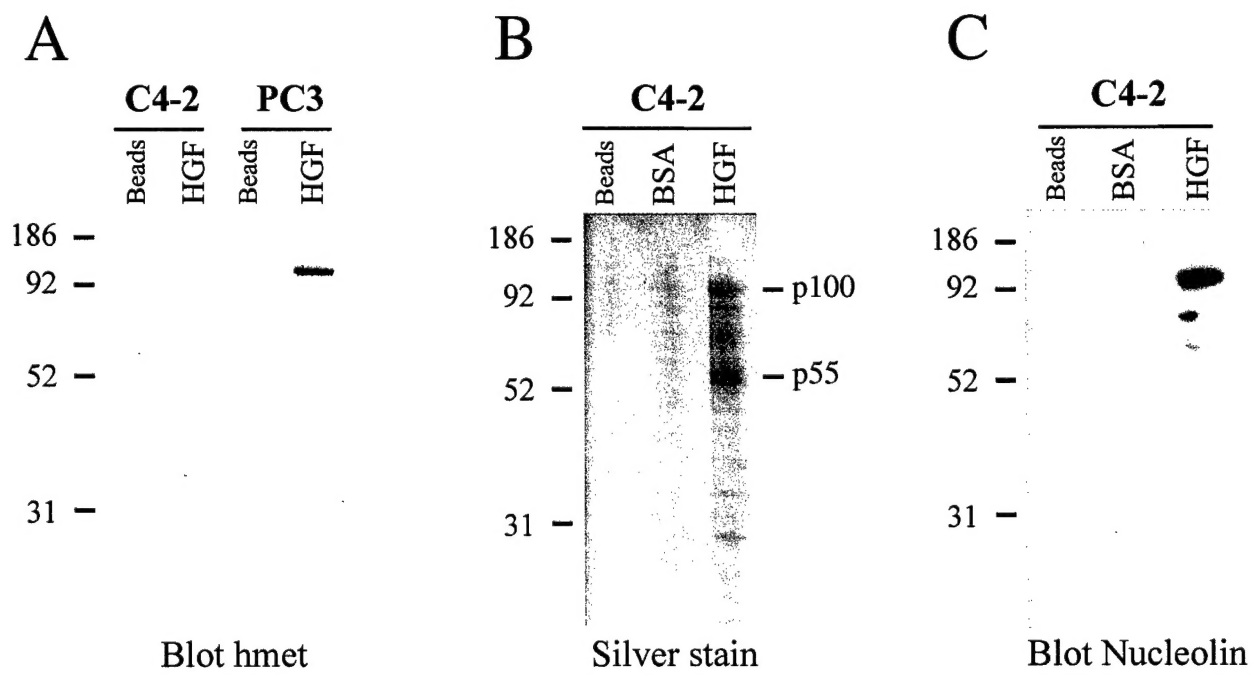**A**

C4-2   PC3
-   +   -   + HGF

186 —

92 —

52 —

Blot hmet

B

C4-2   PC3
-   +   -   + HGF

186 —

92 —

52 —

Blot P-Y

C

C4-2
-   15 30 60 120 Minutes

IP FAK

Blot P-Y

Blot FAK

Figure 9. Edlund et al.

A

C4-2   PC3

Beads HGF   Beads HGF

186 —

92 —   ▬

52 —

31 —

Blot hmet

B

C4-2

Beads BSA HGF

186 —

92 —   — p100

52 —   — p55

31 —

Silver stain

C

C4-2

Beads BSA HGF

186 —

92 —

52 —

31 —

Blot Nucleolin

Figure 10. Edlund et al.